5-2011

Heat transfer measurement in oil-based nanofluids.

Kan Liu
University of Louisville

HEAT TRANSFER MEASUREMENT IN OIL-BASED NANOFLUIDS

By

Kan Liu
B.S., East China University of Science and Technology, 2007

A Dissertation
Submitted to the Faculty of the
Speed School of Engineering of the University of Louisville
in Partial Fulfillment of the Requirements
for the Degree of

Doctor of Philosophy

Department of Chemical Engineering
University of Louisville
Louisville, KY 40292

May 2011

HEAT TRANSFER MEASUREMENT IN OIL-BASED NANOFLUIDS

By

Kan Liu

B.S., East China University of Science and Technology, 2007

A Dissertation Approved on

April 11th, 2011

Date

by the following Dissertation Committee:

Gerold A. Willing (Dissertation Director)

James C. Watters

Eric Berson

Moises Carreon

William Biles

ACKNOWLEDGMENTS

I would like to express my deepest gratitude to my Ph.D advisor, Prof. Gerold A. Willing for his guidance and support during my Ph.D study at University of Louisville. Dr. Willing provided an exciting and relaxing working environment and great opportunities to develop new ideas. It was a very enjoyable time working in his research group.

I would like to thank Clare Brun and Nick Chapman for their help build the heat transfer measurement system.

I would like to thank Prof. James C. Watters, Prof. Eric Berson, Prof. Moises Carreon, and Prof. William Biles for agreeing to be my dissertation committee.

Finally, I would like to thank my family for their encouragement and support, without which this dissertation and research would not have been possible.

ABSTRACT

HEAT TRANSFER MEASUREMENT IN OIL-BASED NANOFLUIDS

Kan Liu

April 11, 2011

Nanoparticles are a class of materials that exhibit unique physical and chemical properties compared to those of the same material at the bulk scale. One method of enhancing the thermal conductivity, and hence the heat transfer coefficient, of a fluid is to add nanoparticles to the fluid creating a so called nanofluid. The term "nanofluids" was coined by researchers at Argonne National Laboratory and refers to a two-phase mixture composed of a continuous liquid phase and dispersed nanoparticles in suspension. Nowadays, nanofluids are considered to be the next-generation heat transfer fluids as they offer exciting new possibilities to enhance heat transfer performance compared to pure liquids.

Heat transfer coefficient of a fluid is the proportionality coefficient between the heat flux that is a heat flow per unit area and the thermodynamic driving force for the flow of heat. It shows how effective heat can be transferred within a system and can be passively enhanced by changing flow geometry, boundary conditions, or by enhancing

thermal conductivity of the fluid. In most existing systems, since the first two of these are set by design, the only method to enhance heat transfer is to enhance heat transfer properties of the fluid.

In this study, we used three sizes of Cu nanoparticles with different particle loadings and dispersed them into PAO formulated motor oil to create nanofluids. Measurements of heat transfer coefficients and other fluid properties were performed. Both base and nanofluids appeared to behave like Newtonian fluids and an up to 25% enhancement of the heat transfer coefficient was observed in the laminar flow regime. The heat transfer coefficient is shown to increase with increasing Reynolds number. However, as fluid temperature increases, the heat transfer coefficient decreased. Various factors including Reynolds number, fluid temperature, nanoparticle size, and nanoparticle loadings are all capable of impacting the enhancement ratio. A consistent downward trend of enhancement ratio with respect to Reynolds number was observed for the nanofluids discussed in this work. Future studies in the turbulent flow regime are needed to confirm this trend. Finally, a theoretical model to predict the heat transfer coefficient of nanofluids is developed based on previously published correlations the results of which are in excellent agreement with the experimental data.

TABLE OF CONTENTS

LIST OF TABLES

LIST OF FIGURES

FIGURE PAGE

CHAPTER I

INTRODUCTION

The first use of the concepts found in 'nano-technology' was in "There's Plenty of Room at the Bottom", a talk given by physicist Richard Feynman at an American Physical Society meeting at California Institute of Technology (Caltech) on December 29, 1959 [1]. Feynman described a process by which the ability to manipulate individual atoms and molecules might be developed, using one set of precise tools to build and operate another proportionally smaller set, and so on down to the needed scale. In the course of this, he noted, scaling issues would arise from the changing magnitude of various physical phenomena: gravity would become less important while the surface tension and van der Waals attraction would become increasingly more significant.

The term "nanotechnology" was first defined by Norio Taniguchi of the Tokyo Science University in a 1974 paper [2] as follows: "'Nano-technology' mainly consists of the processing of separation, consolidation, and deformation of materials by one atom or one molecule." Since that time the definition of nanotechnology has generally been extended to include features as large as 100 nm. Additionally, the idea that nanotechnology embraces structures exhibiting quantum mechanical aspects, such as quantum dots, has further evolved its definition. Also in 1974, the process of atomic layer

deposition, for depositing uniform thin films one atomic layer at a time, was developed and patented by Dr. Tuomo Suntola and co-workers in Finland. In the 1980s, the idea of nanotechnology as a deterministic, rather than stochastic, handling of individual atoms and molecules was conceptually explored in depth by Dr. K. Eric Drexler. His vision of nanotechnology is often called "Molecular Nanotechnology" (MNT) or "molecular manufacturing."

Nanotechnology is the understanding and control of matter at dimensions between approximately 1 and 100 nanometers, where unique phenomena enable novel applications. Encompassing nanoscale science, engineering, and technology, nanotechnology involves imaging, measuring, modeling, and manipulating matter at this length scale. Dimensions between 1 and 100 nanometers are known as the nanoscale. At the nanoscale, unusual physical, chemical, and biological properties can emerge in materials. These properties may differ in important ways from the properties of bulk materials and single atoms or molecules.

Work within the intersecting disciplines at the core of nanotechnology innovation—including physical, life, and social sciences and engineering—has revealed the potential of nanomaterials and nanoscale processes in a number of ways. They can be used to collect and store energy, reinforce materials, sense contaminants, enable life-saving drugs, and shrink and accelerate computational devices in both incremental and paradigm-shifting ways. Furthermore, nanotechnology has enabled development of entirely new materials and devices that can be exploited in each of these and countless other applications [3].

The United States has set the pace for nanotechnology innovation world-wide

with the National Nanotechnology Initiative (NNI). Launched in 2001 with eight agencies, the NNI today consists of the individual and cooperative nanotechnology-related activities of 25 Federal agencies with a range of research and regulatory roles and responsibilities. The ten-year history of U.S leadership in fundamental nanotechnology research and development under the NNI has established a thriving nanotechnology R&D environment. One of the major goals of the National Nanotechnology Initiative strategic plan in 2011 is to advance a world-class nanotechnology research and development program. This program expands the boundaries of knowledge and develops technologies through a comprehensive program of research development. The NNI agencies invest at the frontiers and intersections of many disciplines, including chemistry, engineering, biology, materials science, and physics. The interest in nanotechnology arises from its potential to significantly impact numerous fields, including aerospace, agriculture, energy, healthcare, information technology, and transportation systems. In this strategic plan, fundamental nanoscale phenomena and processes is one of the most important research areas.

An important term "nanofluids" was coined by researchers at Argonne National Laboratory in 1995 and refers to a two-phase mixture composed of a continuous liquid phase and dispersed nanoparticles in suspension [4]. Studies have shown the great potential of nanofluids to enhance thermal properties of their base fluids. As the first step, the preparation of nanofluids [5] is a key step to these enhancements.

The term nanofluid does not simply equate to a liquid-solid mixture. Special requirements including stable suspension, even with low agglomeration of nanoparticles and no chemical change in fluid are needed. To meet these requirements one need to

change the surface properties of suspended particles and to suppress the formation of particle clusters to obtain a stable suspension. Depending on the properties of the nanoparticles and the solution selected, different types of surfactants can be used to enhance stability. Surfactants reduce the surface tension of water by adsorbing at the liquid-gas interface. They also reduce the interfacial tension between oil and water by adsorbing at the liquid-liquid interface. When surfactants assemble in oil, the aggregate is referred to as a reverse micelle. In a reverse micelle, the hydrophilic heads of the surfactants are in the core of the micelle and the hydrophobic tails maintain favorable contact with oil [6-8]. The most commonly used surfactants are thiols, oleic acid, laurate salts. Also, different surfactants may affect the properties of the nanofluids which still need to be more fully investigated. Figure 1.1 shows how cetyl trimethylammonium bromide (CTAB) works as a surfactant on alumina molecule.

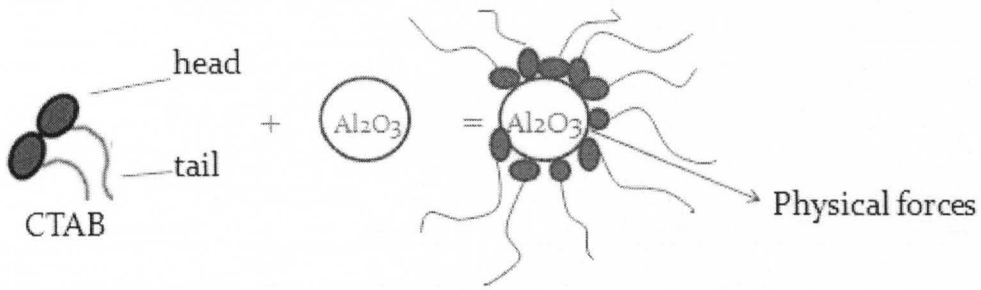

Fig 1.1 Encapsulation of nanoparticle with surfactant molecules

There are two major techniques used to produce nanofluids: the two-step technique and the single step technique. The two-step technique [4] starts with nanoparticles, produced by one of the physical or chemical synthesis techniques, and proceeds to disperse them into a base fluid. It is commonly used in producing of

nanofluids containing oxide nanoparticles as well as carbon nanotubes. The advantage of the two-step technique in terms of eventual commercialization of nanofluids is that inert gas condensation techniques have been scaled up to economically produce tonnage quantities of nanoparticles [9]. Making nanofluids using the two-step technique is challenging, though, because of the results from potential agglomeration of nanoparticles prior to a complete dispersion. This agglomeration is due to the attractive Van der Waals forces between nanoparticles, and causes the particles to quickly settle out of suspension. In fact, agglomeration is a critical issue in all nanopowder technology, including nanofluid technology, and a key step to success in achieving high-performing heat transfer nanofluids is to produce and suspend nearly mono-dispersed or non-agglomerated nanoparticles in liquids. This barrier is exacerbated by the use of oxide nanoparticles that require higher volume concentrations compared to metal particles to achieve the same heat transfer enhancement in nanofluids. At high volume concentrations, the agglomeration problem becomes worse.

The single-step technique [4] simultaneously makes and disperses the nanoparticles directly into a base fluid. It is preferable to the two-step process when making nanofluids containing high-conductivity metals to prevent oxidation. A disadvantage of the single-step technique for nanofluid production is that systems run in batch mode with limited control over several important parameters, including those that control nanoparticle size. Commercial viability would be greatly increased if the single-step technique could be run in a continuous mode.

Metals (Ag, Cu, Fe, and Au), metal oxides (Al_2O_3, CuO), nitride ceramics and carbon nanotubes have been used to produce nanofluids [10-21]. The great potential of

nanofluids in different applications led many researchers to launch projects focusing on nanofluids. Because of this, more and more nanofluid-related research publications have appeared in literature. It can be seen from Figure 1.2 that there have been a total of 990 research articles on nanofluids published from 2001 to 2010 [22]. Different particle sizes, shapes, aspect ratios and volume fractions have been studied by research groups around the world [5, 23-27]. Most studies have focused on the enhancement of the thermal conductivity of nanofluids whereas studies on the enhancement of the heat transfer coefficient have been limited and mostly focused on carbon based nanoparticles. Furthermore, most studies have used water as the base fluid. There are relatively few studies on the effects of nanoparticles on oil-based nanofluids especially for PAO oils.

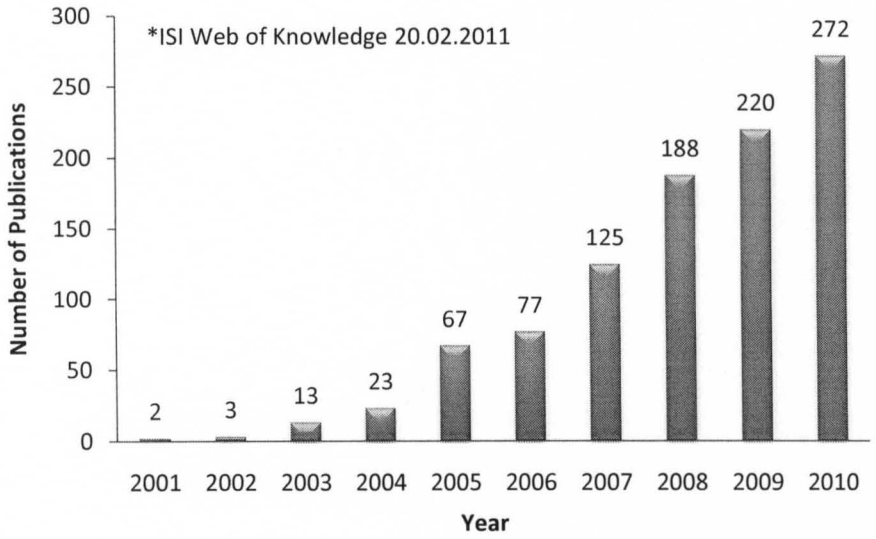

Fig 1.2 Number of published research articles on nanofluids between 2000 and 2010.

Thermal conductivity is the property of a material that indicates its ability to conduct heat. It is a more studied research area than any other nanofluid-related topic. Thermal conductivity of nanofluid is strongly dependent on several factors including

nanoparticle size, shape, volume fraction, base fluid material, temperature, and acidity. Keblinski et al. [28] proposed four possible reasons for the contribution of the nanometer-sized particles to the increase of the thermal conductivity: Brownian motion of the particles, molecular level layering of the liquid at the liquid/solid interface, the nature of the heat transport in the nanoparticles, and the effects of nanoparticle clustering. The transient hot-wire method is the most common way to experimentally measure the thermal conductivity. As shown in Figure 1.3, the transient hot-wire method [29] is a standard transient dynamic technique based on the measurement of the temperature rise at a defined distance from a linear heat source (hot wire) embedded in the test material. If the heat source is assumed to have a constant and uniform output along the length of test sample, the thermal conductivity can be derived directly from the resulting change in the temperature over a known time interval [30]. So far it has been very difficult to develop a sophisticated theory to determine the thermal conductivity but some empirical equations have been developed to estimate the thermal conductivity of nanofluids [31-34].

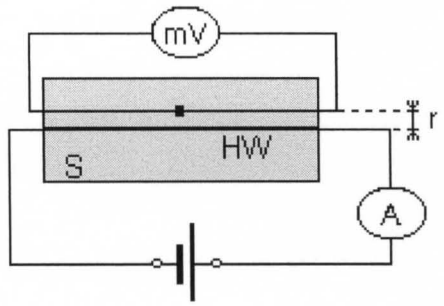

Fig 1.3 Transient hot-wire method.

While increases in the effective thermal conductivity as well as changes in density, specific heat, and viscosity are important indications of improved heat transfer behavior of nanofluids, the net benefit of nanofluids as heat transfer fluids is best determined

through the heat transfer coefficient. Because of the complex morphology and orientation of the nanoparticles dispersed in fluids, there have been few correlations developed for the heat transfer coefficients as compared to the study of thermal conductivity. The heat transfer coefficient is a proportionality constant between the heat flux, i.e. the heat flow per unit area, and the thermodynamic driving force for the flow of heat. There are numerous methods for calculating the heat transfer coefficient in different heat transfer modes, flow regimes and different fluids. Its magnitude relates to the effective heat that can be transferred within a system and can be passively enhanced by changing flow geometry, boundary conditions, or by enhancing thermal conductivity of the fluid.

Nowadays, nanofluids are considered to be the next-generation heat transfer fluids as they offer exciting new possibilities to enhance heat transfer performance compared to pure liquids. They are expected to have superior properties compared to conventional heat transfer fluids, as well as fluids containing micro-sized metallic particles [35]. The main reasons that contributed to this enhancement of heat transfer performance are as [5]:

a) The suspended nanoparticles increase the surface area for heat transfer and the heat capacity of the fluid.
b) The suspended nanoparticles increase the effective thermal conductivity of the fluid.
c) The interaction and collision among particles, fluid and the flow passage surface are intensified.
d) The mixing fluctuation and turbulence of the fluid are intensified.
e) The dispersion of nanoparticles flattens the transverse temperature gradient of the fluid.

Therefore, the heat transfer coefficient of the nanofluids is a function of suspended nanoparticle dimension, volume fraction, fluid flow velocity as well as various fluid properties. In this article, we refer to the heat transfer coefficient of a fluid as the heat transfer coefficient that is measured in our system with certain flow conditions. We can conclude that traditional mechanisms to predict the heat transfer coefficient are no longer applicable to nanofluids. But, prediction of the enhancement of heat transfer coefficient in thermal energy systems will aid in reducing the size of such systems, increasing the energy efficiency, lowering pollution and improving system reliability. However, there has been limited research in these areas when compared to thermal conductivity especially for oil-based nanofluids.

Nanofluids have a great potential in a number of different application areas like transportation, electronics cooling, biomedicine, and nuclear system cooling. For example, a 50/50 ethylene glycol (EG) and water mixture is commonly used as an automotive coolant. Unfortunately, the mixture is a relatively poor heat transfer fluid when compared to pure water. Water/EG mixture based nanofluids with additional nanoparticles are currently being studied to enhance heat transfer performance. [36]. Nanoparticles can improve the heat transfer coefficient of pure ethylene glycol and the resulting nanofluid performs better at low pressure working conditions and smaller coolant system when compared to 50/50 mixture. Therefore, smaller and lighter radiator can be used to increase engine performance and fuel efficiency. Large companies like GM and Ford all have ongoing nanofluid research projects. Nanofluids can also be used as the working fluid for heat pipes in electronic cooling applications where nanofluids can greatly reduce the thermal resistance of the heat pipe when compared to conventional

deionized water. In the biomedical field, iron-based nanoparticles could be used as delivery vehicles for drugs or radiation without damaging nearby tissue to circumvent side effects of traditional cancer treatment methods. Such particles could be guided in the bloodstream to a tumor using magnets external to the body [4].

Motor oil is a lubricant used in internal combustion engines for motor or road vehicles such as cars and motorcycles, and heavier vehicles such as buses and commercial trucks. Lubricating oil creates a separating film between surfaces of adjacent moving parts to minimize direct contact between them, decreasing heat caused by friction and reducing wear, thus protecting the engine. In use, motor oil transfers heat through convection as it flows through the engine by means of air flow over the surface of the oil pan, oil cooler and through the buildup of oil gases evacuated by the Positive Crankcase Ventilation (PCV) system. Motor oils today are mainly blended from base oils composed of various hydrocarbons (mineral, poly-alpha-olefins (PAO), etc. [37]), and are thus organic compounds consisting entirely of carbon and hydrogen.

Most motor oil has many different chemicals in it with very different properties. The temperature at which the oil starts burning is called the flash point. It is determined by the chemicals that burn at the lowest temperature. The higher the flash point, the more stable the oil is at high temperatures and the less the oil in the engine will burn. The pour point is the temperature at which the oil stops flowing like a liquid. The lower this number is, the better protected the engine is when it's cold. The thickness of the oil, that is the resistance the oil offers to motion, is called the viscosity. The viscosity depends on all of the various chemicals in the oil and how they react to each other and to heat. Importantly, as the oil heats up, it thins out, that is the viscosity goes down. The better the

oil is at retaining its viscosity at high temperatures, the higher the viscosity index. All of these properties depend on all the chemicals in the oil.

The high and low temperature performances of oils are described by the Viscosity Index (VI). The VI indicates how much the viscosity of the oil changes as the temperature is increased. In the late 1990s, a process was invented yielding base oils with VIs over 120 [38] compared to conventional oils which generally have VIs of less than 100. These base oils are called Group III or "unconventional base oils." The higher the VI, the fewer additives are necessary to achieve the required viscosity.

Synthetic oils were originally designed for the purpose of having pure base oil with excellent properties [39]. By starting from scratch and building up oil molecules from little pieces, almost every molecule in the oil is just like every other molecule, and therefore the properties are exactly what is designed in and not compromised by impurities. Synthetics were originally a reaction to the relatively poor refining processes available from about 1930 to about 1990. The original synthetics were designed for the Army Air Force in World War II, because they could not make their high performance turbo-charged radial engines stay alive on the available motor oils of the time [38].

One process for making synthetic base oils is to start with a chemical called an olefin, and makes new molecules by attaching them to each other in long chains. A poly-alpha-olefin (PAO) is a polymer made by polymerizing an alpha-olefin which is an alkene where carbon-carbon double bond starts at the α-carbon atom. In transportation applications, pure synthetic oils, mostly made up of PAO, have a much higher flash point than traditional petroleum oils which means they will hold up better in high temperature environments. The primary advantage of a PAO base oil is that all the molecules in the

base oil are nearly identical, so it is easy to get the base oil to behave in a predictable manner. However, due to the high price of producing PAO oils, most of the synthetic oils on the market today are made of Group III oils. Oil companies use a blend of mostly Group III oils and a smaller amount of true synthetics that can produce a product that has nearly the same properties as pure synthetic oil. The molecular uniformity of commercialized PAO formulated motor oils promotes superior lubrication and friction reduction, therefore promotes superior heat control, wear control and energy efficiency. Their uniformity also helps synthetics maintain their protective viscosity in high-temperature operations, which also promotes superior wear control.

In this study, we examine the various factors that could potentially impact the enhancement of heat transfer coefficient of oil-based nanofluid including nanoparticle size, weight fraction, Reynolds number and fluid temperature. PAO formulated oil is used as the base fluid. Copper nanoparticles are added into the PAO oil to make the nanofluids. The enhancement of heat transfer coefficient is the main focus of this study as well as several other fluid properties. Optimized nanoparticle size and concentration are expected to be found that will maximize the enhancement of heat transfer performance. A theoretical model is used based on published models to predict heat transfer coefficient of PAO oil-based nanofluids.

CHAPTER II

LITERATURE REVIEW

1. Experimental Research on Thermal Conductivity of Nanofluids

The enhancement of thermal conductivity is one of the most studied areas of nanofluids for heat transfer purposes, and a big portion of these studies have focused on automotive applications. Various parameters including particle size, particle concentration, particle material, base fluid material, and operating temperature have been studied to determine if they would impact the enhancement of thermal conductivity of nanofluids.

The effect of particle size on thermal conductivity of spherical nanoparticles was studied. Lee et al. [40], Wang et al. [41] and Xie et al. [42] have all measured the enhancement of thermal conductivity using Al_2O_3 nanoparticles with sizes of 28nm, 38nm and 60nm, respectively dispersed in water. The enhancement ratio increased with increasing volume concentration of nanoparticles. The larger 60nm particles showed the highest enhancement. Interestingly though, it was the 38nm particle that showed the least enhancement and not the smaller particle of 28nm. Because of this, no clear conclusions can be drawn from the results. Similar comparisons can be made from the work of three groups who studied different sizes of Al_2O_3 nanoparticles dispersed in ethylene glycol. This time, the intermediate-sized particle of 28nm exhibited the best enhancement while

the other two sizes (15nm and 60nm) showed almost identical results.

Volume concentration of nanofluids on the enhancement of thermal conductivity was the most extensively studied parameter. Most research groups [11, 14, 40, 42-47] used certain types of nanoparticle with different concentrations up to 5% to make nanofluids and measure the thermal conductivity. Particle size or base fluid material may vary but the general trend is clear: thermal conductivity enhancement increases with increased particle volume concentration. (Weight fraction was used in some publications.)

The effect of particle material on the enhancement of thermal conductivity is hard to find since different research groups used different sizes of nanoparticles and conducted experiments under different conditions. Comparing the results from Wang et al. [41] (28nm Al_2O_3/water, 23nm CuO/water), Lee et al. [40] (24nm CuO/water), Das et al. [44] (29nm CuO/water), and Xie et al. [26] (26nm SiC/water), shows that particle material has little effect on the enhancement for those relatively low thermal conductivity particles. Similar results were found for ethylene glycol (EG) based nanofluids by comparing the data from Xie et al. [26, 42] (26nm Al_2O_3/EG, 26nm SiC/EG), Wang et al. [41] (28nm Al_2O_3/EG), Lee et al. [40] (24nm CuO/EG).

Water and ethylene glycol are the two most commonly used base fluids. A study by Xie and colleagues [48] used 60nm Al_2O_3 dispersed in these two base fluids and oil to measure the enhancement of thermal conductivity. Results showed increased thermal conductivity enhancement for heat transfer fluids with lower thermal conductivity. Water is the best heat transfer fluid with the highest thermal conductivity of the fluids compared. But it showed the least enhancement around 10%-23% while Al_2O_3/oil nanofluid showed a maximum enhancement of 38%. Although this trend was not supported by results from

all research groups, generally it was the case. This result is encouraging because heat transfer enhancement is often most needed when poorer heat transfer fluids are involved. All results discussed above are shown in Table 1. Types of nanofluids and testing parameters are listed with enhancement ratio obtained.

Table 1 Thermal conductivity enhancements

Author/Year	Nanofluid	Particle size (nm)	Concentration (vol%)	Enhancement ratio
Lee et al./1999[40]	Al_2O_3/water	38.4	1.00 – 4.30	1.03 – 1.10
	CuO/water	23.6	1.00 – 3.41	1.03 – 1.12
	Al_2O_3/ethylene glycol	38.4	1.00 – 5.00	1.03 – 1.18
	CuO/ethylene glycol	23.6	1.00 – 4.00	1.05 – 1.23
Wang et al./1999[41]	Al_2O_3/water	28	0.19 – 1.59	1.01 – 1.10
	CuO/water	23		
	Al_2O_3/ethylene glycol	28	5.00 – 8.00	1.25 – 1.41
	CuO/ethylene glycol	23	6.20 – 14.80	1.24 – 1.54
	Al_2O_3/engine oil	28	2.25 – 7.40	1.05 – 1.30
	Al_2O_3/pump oil	28	5.00 -7.10	1.13 – 1.20
Xie et al./2002[26]	SiC/water	26 sphere	0.78 – 4.18	1.03 – 1.17
		600 cylinder	1.00 – 4.00	1.06 – 1.24
	SiC/ethylene glycol	26 sphere	0.89 – 3.50	1.04 – 1.13
		600 cylinder	1.00 – 4.00	1.06 – 1.23
Xie et al./2002[48]	Al_2O_3/water	60.4	5.00	1.23
	Al_2O_3ethylene glycol	60.4	5.00	1.29
	Al_2O_3/pump oil	60.4	5.00	1.38
Das et al./2003[44]	CuO/water			
	(21°C)	28.6	1.00 – 4.00	1.07 – 1.14
	(36°C)	28.6	1.00 – 4.00	1.22 – 1.26
	(51°C)	28.6	1.00 – 4.00	1.29 – 1.36

In general, the thermal conductivity of nanofluids is more temperature sensitive

than that of the base fluid. Consequently, the thermal conductivity enhancement of nanofluids is also temperature-sensitive. Das et al. [44] used nanofluids based on 38nm Al_2O_3 dispersed in water to measure thermal conductivity under three different temperatures at 21°C, 36°C and 51°C. Results clearly showed that enhancement increased as temperature was increased. This trend is supported by many other research groups [12, 49, 50] except Masuda et al. [43] who concluded that enhancement of thermal conductivity decreased with increased temperature. This trend is also important for engineering applications where most fluids operate at elevated temperatures.

Finally, PAO oil-based nanofluids seem to exhibit best enhancement of thermal conductivity. Both Marquis et al. [16] and Yang et al. [51] used carbon nanotubes/PAO oil nanofluids and observed thermal conductivity increase of 183% and 161%, respectively. Over 100% enhancement was report by Shaikh et al. [27] using nanofluids with carbon nanofiber and exfoliated graphite dispersed in PAO oil. Other parameters like pH value, additive type and concentration, and types of surfactants are not discussed due to limited data provided. A complete summary of results by different research groups are listed in Appendix A.

2. Experimental Research on Heat Transfer Coefficient

When put into application, the heat transfer coefficient of a nanofluid is more important than the thermal conductivity as this determines how effectively the heat can be transferred within a system. If nanofluids can improve the heat transfer coefficient of thermal energy systems, they can facilitate the reduction in size of such systems and lead to increased energy and fuel efficiencies, lower pollution, and improved reliability. To

this end, it is essential to directly measure the heat transfer performance of nanofluids under flow conditions typical of specific applications. While not as common as reports on the enhancement of thermal conductivity in nanofluids, there are still several significant studies on the enhancement of the heat transfer coefficient under flow conditions. Most heat transfer studies were presented using Nusselt number *Nu*, which is the ratio of convective to conductive heat transfer across the boundary. It is defined as:

$$Nu = \frac{h \cdot D}{k} \tag{1}$$

where h is the heat transfer coefficient, D is the diameter of the tube, and k is thermal conductivity of the fluid.

2.1 Results based on types of base fluid

Choi [52] pointed out that heat transfer coefficients should increase with fluid flow rates or with increasing thermal conductivities of the fluid provided that other properties of the nanofluid system, such as heat capacity, density and viscosity, are kept the same. Most studies on enhancement of heat transfer performance used water or ethylene glycol as the base fluid. Li et al. [53] experimentally investigated a 35 nm Cu/deionized water nanofluid flowing in a tube with constant wall heat flux and showed that the ratio of the Nusselt number for the nanofluid to that of pure water under the same flow velocity varies from 1.05 to 1.14 by increasing the volume fraction of nanoparticles from 0.5% to 1.2%, respectively. In other words, the heat transfer performance was enhanced by a maximum of 14% by using Cu/water nanofluids. Xuan et al. [19] investigated heat transfer of Cu/water nanofluid under constant wall heat flux in turbulent flow regime and concluded that convective heat transfer enhancement of the nanofluid may be related to

the thermal conductivity increase or the random movement and dispersion of nanoparticles within nanofluid. They proposed a new correlation based on a dispersion model and considered the effect of volume fraction and size of the nanoparticles to account for the enhancement. Wen et al. [11] have studied Al_2O_3/water nanofluid heat transfer in laminar flow under constant wall heat flux and reported an increase in nanofluid heat transfer coefficient with Reynolds number and nanoparticle concentration particularly at the entrance region. They expressed that the thermal developing length for a nanofluid was greater than that for pure water. Based on this, they concluded that the reason for the heat transfer enhancement for nanofluids is due the decreased thermal boundary layer thickness arising from the non-uniform distribution of thermal conductivity and viscosity resulting from Brownian motion of nanoparticles. Putra et al. [18] have reported the suppression of the natural convective heat transfer in a nanofluid of Al_2O_3/water and CuO/water and concluded that this could be due to several factors such as the settling of the nanoparticles and the velocity difference between the nanoparticles and the main fluid.

Results on the heat transfer performance of oil-based nanofluids are relatively limited but there are still several studies that are particularly significant to this work. Chun et al.[54] determined that heat transfer coefficients increased as particle loading increased from 0 to 0.5 vol% for Al_2O_3/transformer oil nanofluids. It was also found that over a Reynolds number (Re) range of 100 to 450, larger nanoparticle sizes (43nm) showed a slight enhancement in heat transfer coefficient when compared to smaller nanoparticle sizes (27-43nm). A more interesting result is that the rod-like alumina (7 nm diameter with an aspect ratio of 50 to 200) dispersed in oil displayed higher heat transfer

coefficients at lower Re but lower heat transfer coefficients at higher Re when compared to the larger nanoparticles over the Re range of 100 to 450. The researchers postulate that this may be due to alignment of the rods at the thermal boundary layer in the pipe at lower Re.

Choi and colleagues [55] used spherical and rod shape Al_2O_3 and spherical AlN nanoparticles dispersed in transformer oil to make nanofluids. All three types of nanofluids showed a small enhancement in the heat transfer coefficient at a Reynolds number range of 100 to 500. A maximum of 20% increase was observed for the AIN/transformer oil based nanoparticles at a volume fraction of 0.5%.

Yang et al. [24] found that at a graphite nanoparticle loading of 2 vol%, a nanofluid based on mixture of two synthetic oil showed little enhancement of the heat transfer coefficient, but at a particle loading of 2.5 vol%, there was a 22% increase in the heat transfer coefficient at a temperature of 50°C over a Re of 5 to 110. As the temperature increased to 70°C, the enhancement of heat transfer coefficient decreased slightly to 15%. The researchers postulated that this decrease in enhancement could be due either to an increased alignment in the particles at higher temperatures which would lead to lower viscosities or a depletion of particles near the wall. Results discussed above are summarized in Table 2.

Table 2 Heat transfer enhancements

Author/Year	Nanofluid	Particle size (nm)	Concentration (vol%)	Enhancement ratio
Putra et al./2003[18]	Al_2O_3/water (L/D=0.5)	131.2	1.00	0.85 – 1.02
		131.2	4.00	0.70 – 0.85
	Al_2O_3/water (L/D=1.0)	131.2	1.00	0.87 – 1.04
		131.2	1.00	0.63 – 0.82
Xuan et al./2003[19]	Cu/water	<100	0.30	0.99 – 1.05
		<100	0.50	1.01 – 1.08
		<100	0.80	1.07 – 1.13
		<100	1.00	1.13 – 1.15
		<100	1.20	1.14 – 1.21
		<100	1.50	1.23 – 1.27
		<100	2.00	1.25 – 1.35
Wen et al./2004[11]	Al_2O_3/water (x/D=63)	42	0.60	1.04 – 1.12
		42	1.00	1.09 – 1.22
		42	1.60	1.25 – 1.38
	Al_2O_3/water (x/D=116)	42	0.60	1.10 – 1.20
		42	1.00	1.12 – 1.20
		42	1.60	1.26 – 1.35
Yang et al./2005[24]	Graphite/ transmission Fluid (50°C)	1000-2000x2	0.77	0.97 – 1.02
		0-40	0.97	1.21 – 1.31
	Graphite/ transmission Fluid (70°C)	1000-2000x2	0.77	0.97 – 1.03
		0-40	0.97	1.14 – 1.29
	Graphite/mixture of two syn. oils (50°C)	1000-2000x2	0.75	0.99 – 1.05
		0-40	0.75	1.01 – 1.05
	Graphite/mixture of two syn. oils (70°C)	1000-2000x2	0.75	1.05 – 1.15
		0-40	0.75	1.05 – 1.13
Choi et al./2008[55]	Al_2O_3 (sphere)/ pure oil	13	0.5	1.01 – 1.03
	Al_2O_3 (fiber)/pure oil	2 x 20-200	0.5	1.14 – 1.17
	AlN/pure oil	50	0.5	1.24 – 1.29

2.2 Results based on flow conditions

The study of the enhancement heat transfer coefficients of nanofluids is often divided by fluid conditions including laminar flow, turbulent flow, and pool boiling. Laminar flow refers to flow with Reynolds number less than 2100 and turbulent flow refers to flow with Reynolds number larger than 4000. Flow with Reynolds number between 2100 and 4000 is called transition flow.

Several studies have been conducted in the laminar flow regime. Wen et al. [11] studied Al_2O_3/water nanofluids in a Reynolds number range from 700 to 1950. Enhancement of the heat transfer coefficient was observed for nanofluids with various particle concentrations. But there was no observed influence of the Reynolds number as the enhancement ratio stayed close to constant in this laminar flow regime. Heris et al. [56] also used Al_2O_3/water to measure the enhancement of the heat transfer coefficient. At particle volume concentrations below 2%, the heat transfer enhancement is comparable with Wen's work with the enhancement rising even higher as particle volume concentration increases above 2%. This trend is consistent with the increase of thermal conductivity based on increased particle volume concentration, but the heat transfer enhancement is larger than the thermal conductivity enhancement. The results for flow at the lower particle volume concentrations are in the same range as Wen's results, showing little effect of the Reynolds number heat transfer enhancement. However, at volume concentrations above 2%, an increase in Reynolds number is seen to have a positive effect on heat transfer enhancement. Nanofluid heat transfer results for multi-walled carbon nanotubes (MWCNTs) in water show a very high heat transfer enhancement [49] at

a Re number range of 800-1200. In this range of intermediate laminar flow, heat transfer enhancement ratio rises rapidly at the highest values of Reynolds number.

For oil-based nanofluids, studies covered only a small part of the Reynolds number range. Results for graphite particles in automotive transmission fluid show no enhancement at relatively lower particle volume concentrations, while increasing to a 25% enhancement at a relatively higher volume concentration of approximately 1%. In synthetic oil mixtures, the trends are much the same where nanofluids made from different sources of graphite particles were used. All experiments covered a Reynolds number range from 10 to 110 and no effect of Reynolds number on the enhancement of heat transfer coefficient was observed.

The turbulent flow regime is hard to reach due to limitations of lab equipments. Therefore, very few research groups were able to study enhancement of heat transfer coefficient in the turbulent flow regime. Pak and Cho measured heat transfer performance of Al_2O_3/water and TiO_2/water nanofluids in the turbulent flow regime. There is little or no effect of Reynolds number on the heat transfer enhancement. Similar conclusions can be made from Xuan and Li's work [19], where Cu/water nanofluids were used.

Some researchers have used a correlation calculation to compare the enhancement of heat transfer to the enhancement of thermal conductivity for turbulent flow. One can predict the Nusselt number of the base fluid with reasonable accuracy by using a long-standing heat transfer correlation for turbulent flow, like the Dittus-Boelter correlation [57]. Then, using the increased thermal conductivity of the nanofluid in the same Dittus-Boelter correlation as a rough simulation of the nanofluid, one can predict a Nusselt number for the nanofluid. In so doing, the Dittus-Boelter correlation often

underpredicts the measured nanofluid Nusselt number. For heated turbulent flow, the base fluid Nusselt number is proportional to the thermal conductivity to the 0.6 power. Thus, even if the enhancement ratios for thermal conductivity and Nusselt number were the same, the actual heat transfer would exceed the prediction by the heat transfer correlation because the thermal conductivity in it appears to only the 0.6 power. Some authors have attributed the increased heat transfer enhancement above the thermal conductivity enhancement to particle-fluid interactions.

Long-standing heat transfer correlations for turbulent flow heat transfer in base fluids have also been used as the basis of the development of heat transfer models in turbulently flowing nanofluids, although the effort has been very limited. Typically, nanofluid heat transfer predictive equations were modified from traditional equations such as the Dittus-Boelter equation or the Gnielinski equation [58] with empirical parameters added. Such equations are only valid for specific nanofluids in small parameter ranges. More experimental and theoretical studies are needed before general models can be developed.

It is worth mentioning that the data for both laminar and turbulent flow are not enough to draw the conclusion that the enhancement of heat transfer is a function of particle size. The thermal conductivity enhancement had been seen to increase with particle size, but more experimental data are needed to establish such a trend with regard to the enhancement of heat transfer coefficient.

Table 3 Pool boiling heat transfer enhancements

Author/Year	Nanofluid	Particle size (nm)	Concentration (vol%)	Enhancement ratio
Das et al./2003[59]	Al_2O_3/water (smooth cylindrical surface)	38	1.00	0.72 – 0.80
		38	2.00	0.69 – 0.76
		38	4.00	0.60 – 0.65
	Al_2O_3/water (rough cylindrical surface)	38	1.00	0.65 – 0.69
		38	2.00	0.64 – 0.69
		38	4.00	0.57 – 0.60
Das et al./2003[60]	Al_2O_3/water (4mm tube)	58.4	1.00	0.79 – 0.85
		58.4	4.00	0.46 – 0.55
	Al_2O_3/water (6.5mm tube)	58.4	1.00	0.71 – 0.79
		58.4	4.00	0.64 – 0.71
	Al_2O_3/water (20mm tube)	58.4	1.00	0.83 – 0.85
		58.4	4.00	0.64 – 0.70
Bang et al./2005[61]	Al_2O_3/water	47	0.50	0.75 – 0.92
		47	1.00	0.78 – 0.89
		47	2.00	0.70 – 0.83
		47	4.00	0.68 – 0.83
Wen et al./2005[62]	Al_2O_3/water	10 - 50	0.08	1.06 – 1.22
		10 - 50	0.18	1.12 – 1.29
		10 - 50	0.24	1.19 – 1.36
		10 - 50	0.32	1.24 – 1.40

A few experiments were focused on pool boiling for nanofluids. From Das and colleagues' work [44], the enhancement ratio decreases as particle volume concentration increases, in contrast to the enhancement of thermal conductivity results. The author noted particle coating on the heat surfaces, and concluded that the poor nanofluid performance was due to particles coming out of suspension and depositing on the heated surfaces. The experimental parameters used by Bang et al. [61] are in the same range as Das and colleagues' work, and so is the heat transfer enhancement ratio. The addition of nanoparticles decreased the heat transfer rate, and the degradation became worse as

particle volume concentration was increased. However, at very low particle volume concentrations (less than 0.32%), Wen et al.'s study [62] shows heat transfer enhancement for pool boiling of this nanofluid. Also, the usual trend is observed in their data, wherein the heat transfer enhancement increases with increased particle volume concentration up to 0.32%. Clearly, there is a need for more experimental work in this area. A summary of results is shown in Table 3.

3. Theoretical Modeling of Nanofluids

3.1. Correlations of thermal conductivity

For theoretical modeling purposes, we can define a nanofluid as a mixture of two parts. One is a continuous base fluid and the other is the discontinuous solid nanoparticles. Because the microstructures of nanofluids are not completely known, it is impossible to effectively determine physical properties including heat transfer coefficient. Experimenters usually have to make some reasonable assumptions on the microstructures of the mixtures to better estimate those properties.

In this project, the main focus was on determining heat transfer coefficient correlations that could fit the experimental data obtained. Since most correlations use dimensionless number called Nusselt number *Nu* to represent heat transfer performance, which is a function of both thermal conductivity and heat transfer coefficient, we need to predict thermal conductivity of nanofluids used in this project based on developed correlations to obtain the heat transfer coefficient.

Maxwell was the first to investigate conduction through suspended particles. He developed the Maxwell equation [31] considering a very dilute suspension of spherical

particles by ignoring the interactions between particles, which is defined as:

$$k_e = k_m + 3\nu_p \frac{k_p - k_m}{2k_m + k_p - \nu_p(k_p - k_m)} k_m \tag{2}$$

where k_m is the thermal conductivity of a matrix in which all the spherical particles are embedded in and k_p is the thermal conductivity of spherical particles. Note that this equation is only a first-order approximation and is applicable only to mixtures low particle concentrations.

Hamilton and Crosser [32] established a correlation to estimate effective thermal conductivity, k_{eff}, of macroscopic solid-liquid mixtures, which is defined in the following equation:

$$\frac{k_{eff}}{k_f} = \frac{k_p + (n-1)k_f - (n-1)\Phi(k_f - k_p)}{k_p + (n-1)k_f + \Phi(k_f - k_p)} \tag{3}$$

where k_f and k_p are the thermal conductivities of the fluid and particles, respectively. Φ is the volume fraction of the particles, and n is the empirical shape factor. Large aspect ratio particles such as carbon nanotubes (CNT) have high values of n, which means they have great potential for enhancement of thermal conductivity since the result of the right side of Eq.(3) will increase with increasing n.

A number of correlations have been developed based on the Maxwell equation. Various factors including particle shape, distribution, and particle shell structure are taken into consideration in developing these correlations. To improve the predictive ability of these correlations, mechanisms of thermal conductivity have been formulated specifically for nanoscale application to account for the effects of nanoparticle Brownian motion, the nanoparticle-matrix interfacial layer, and nanoparticle clustering/aggregation.

Yu and Choi [34] introduced another formula for calculating thermal conductivity

of nanofluids, which is expressed in the following equation:

$$k_{eff} = \left[\frac{k_p+2k_w+2(k_p-k_w)(1+\beta)^3\phi}{k_p+2k_w-(k_p-k_w)(1+\beta)^3\phi}\right]k_w \quad (4)$$

where β is the ratio of the nanolayer thickness to the original particle radius. In a nanoparticle-in-liquid suspension, the nanolayer is considered to be a solid-like layer around the nanoparticles. Normally β=0.1 is used to calculate the thermal conductivity of nanofluid. This modification of the Maxwell model considered the impact of the nanolayer and is a good fit for smaller size nanoparticle based nanofluids.

Murshed et al. [33] established the Bruggeman model for calculating the thermal conductivity of nanofluids, which is defined as:

$$k_{eff} = \frac{1}{4}[(3\phi-1)k_p + (2-3\phi)k_w] + \frac{k_w}{4}\sqrt{\Delta} \quad (5)$$

$$\Delta = [(3\phi-1)^2(k_p/k_w)^2 + (2-3\phi)^2 + 2(2+9\phi-9\phi^2)(k_p/k_w)] \quad (6)$$

By taking particle agglomeration into consideration, Timofeeva et al. [63] introduced the effective medium theory for computing thermal conductivity of nanofluids, which is expressed as follows:

$$k_{eff} = [1+3\phi]k_w \quad (7)$$

In summary, most of the correlations developed based on the physical mechanisms of the nanoparticle-matrix interfacial layer effect, nanoparticle Brownian motion effect, or nanoparticle aggregate effect usually involve some empirical parameters. Those parameters must be obtained before they can be used to predict thermal conductivity of a nanofluid. This requirement greatly limits the use of those correlations. Furthermore, instead of one single mechanism, the combined effect of two or more mechanisms may contribute to the enhancement of thermal conductivity. This will be an

important issue in future research on physical mechanisms of the enhancement of thermal conductivity of nanofluids.

3.2 Correlations of heat transfer coefficient

Theoretical models for heat transfer coefficient calculation are usually presented using Nusselt number *Nu*. In general, *Nu* of a nanofluid may be expressed as follows:

$$Nu_{nf} = f\left\{Re_{nf}, Pr_{nf}, \frac{k_d}{k_f}, \frac{(\rho c_p)_d}{(\rho c_p)_f}, \Phi, dimensions\ and\ shape\ of\ particles\right\} \tag{8}$$

where Re_{nf} is the Reynolds number of the nanofluid, Pr_{nf} is the Prandtl number of the nanofluid, k_d is the thermal conductivity of the nanoparticle, k_f is the thermal conductivity of the base fluid, $(\rho c_p)_d$ is the heat capacity of the nanoparticle, $(\rho c_p)_f$ is the heat capacity of the base fluid, and Φ is the volume fraction of the nanofluid.

Considering that nanofluids consist of small size particles and low concentrations in base fluids, some early studies of correlations for homogenous liquid systems might be applied to determine the *Nu* for nanofluids. A commonly used correlation is the Dittus–Boelter heat transfer correlation [64] for fluids in turbulent flow. This correlation is applicable when forced convection is the only mode of heat transfer; i.e., there is no boiling, condensation, significant radiation, etc. It is defined as:

$$Nu = 0.023 Re^{0.8} Pr^{0.4} \tag{9}$$

Another correlation for convective heat transfer of laminar flow in tubes is the Seider-Tate equation [65],

$$Nu = 1.86 Re^{1/3} Pr^{1/3} \left(\frac{D}{L}\right)^{1/3} \left(\frac{\mu_b}{\mu_w}\right)^{0.14} \tag{10}$$

where $(\frac{\mu_b}{\mu_w})^{0.14}$ is the radial variation of fluid properties and natural convection effect. μ_b and μ_w are the dynamic viscosity at the bulk fluid temperature and dynamic viscosity at boundary surface temperature, respectively. This equation can be more accurate compared to Dittus–Boelter equation as it takes into account the change in viscosity due to temperature change between the bulk fluid average temperature and the heat transfer surface temperature.

The Oliver correlation [66] for horizontal flow in tubes is:

$$Nu\left(\frac{\mu_w}{\mu_b}\right)^{0.14} = 1.75[Gz + 5.6\,x\,10^{-4}(Gr \cdot Pr \cdot L/D)^{0.70}]^{1/3} \quad (11)$$

where Gz is the Graetz number, $Gz = \frac{WCp}{kL}$, Gr is the Grashof number. The Eubank and Proctor correlation [67] for laminar flow in horizontal tube is:

$$Nu\left(\frac{\mu_w}{\mu_b}\right)^{0.14} = 1.75[Gz + 12.6(Gr \cdot Pr \cdot D/L)^{0.40}]^{1/3} \quad (12)$$

For both Eq. (11) and (12), the first term Gz is contributed by the forced convection mechanism, and the second term which includes Grashof number, Prandtl number, and the ratio of L/D are intended to account for the effect of the natural convection. Therefore, we can estimate the relation between those variables which divides the forced convection from the natural convection regime based on the magnitude of the two terms.

The modeling of heat transfer coefficients of nanofluids is gaining attention from researchers but it is still at its early stage since most the correlations developed are modified from those traditional correlations discussed above. More extensive study on the modeling of heat transfer coefficient and more experimental data are needed in future study. The theoretical modeling of heat transfer coefficient of nanofluids is discussed later in this dissertation.

CHAPTER III

METHODS AND MATERIALS

1. Preparation of Nanofluids

Three different particle sizes (25nm, 40-60nm, 60-80nm) of spherical shaped copper nanopowders (purity: 99.9%) were obtained from Skyspring Nanomaterials (Houston, Texas, USA). 100% Poly-alpha-olefin (PAO) formulated motor oil was purchased from Amsoil Inc. (Superior, Wisconsin, USA). 1-Dodecanethiol, was obtained from Alfa Aesar (Ward Hill, Massachusetts, USA) and used as a surfactant. Each size of

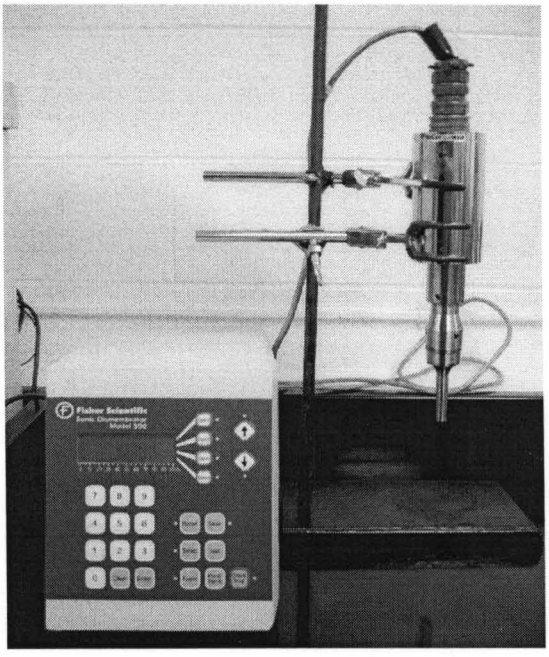

Fig 3.1 Model 500 Sonic Dismembrator.

copper nanoparticles were suspended in the PAO oil at weight percentages of 0.25, 1.0, 1.5, and 2.0 using a Model 500 Sonic Dismembrator from Fisher Scientific (shown in Figure 3.1) that is able to deliver up to 400 watts of power. Due to the lack of functional groups in these very hydrophobic molecules, special surfactants are needed to disperse nanoparticles uniformly. In this work, dodecanethiol was added to help stabilize fluid suspension and the amount of dodecanethiol was carefully controlled based on the total available surface area of the copper nanoparticles. The hydrophilic groups (heads) of the surfactant are attached to the surface of copper nanoparticles by physical forces while their hydrophobic groups (tails) maintain favorable contact with oil. Each sample is sonicated for 60min. All the samples were kept at least 48 hours after sonicating and shaken well before further testing. All experimental fluids are list in Table 4. Notice that only three concentrations of nanofluids were made for 40-60nm Cu nanoparticles due to the limited amount of 40-60nm Cu nanopowder provided.

Table 4 Experimental fluids

	Nanoparticle	Base fluid	Particle Loading
Cu25-1	25nm Cu	PAO oil	0.25 wt%
Cu25-2	25nm Cu	PAO oil	1.0 wt%
Cu25-3	25nm Cu	PAO oil	1.5 wt%
Cu25-4	25nm Cu	PAO oil	2.0 wt%
Cu40-2	40-60nm Cu	PAO oil	1.0 wt%
Cu40-3	40-60nm Cu	PAO oil	1.5 wt%
Cu40-4	40-60nm Cu	PAO oil	2.0 wt%
Cu60-1	60-80nm Cu	PAO oil	0.25 wt%
Cu60-2	60-80nm Cu	PAO oil	1.0 wt%
Cu60-3	60-80nm Cu	PAO oil	1.5 wt%
Cu60-4	60-80nm Cu	PAO oil	2.0 wt%

2. Experimental Setup

Heat transfer coefficients of prepared base and nanofluids were measured using a lab-built test rig. A schematic of the heat transfer test rig is shown in Figure 3.2. The entire system is made from ¼ inch stock copper tubing and fittings. In the flow system, a copper pipe serving as a reservoir for the nanofluids is capable of holding 2 liters of fluid. The fluid flows from the reservoir through a variable speed gear pump (Grainger 6NY97). The gear pump is sized to cover a wide range of flowrates up to 4.8 gal/min. Based on the properties of the nanofluid, particularly viscosity, the pump will cover a Re range from 50 to 7000. Flowrates are measured using an inline flowmeter connected into an electronic readout. From here the fluid flows through a copper coil held in a hot water bath which can maintain the test fluid at any temperature from room temperature up to 96°C. The fluid then enters the heat exchange section. There are two thermocouples placed in the fluid at both the inlet and outlet of this section. The section itself is formed form ¼ inch high thermal conductivity copper refrigerator tubing. Six type-T thermocouples are attached equidistant along the exterior of the copper tube in this section. The entire heat exchange section is wrapped in heat tape which provides a constant heat flux to the fluid. Two layers of insulation are wrapped around the heating tape to ensure low environmental heat loses within the heat exchange section. Temperatures are monitored in real time using a Labview program designed for the system. The program also provides real time calculation of the heat transfer coefficient based on the fluid properties and flowrates.

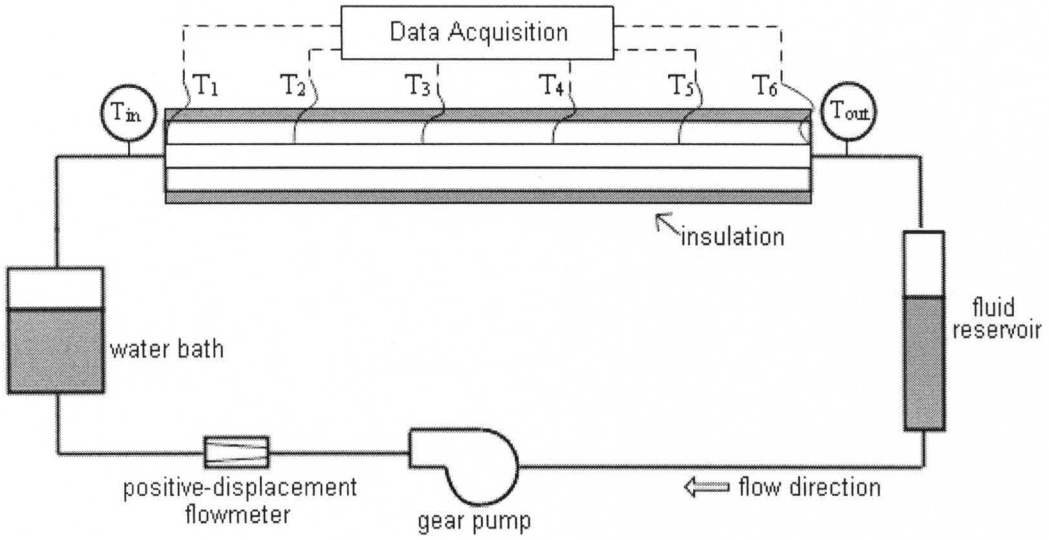

Fig 3.2 Schematic of heat transfer test rig.

The heat transfer measurement procedures are: 1) set up water bath temperature and fill the reservoir with test fluid; 2) Start the pump and circulate the fluid until inlet fluid temperature is stable at the bath temperature; 3) Set up desired flow rate and heating tape power; 4) Record data after the system reaches a steady state (usually in 20-30min). By using control variables including heating power, inlet fluid temperature and fluid flow rate, we conducted a series of heat transfer coefficient tests of base and nanofluids. The ratio of heat transfer coefficient of nanofluid to base fluid was calculated to determine if there was any enhancement.

To prevent coating of the nanoparticles inside the heat transfer test rig, kerosene was used to flush the system twice for 20 minutes between test fluids. For preliminary tests, hexane was used after the kerosene flush to flush the residual kerosene. Due to the low boiling point of hexane (69°C), we could elevate the water bath temperature to evaporate the hexane residual inside the system. Later in this project, we used the base motor oil to flush the residual kerosene.

Heat transfer coefficient is defined by:

$$h = \frac{\Delta Q}{A \cdot \Delta T \cdot \Delta t} \tag{13}$$

where ΔQ is the heat input or heat loss, A is the surface area, ΔT is the temperature difference between solid surface and surrounding fluid area, and Δt is the time period.

In this study, heat transfer coefficient is calculated using the following equation:

$$h = \frac{\frac{(T_{out} - T_{in}) \cdot cp \cdot \rho \cdot q}{\pi \cdot d \cdot L}}{\Delta T} \tag{14}$$

where T_{out} and T_{in} are the outlet and the inlet temperature of the heat exchange section, respectively. c_p is the specific heat of the fluid, ρ is the density of the fluid, q is volumetric flow rate, d and L are the diameter of the tube and total length of the heat exchange section, respectively. ΔT is the average temperature difference between surface of the tube and the fluid.

Another commonly used value is called the Nusselt number Nu. In heat transfer at a boundary (surface) within a fluid, the Nusselt number is the ratio of convective to conductive heat transfer across the boundary. Named after Wilhelm Nusselt, it is a dimensionless number, which is defined as:

$$Nu = \frac{h \cdot D}{k} \tag{1}$$

where h is the heat transfer coefficient, D is the diameter of the tube, and k is thermal conductivity of the fluid.

All collected data were then input into a spreadsheet where the equations for calculating heat transfer coefficient, Reynolds number, and several other parameters. Figure 3.3 shows an example of the spreadsheet for base fluid at a water bath temperature of 40°C.

A	D	E	F	G	H	I	J
current	20-Oct	20-Oct	20-Oct	20-Oct	20-Oct	20-Oct	20-Oct
fluid				base			
% power				50% T=40C			
Flow cc/s	10	20.1	30.1	40	60.1	80	97.9
inlet	40.9	41.16	41.13	41.35	41.98	42.86	44.85
1	47.09	46.92	46.43	46.35	46.6	47.25	48.99
2	59.84	57.84	56.58	55.9	55.52	55.68	56.97
3	61.76	58.84	57.12	56.19	55.56	55.54	56.65
4	65.78	62.11	60.13	58.97	58	57.77	58.8
5	66.4	62.21	59.93	58.61	57.46	57.15	58.12
6	68.84	62.84	59.87	58.12	56.49	55.88	56.96
outlet	60.91	54.1	51.55	50.06	48.44	47.92	49.06
density	873.6	873.6	873.6	873.6	873.6	873.6	873.6
viscosity	0.0246	0.0283	0.0298	0.0305	0.0311	0.0309	0.0291
specific heat	2050	2050	2040	2040	2040	2040	2040
therm cond	0.1396	0.1396	0.1396	0.1396	0.1396	0.1396	0.1396
T_{out}-T_{in}	20.01	12.94	10.42	8.71	6.46	5.06	4.21
avg ΔT	10.67	10.80	10.31	9.97	9.71	9.48	9.12
total heat in	358	466	559	621	692	721	735
avg heat flow	21,802	28,339	34,006	37,775	42,095	43,890	44,688
Nusselt #	70.3	90.2	113.4	130.3	149.0	159.2	168.5
Reynolds #	94.4	164.4	234.0	303.5	447.7	599.9	779.6
Prandtl #	360.6	416.0	435.6	446.3	454.6	451.6	425.3
Graetz #	149.9	301.2	448.9	596.5	896.2	1193.0	1459.9
$\Delta T_{fluid}/\Delta T_{wall}$	1.876	1.198	1.010	0.874	0.665	0.534	0.462
heat transf coeff	2044	2624	3297	3791	4334	4631	4902

Fig 3.3 Spreadsheet for heat transfer coefficient calculation.

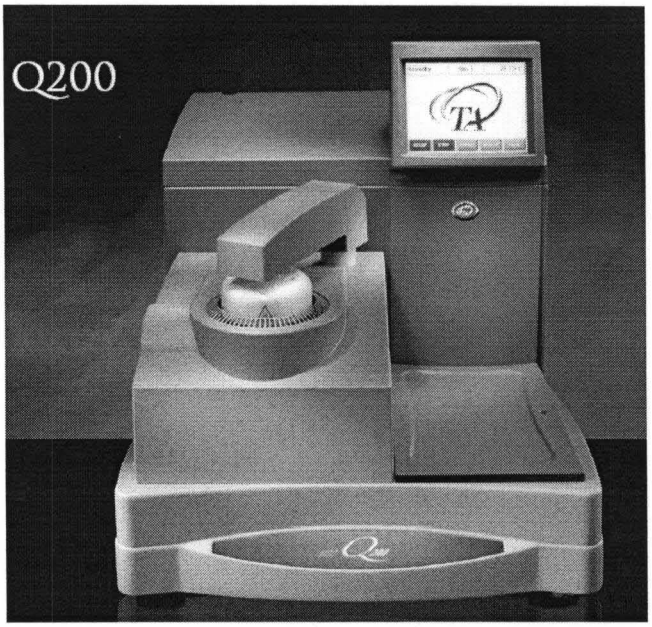

Fig 3.4 TA Instruments Q200 Differential Scanning Calorimeter.

Specific heat was measured by a Q200 Differential Scanning Calorimeter from TA Instruments (shown in Figure 3.4). Differential Scanning Calorimetry (DSC) is a thermoanalytical technique in which the difference in the amount of heat required to increase the temperature of a sample and reference is measured as a function of temperature. Both the sample and reference are maintained at nearly the same temperature throughout the experiment. Generally, the temperature program for a DSC analysis is designed such that the sample holder temperature increases linearly as a function of time. The technique was developed by E.S. Watson and M.J. O'Neill in 1960 [68], and introduced commercially at the 1963 Pittsburgh Conference on Analytical Chemistry and Applied Spectroscopy. The term DSC was coined to describe this instrument which measures energy directly and allows precise measurements of heat capacity [69].

Viscosity was measured by a cone and plate DV-III Digital Rheometer from Brookfield Engineering Laboratories (shown in Figure 3.5). The rheometer uses a calibrated spring to drive a spindle that is immersed in the test fluid. A viscous drag force of the test fluid against the spindle is created due to the rotation of the spindle, which is determined by the deflection of the spring. Spin speed of the spindle was manually controlled so that we were able to measure the test fluid under various shear rates to determine if the corresponding shear stress increased linearly with the increasing shear rate, which is the definition of Newtonian fluid. Identification of the oil based Cu nanofluids as either Newtonian or non-Newtonian fluids is particularly important to this project and will be discussed later.

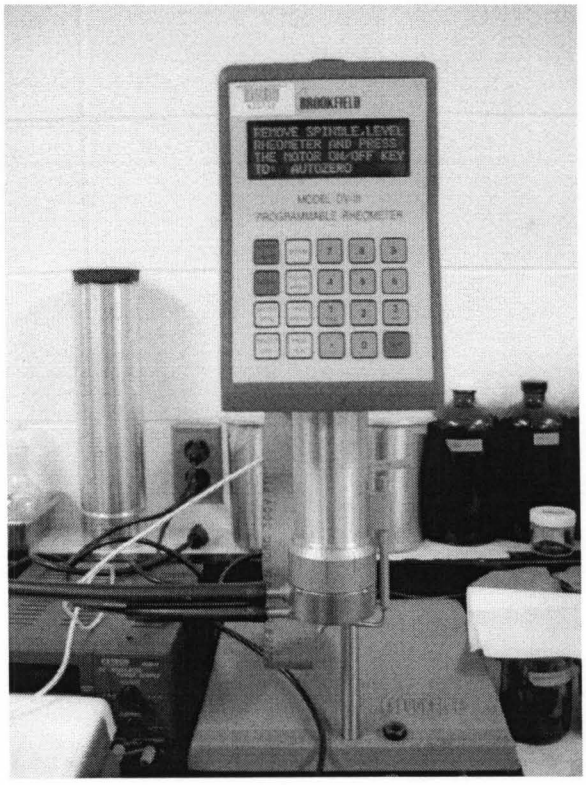

Fig 3.5 Brookfield DV-III Rheometer.

The density of nanofluids is calculated using the correlation proposed by Pak and Cho [17], which is defined as:

$$\rho_{nf} = \phi\rho_p + (1-\phi)\rho_{bf} \tag{15}$$

where ρ_{nf} is the density of the nanofluid, ϕ is the weight fraction of the nanoparticles, and ρ_p and ρ_{bf} are the density of the Cu nanoparticle and base fluid, respectively. Reynolds number was calculated using the following equation:

$$Re = \frac{\rho VL}{\mu} \tag{16}$$

where ρ is the density of the test fluid, V is the mean velocity of the test fluid, L is the diameter of the test tube, and μ is the dynamic viscosity of the fluid.

CHAPTER IV

RESULTS

1. Preliminary Results

For the first two years of this project, we worked with a well-known lubricant manufacturing company to measure the heat transfer coefficient of five samples using a lab-built heat transfer test rig. These samples were oil based nanofluids but the nanoparticles and other additives were unknown. Table 5 shows the code name for each base fluid and its corresponding nanofluid. Results for heat transfer tests are shown in Figure 4.1.1 – 4.1.6. All figures are plotted showing heat transfer coefficient as a function of Reynolds number.

Table 5 Preliminary test fluid samples

	Base fluid	Nanofluid
Base/nano#1	504-250-5B	504-252-7B
Base/nano#2	504-257-2B	504-257-6A
Base/nano#3	7451-120-1	7451-121-1
Base/nano#4	7451-135-3	7451-143-1
Base/nano#5	145-1	145-2

Test fluid T504-250-5B and T504-252-7B (Base and nanofluid#1) were tested

twice in Dec. 2008 (Figure 4.1.1) and in March 2009 (Figure 4.1.2). Each measurement was conducted twice under same conditions to ensure accuracy. Specific heat capacity and viscosity data of the nanofluid are assumed to be the same as the base fluid as specified by the supplier. As is shown in Figure 4.1.1 nanofluid#1 exhibited a higher heat transfer coefficient than base fluid#1. Specifically, at both temperatures, the enhancement in the heat transfer coefficient from the nanofluid as compared to the base fluid increases with increasing in the Re. It should be noted that the maximum Re that can be achieved is related to temperature of the fluid since Re is inversely proportional to viscosity and viscosity decreases with increasing temperature. Consistent results were produced in March 2009 using same base and nanofluid#1 (Figure 4.1.2). Under the same conditions, the nanofluid again showed higher heat transfer coefficient than base fluid#1. However, the enhancement ratio decreased from 1.288 to 1.092 as the Reynolds number is increased at temperature of 80°C.

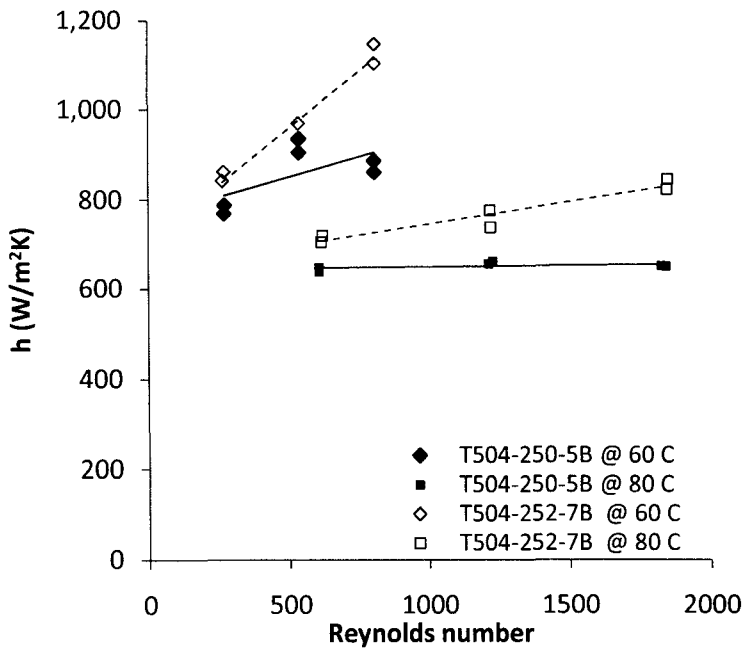

Fig 4.1.1 Heat transfer coefficient as a function of Re for Base/nano#1 (Dec 2008).

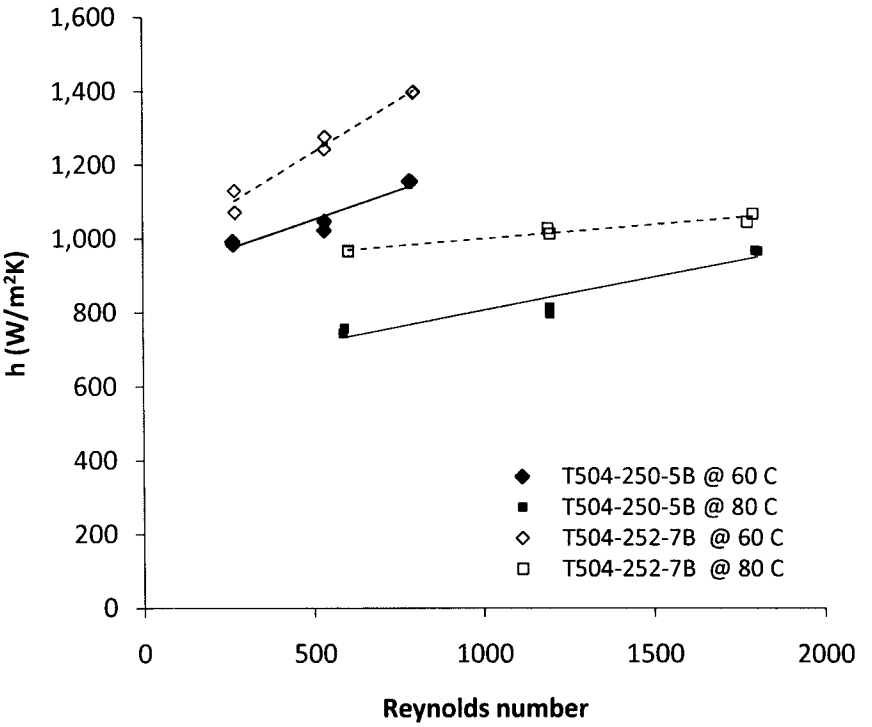

Fig 4.1.2 Heat transfer coefficient as a function of Re for Base/nano#1 (Mar 2009).

Not all the nanofluids showed an enhancement in their heat transfer coefficient when compared to their base fluids. Different additives were added into base fluid#2 (T504-257-6A) to make nanofluid#2 (T504-257-2B). Heat transfer test started in January 2009 and results are plotted in Figure 4.1.3. It can be seen that there is almost no enhancement for nanofluid#2 at both temperatures. Heat transfer coefficient increased linearly with increasing Reynolds number.

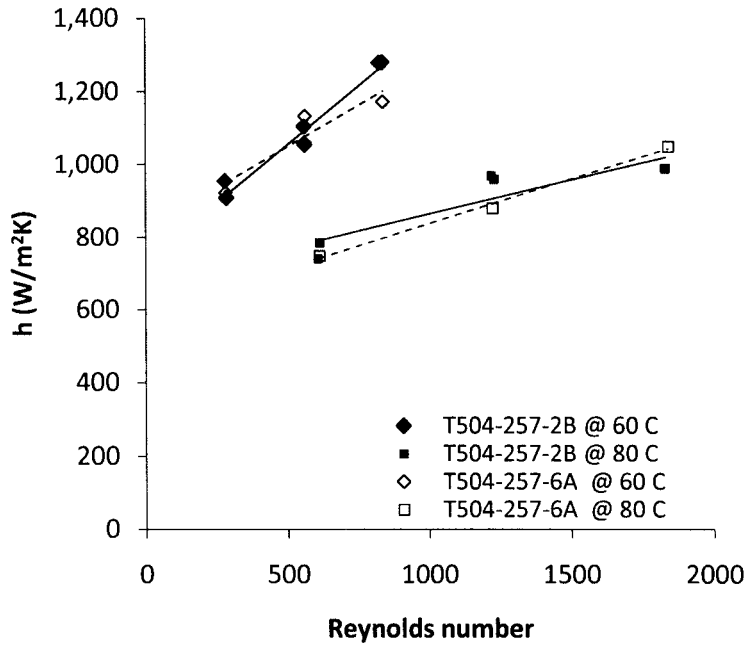

Fig 4.1.3 Heat transfer coefficient as a function of Re for Base/nano#2 (Jan 2009).

After the test of base and nanofluid#2, the heat transfer measurement system was then modified to allow higher temperatures (96°C) to obtain a better approximation of actual engine operating temperatures in an automobile. At the higher operating temperature of 96°C, the Reynolds number would increase significantly due to the decrease in viscosity. Base fluid#3 (C7451-120-1) and its nanofluid (C7451-121-1) were tested at two temperatures (80°C and 96°C) in a Reynolds number in the range of 1000 to 4000, which covered the laminar flow and transition flow regimes. Figure 4.1.4 shows that a small enhancement was observed at fluid temperature of 80°C. At 96°C, the enhancement decreased with the increase of Reynolds number. At a maximum flow rate, the transition flow regime was reached and no enhancement was observed.

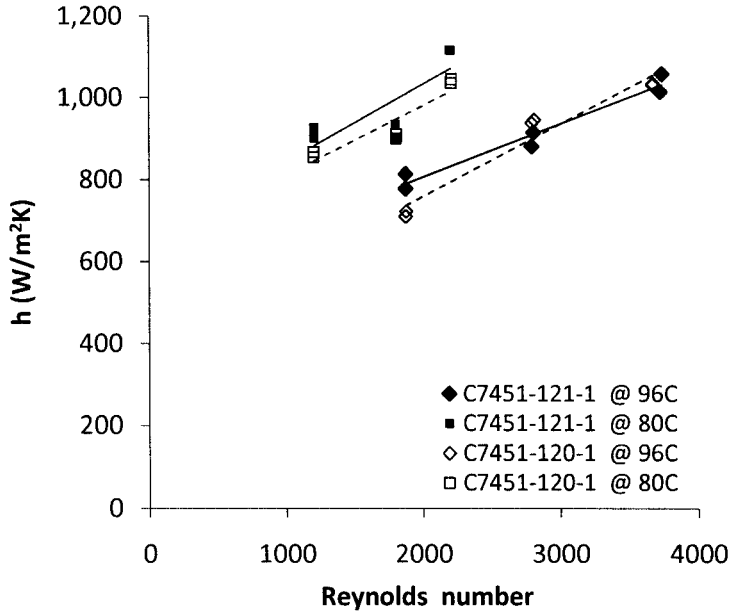

Fig 4.1.4 Heat transfer coefficient as a function of Re for Base/nano#3 (May 2009).

Base and nanofluid#4 (C7451-135-3 and C7451-143-1) and base and nanofluid#5 (C7451-145-1 and C7451-145-2) were tested between June and July of 2009. All fluids were measured at a single temperature of 80°C. It can be seen from Figure 4.1.5 that nanofluids showed a small enhancement over its base fluid at a Reynolds number range of 600 to 2200. This enhancement increased with increasing Reynolds number. Results for base and nanofluids#5 were plotted in Figure 4.1.6. In contrast to base and nanofluid#4, the heat transfer coefficient of nanofluid#5 is consistently lower than base fluid#5.

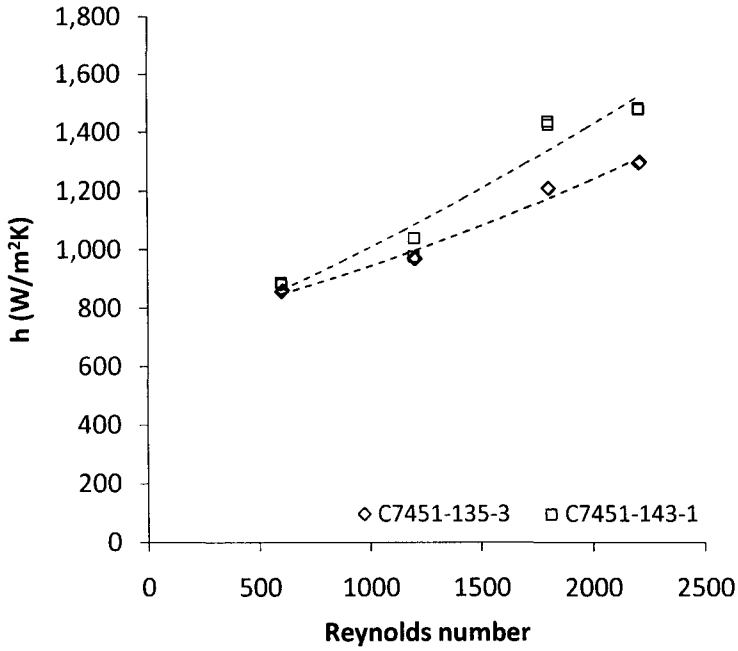

Fig 4.1.5 Heat transfer coefficient as a function of Re for Base/nano#4 (Jun 2009).

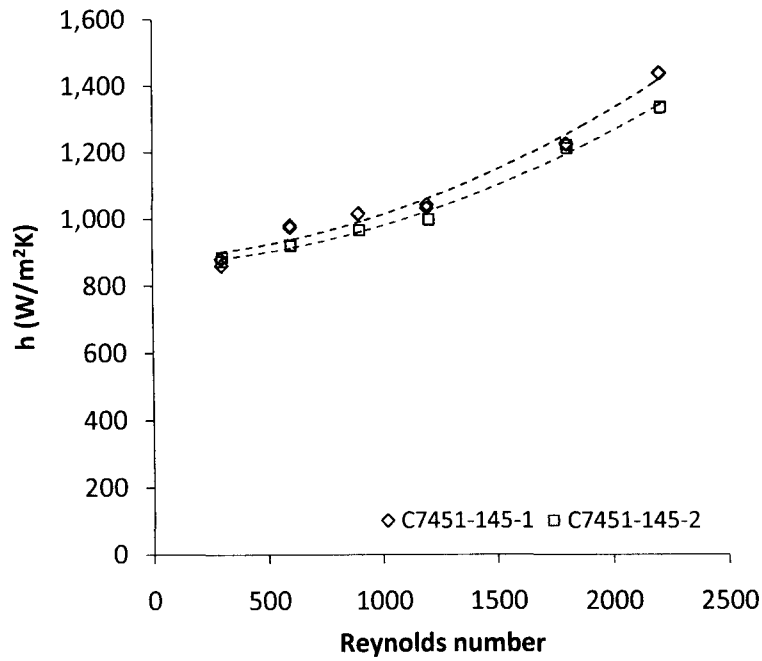

Fig 4.1.6 Heat transfer coefficient as a function of Re for Base/nano#5 (July 2009).

While heat transfer measurements for nanofluids and base oils are reproducible within a single measurement session, there seems to be a longer term trend of decreasing values over a period of several weeks. This trend can be seen in Figure 4.1.7 and Figure 4.1.8 which show four measurements at two temperatures for nanofluid#3 (C7451-121-1) and its base fluid#3 (C7451-120-1) from March 4th to May 18th at a temperature of 95°C. As the fluid ages, the measured trends of the heat transfer coefficient increasing with Re are consistent. However the absolute values of the heat transfer coefficient declines steadily.

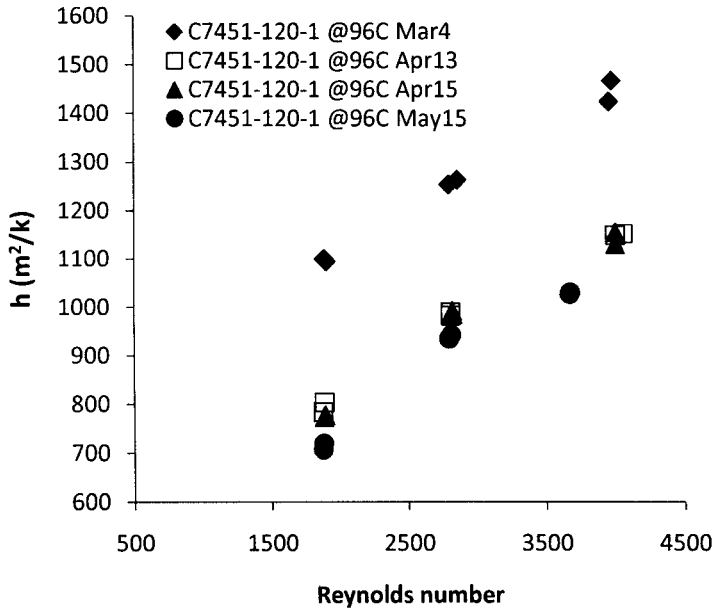

Fig 4.1.7 Measured heat transfer values for base fluid #3 decreases over a ten week period.

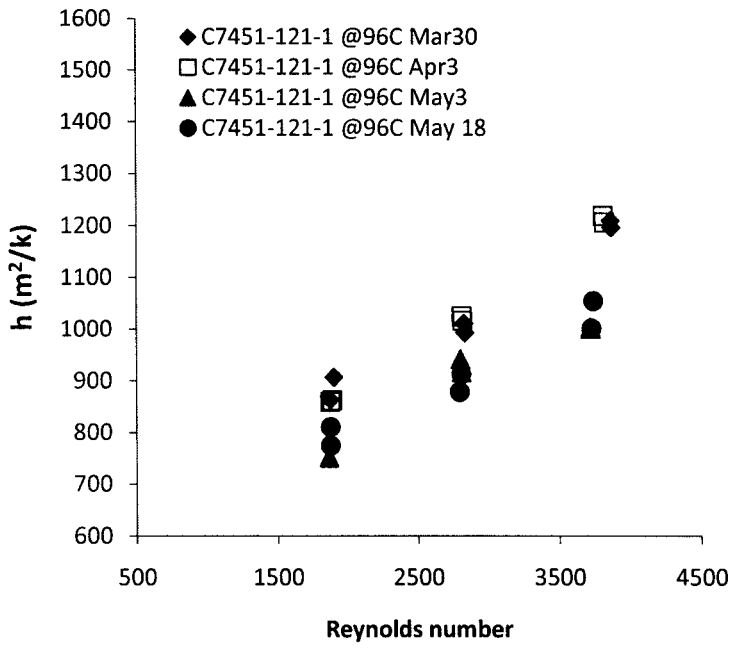

Fig 4.1.8 Measured heat transfer values for nanofluid#3 decreases over a ten week period.

2. Specific Heat Test Results

Specific heat measurements for all copper nanoparticle based nanofluids and base fluids were conducted to ensure accuracy in the calculation of the heat transfer coefficient. Heat flow increase as the increasing temperature (30°C to 90°C) was measured using DSC. Specific heat is shown to increase linearly with rising temperature. The base fluid shows the highest specific heat value. As weight fraction of nanoparticles is increased, the value of specific heat of nanofluid decreases. Results are plotted in Figure 4.2.1 – 4.2.3. The last number (-1, -2, -3, -4) on the name of each nanofluid represents its weight percentage (0.25, 1.0, 1.5, 2.0).

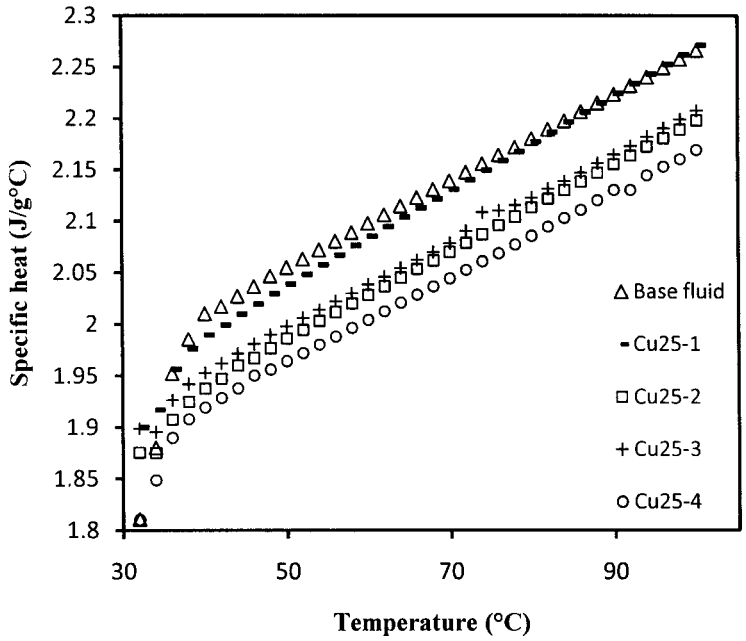

Fig 4.2.1 Specific heat test for Cu25 nanofluids.

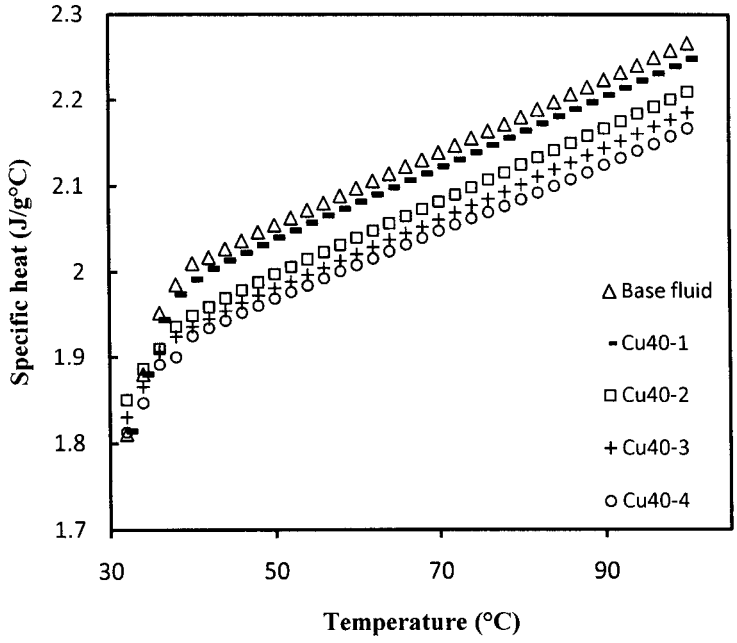

Fig 4.2.2 Specific heat test for Cu40 nanofluids.

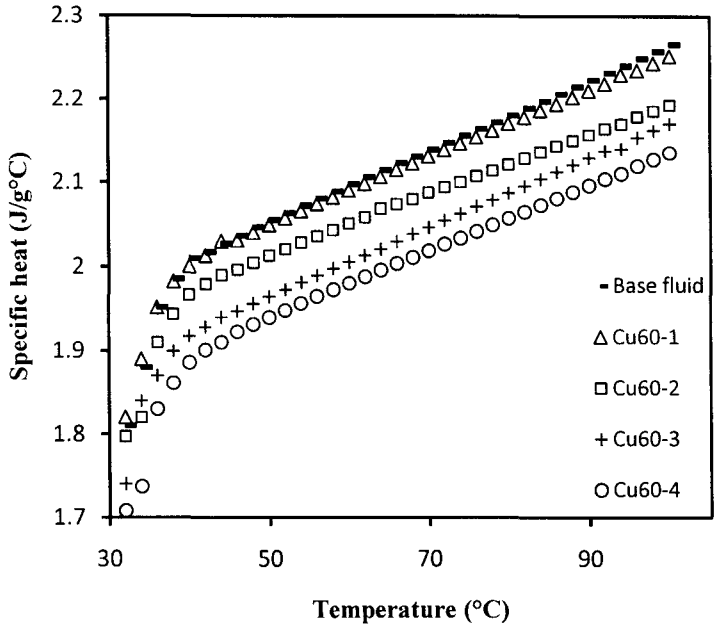

Fig 4.2.3 Specific heat test for Cu60 nanofluids.

3. Viscosity Test Results

Viscosities of base and nanofluids were measured using a cone and plate Brookfield DV-III Rheometer at a temperature range from 30°C to 90°C. Results for base and nanofluids with weight fraction of 2.0% are shown in Figure 4.3.1 – 4.3.4. Viscosity is independent of shear rate for all test fluids which indicates a Newtonian behavior based on Newton's law of viscosity.

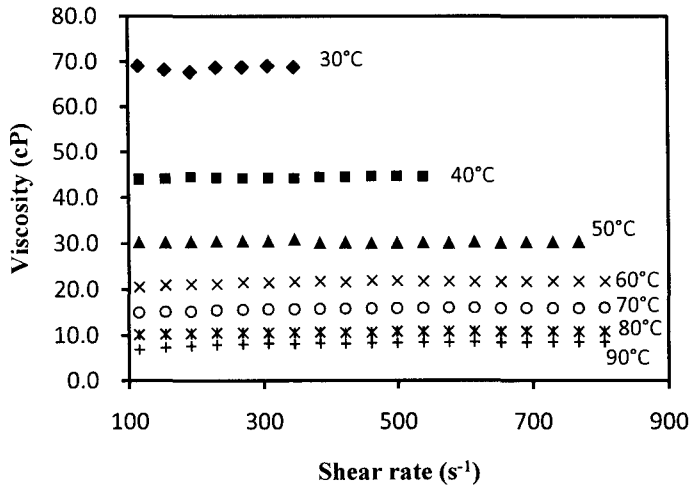

Fig 4.3.1 Viscosity test for base fluid at various temperatures.

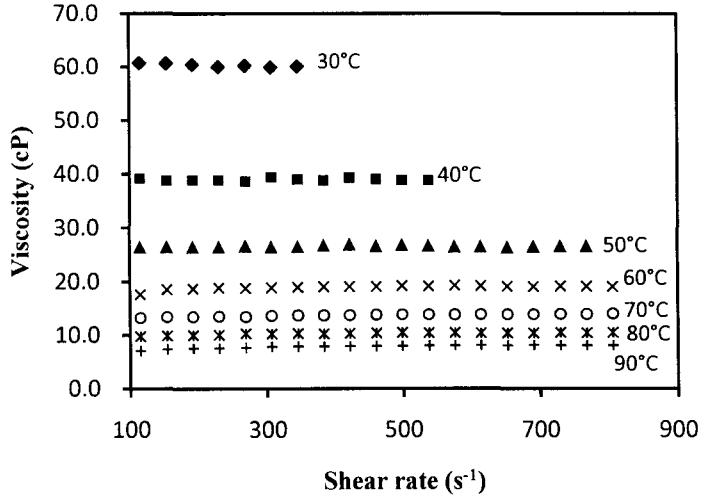

Fig 4.3.2 Viscosity test for Cu25-4 nanofluid at various temperatures.

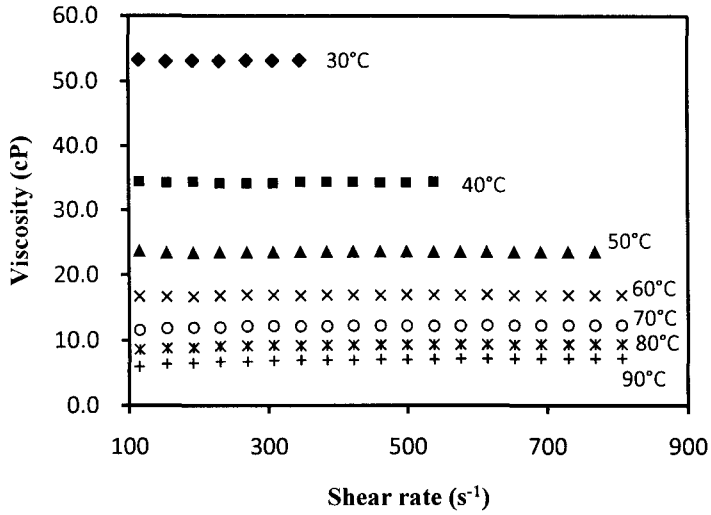

Fig 4.3.3 Viscosity test for Cu40-4 nanofluid at various temperatures.

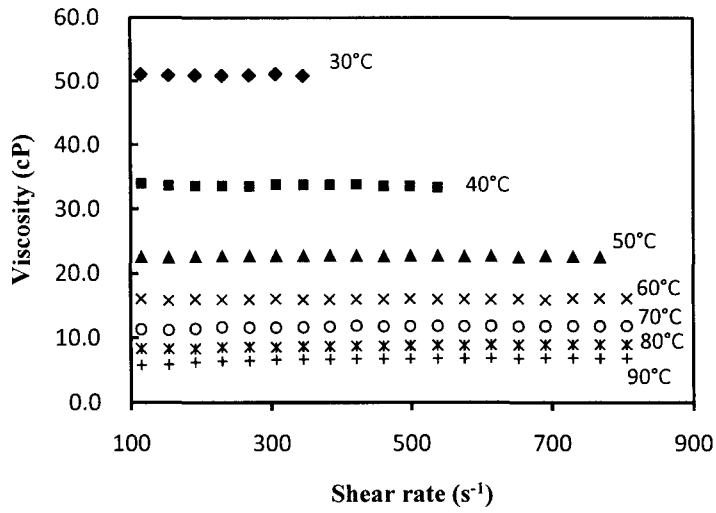

Fig 4.3.4 Viscosity test for Cu60-4 nanofluid at various temperatures.

4. Heat Transfer Coefficient Test Results

After viscosity and specific heat test, heat transfer measurements were started.

Two liters of test fluid were made and added into the heat transfer test rig. Each fluid was tested at various flow rates and temperatures using the procedure discussed earlier. Each measurement was conducted twice under the same flow conditions to ensure repeatability. Some of these results are shown below in Figure 4.4.1.1 – 4.4.3.5. Complete results can be seen in Appendix C. All measurements for base and nanofluids show increasing heat transfer coefficient as both the flow rate and Reynolds number increases.

4.1 25nm Cu nanofluids (Cu25)

Four weight percentages (0.25, 1.0, 1.5, 2.0) of Cu25 nanofluids were tested. Results of heat transfer coefficient measurement for three fluid temperatures are shown in Figure 4.4.1.1. – 4.4.1.3.

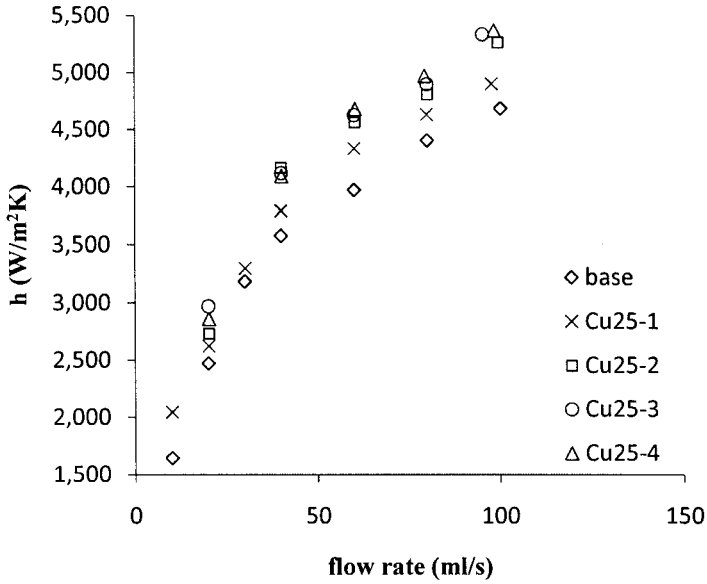

Fig 4.4.1.1 Heat transfer coefficient (h) as a function of flow rate at 40°C.

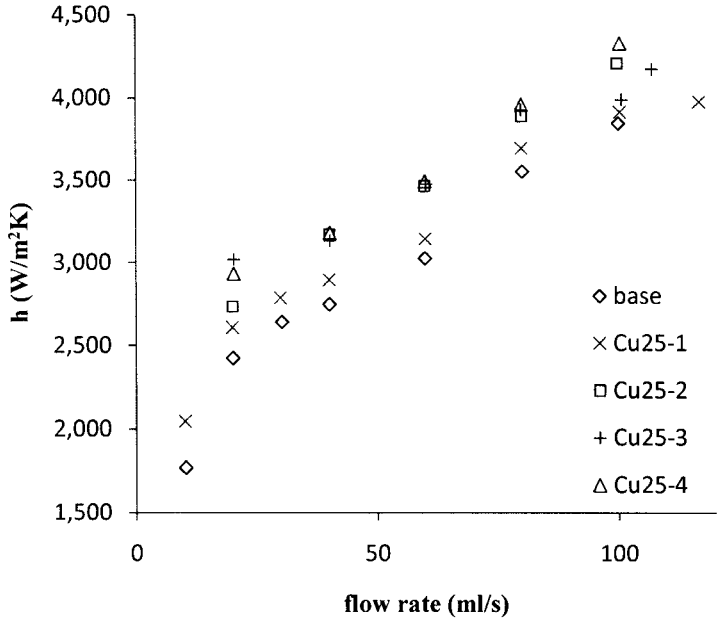

Fig 4.4.1.2 Heat transfer coefficient (h) as a function of flow rate at 65°C.

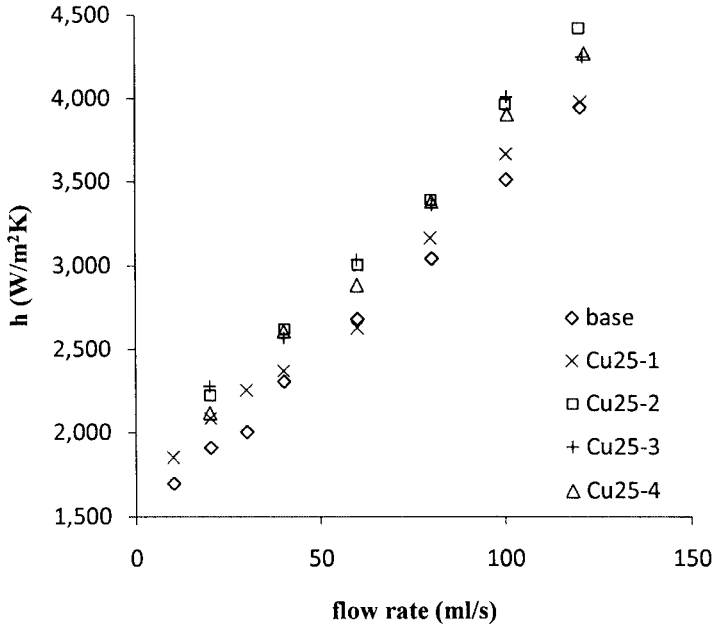

Fig 4.4.1.3 Heat transfer coefficient (h) as a function of flow rate at 90°C.

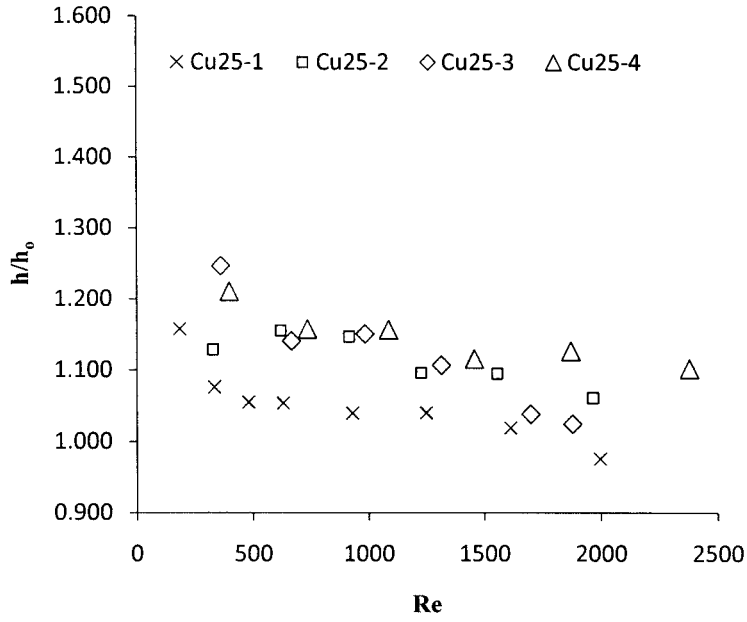

Fig 4.4.1.4 Enhancement ratio (h/h_0) as a function of Reynolds number (Re) at 65°C.

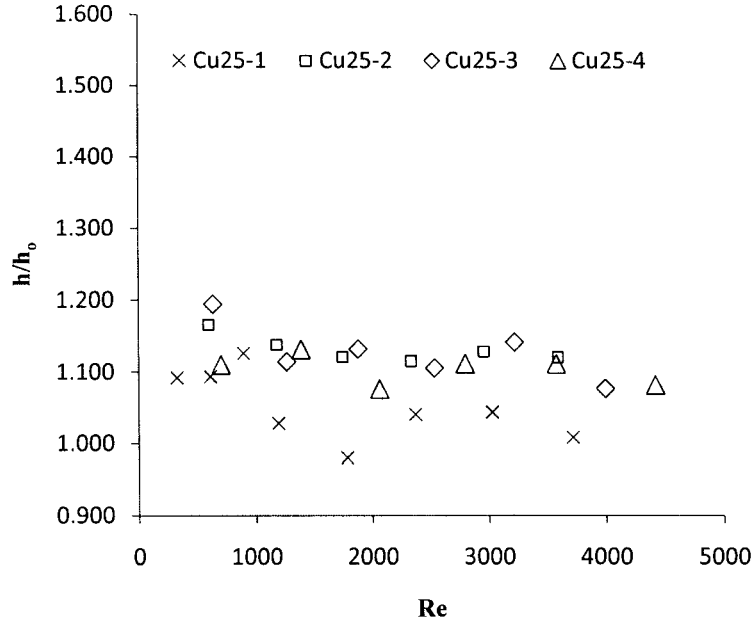

Fig 4.4.1.5 Enhancement ratio (h/h_0) as a function of Reynolds number (Re) at 90°C.

Based on these results, the enhancement ratio of nanofluid to base fluid h/h_0 are calculated. These results are presented in Figure 4.4.1.4 and Figure 4.4.1.5. The maximum enhancement of 25% is found for Cu25-3 at an inlet fluid temperature of 65°C and a Reynolds number of around 400.

4.2 40-60nm Cu nanofluids (Cu40)

Only three weight percentages (1.0, 1.5, 2.0) of Cu40 nanofluids were made and tested due to the limit supply of 40nm nanoparticles. Results are shown in Figures 4.4.2.1. – 4.4.2.6. A maximum enhancement of 16.4% is obtained for Cu40-3 nanofluids at 40°C.

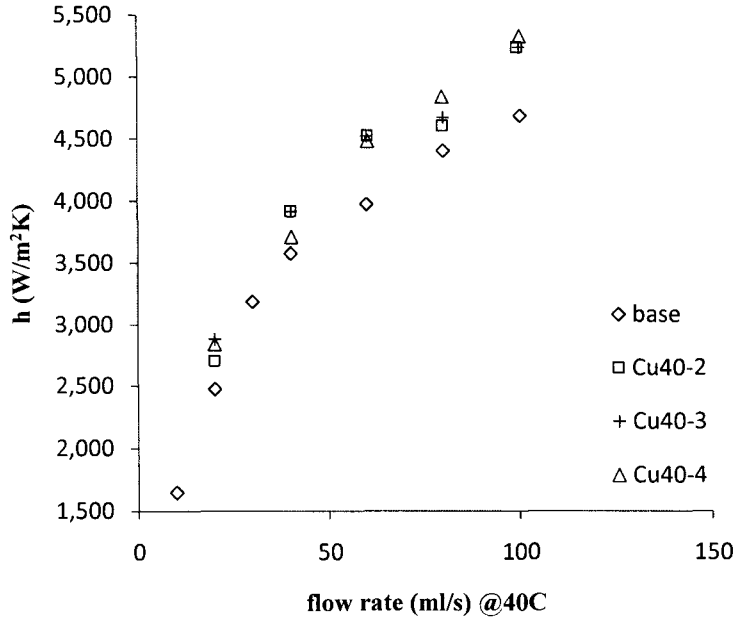

Fig 4.4.2.1 Heat transfer coefficient (h) as a function of flow rate at 40°C.

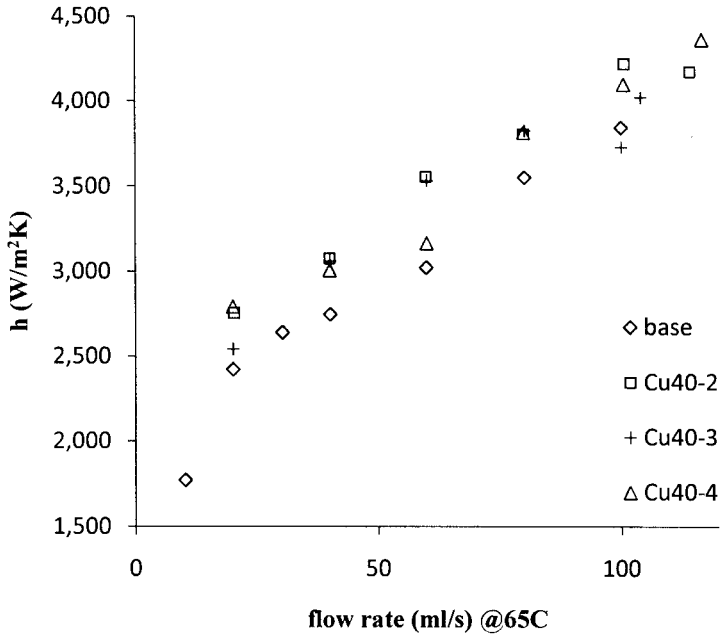

Fig 4.4.2.2 Heat transfer coefficient (h) as a function of flow rate at 65°C.

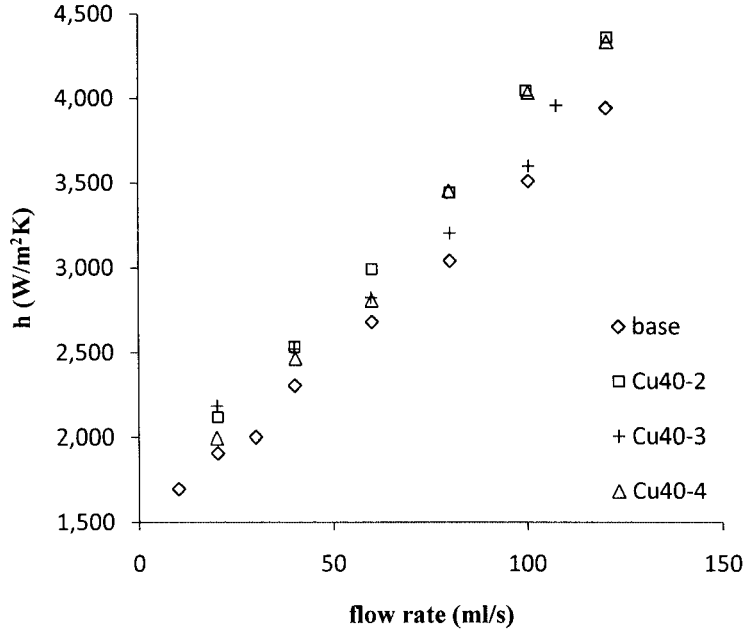

Fig 4.4.2.3 Heat transfer coefficient (h) as a function of flow rate at 90°C.

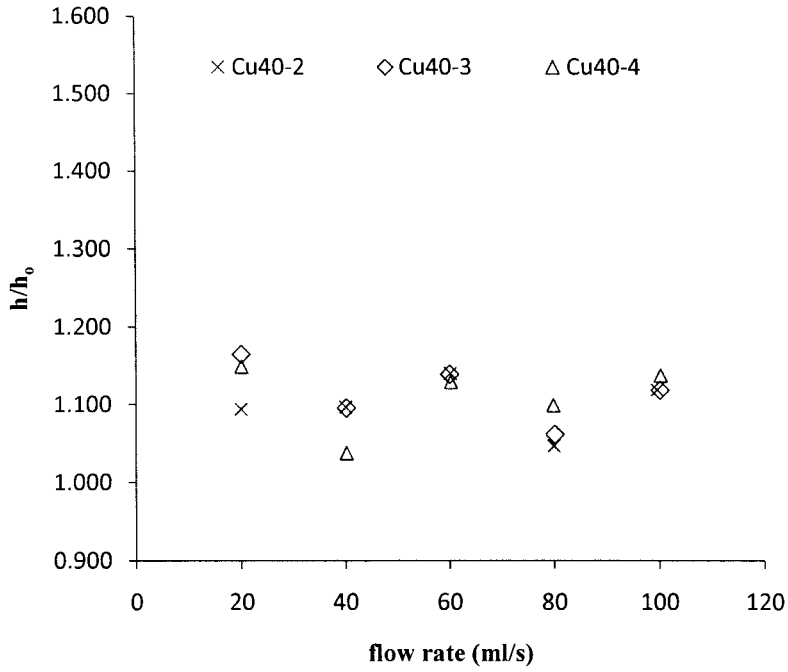

Fig 4.4.2.4 Enhancement ratio (h/h_0) as a function of Reynolds number (Re) at 40°C.

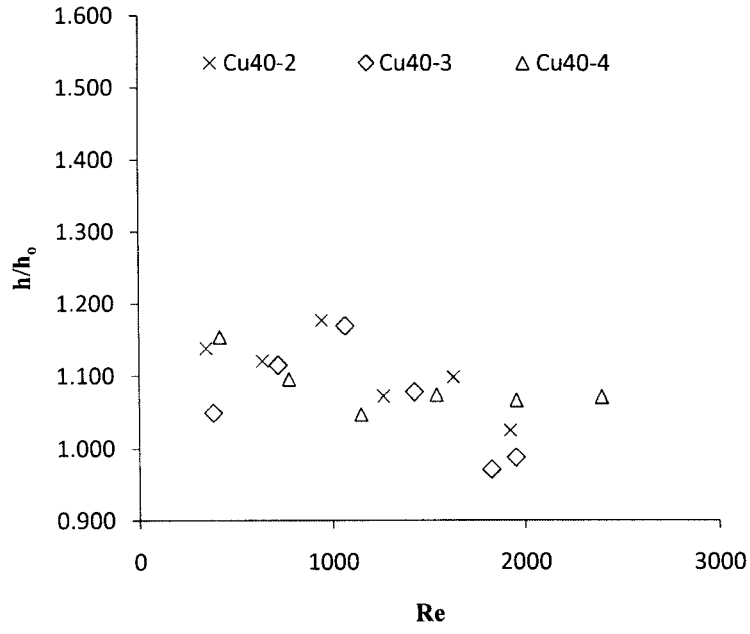

Fig 4.4.2.5 Enhancement ratio (h/h_0) as a function of Reynolds number (Re) at 65°C.

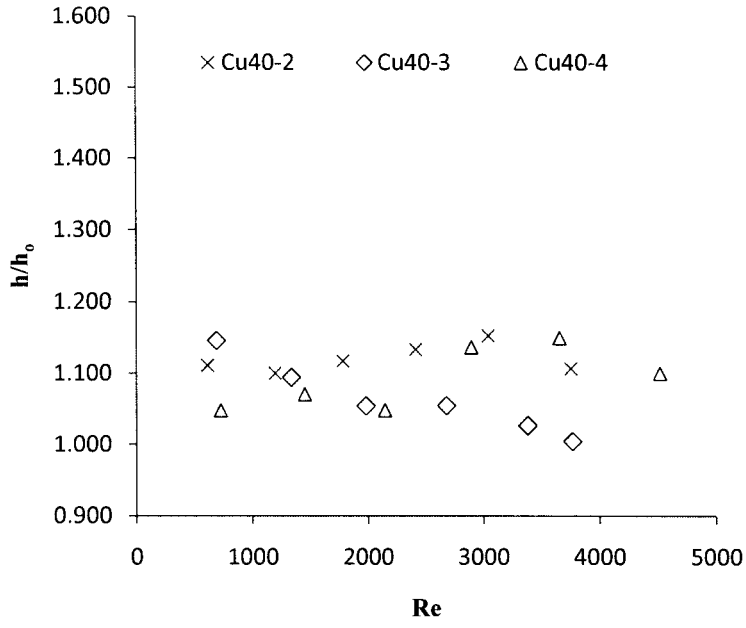

Fig 4.4.2.6 Enhancement ratio (h/h_0) as a function of Reynolds number (Re) at 90°C.

4.3 60-80nm Cu nanofluids (Cu60)

Four weight percentages (0.25, 1.0, 1.5, 2.0) of Cu60 nanofluids were tested. Results are shown in Figures 4.4.3.1. – 4.4.3.5. Nanofluid with a weight fraction of 2.0% exhibits a maximum enhancement of 21% at 40°C.

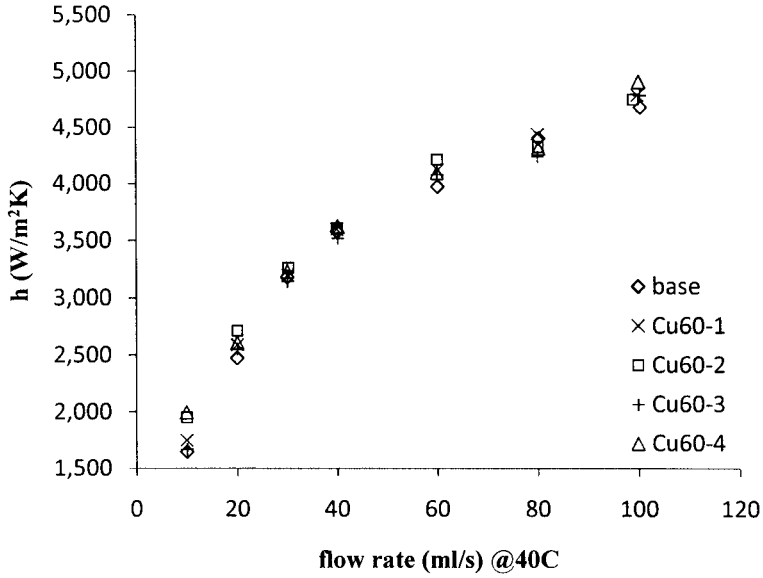

Fig 4.4.3.1 Heat transfer coefficient (h) as a function of flow rate at 40°C.

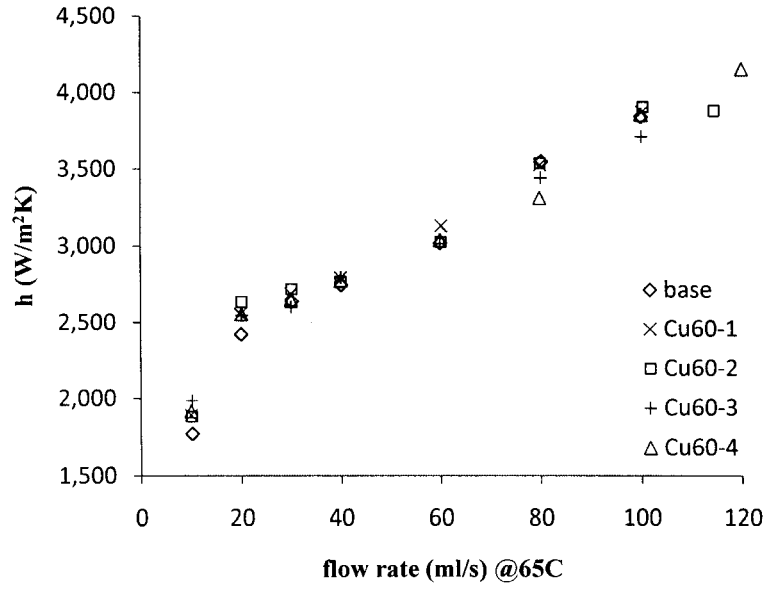

Fig 4.4.3.2 Heat transfer coefficient (h) as a function of flow rate at 65°C.

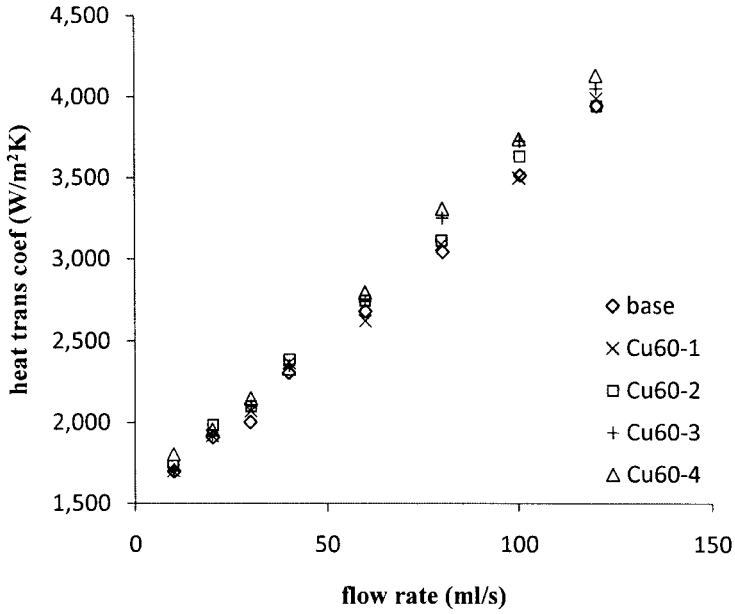

Fig 4.4.3.3 Heat transfer coefficient (h) as a function of flow rate at 90°C.

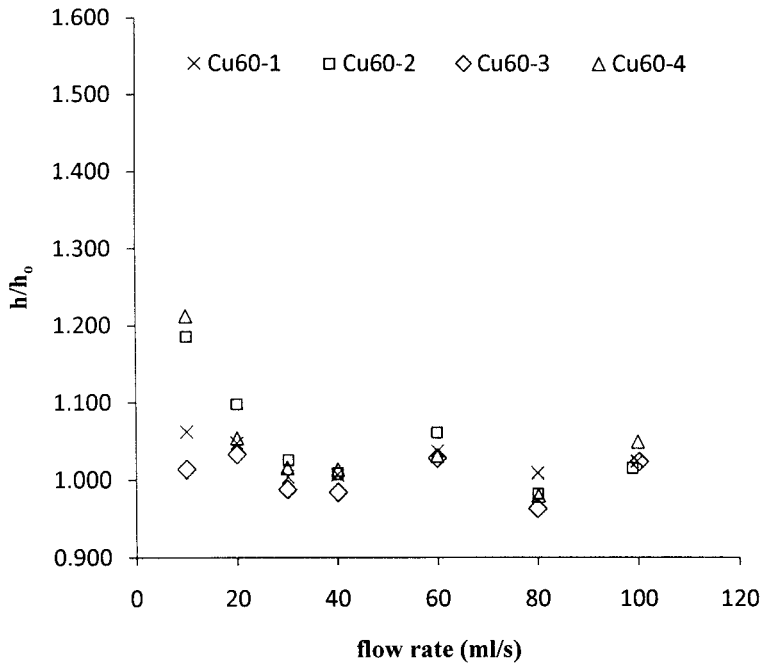

Fig 4.4.3.4 Enhancement ratio (h/h_0) as a function of Reynolds number at 40°C.

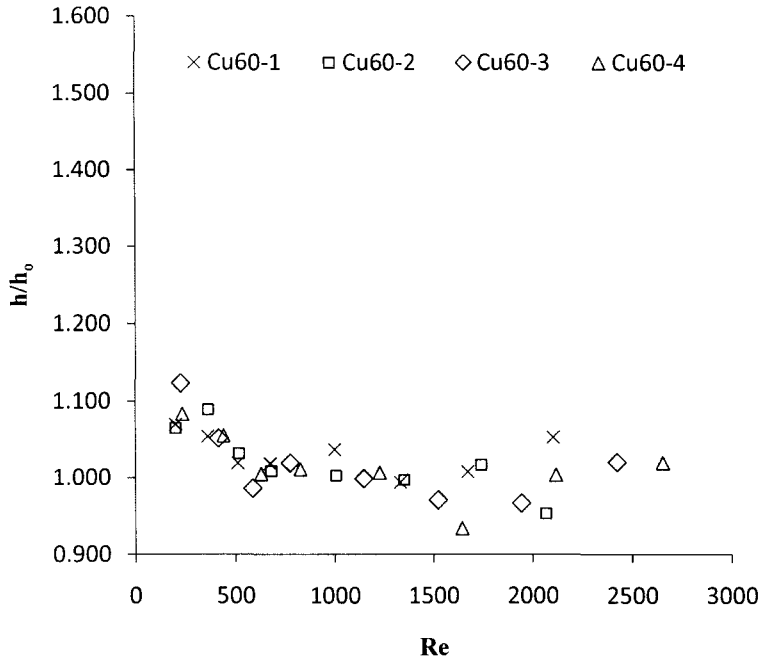

Fig 4.4.3.5 Enhancement ratio (h/h_0) as a function of Reynolds number at 65°C.

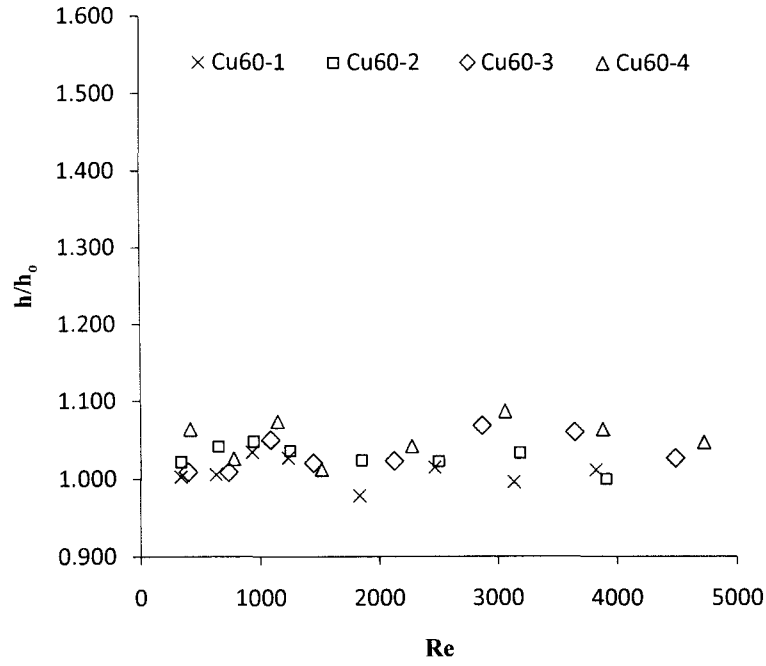

Fig 4.4.3.6 Enhancement ratio (h/h_0) as a function of Reynolds number at 90°C.

CHAPTER V

DISCUSSION

1. Preliminary Results

Five different pairs of base and nanofluids as provided were tested during the initial system and procedural development period. Through this process, several trends became evident even though specific information about the fluids being tested was severely limited.

From the results presented in the previous chapter, the heat transfer measurements are reproducible within a single measurement. But there is a longer term trend of decreasing heat transfer coefficient values over a period of time as shown in Figures 4.1.7 and 4.1.8. One potential source of this drift is the buildup of a coating on the tube wall of the heat exchange section which may result in a reduction in the heat transfer coefficient. Another explanation is that the decrease could be due to the kerosene residue in the system. Kerosene was used to flush the system between runs to remove the residual test fluid and particles but the kerosene could not be completely drained out prior to the start of another test run. As kerosene has a poor heat transfer properties, the residual kerosene mixed with the new test fluid could decrease the heat transfer coefficient.

When changing fluids, our standard flush technique involved draining the system of the previous test fluid, refilling with kerosene, circulating the kerosene for a period of

time, draining the kerosene and refilling the system with the new test fluid. The thoroughness of the drain steps and the time and intensity of kerosene circulation were somewhat variable. Residual amounts of fluid or kerosene could affect subsequent measurements. In order to evaluate the effectiveness of this flush procedure, we made a series of measurements at a standard condition of 40°C and 30 ml/s flow rate. These results are shown in Figure 5.1.1.

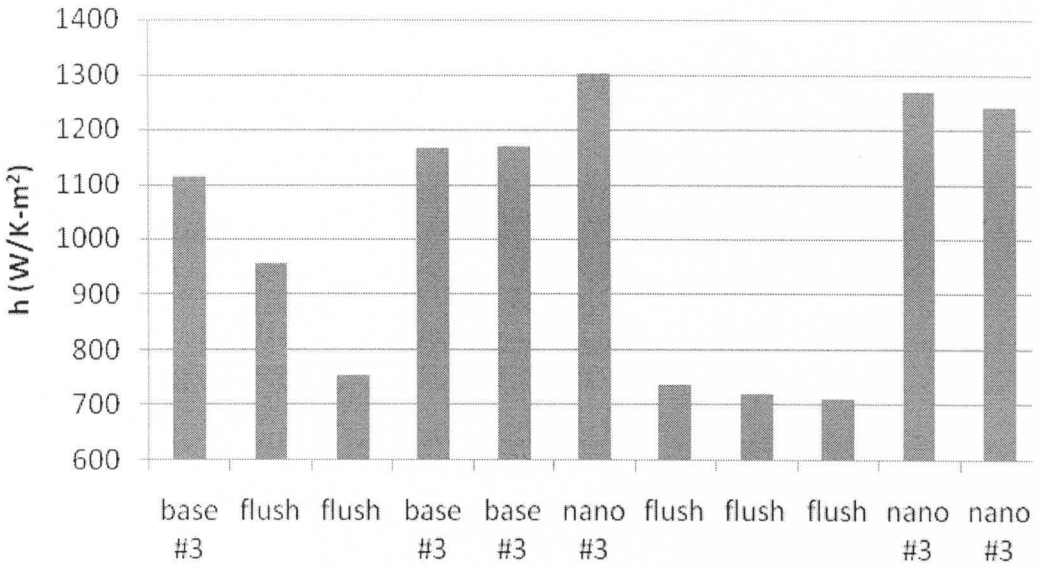

Fig. 5.1.1 Flush effectiveness experiment measured heat transfer coefficient at 40°C and 30 ml/s after a series of fluid changes. The measurements were taken sequentially and displayed from left to right in the bar chart above.

The experiment started with a measurement for the heat transfer coefficient of base oil #3, yielding a value of 1113 W/K-m^2. After draining that oil and refilling with kerosene, the heat transfer of the kerosene was measured as 958 W/K-m^2. Draining and refilling with new kerosene yielded a value 755 W/K-m^2. It seems that the initial flush step left residual oil in the system. Assuming that the second measurement for kerosene is

a more accurate value for kerosene in a "clean" system, we use this value as a baseline for assuring that the flush process restores the system to a consistent state.

The fourth step in this experiment started with a refilling of the system with base oil. The heat transfer measurement of 1166 W/K-m^2 is somewhat higher than the initial measurement, suggesting that the double flush may have removed a residual coating on the tube interior. Draining and refilling the system with base oil (no flush) resulted in a new heat transfer value of 1170 W/K-m^2, very close to the previous measurement. Again draining the base oil and refilling with nanofluid #3 yielded a heat transfer coefficient of 1300 W/K-m^2, significantly higher than that of the base fluid.

Adopting a somewhat more intense procedure for draining and flushing, we refilled the system with kerosene three times, measuring heat transfer coefficients of 738, 721 and 714 W/K-m^2, consistent with our "baseline" value of 755 and indicating a "clean" system. Refilling twice with nanofluid#3 yielded 1268 and 1240 W/K-m^2, which is a little lower than the initial nanofluid measurement but still significantly higher than that of the base fluid.

From all the results obtained during this development period, some of the conclusions that can be drawn seem to agree well with what has been reported in literature. As shown in Figures 4.1.1 – 4.1.6, there is always a decrease in the heat transfer coefficient as well as a decrease in the enhancement of the heat transfer coefficient as the temperature is increased. This could potentially be an important issue in transportation applications since the working temperature of motor oil is typically more than 100°C. The possibility of the decrease in heat transfer coefficient as the fluid ages or as a coating is built up has not been reported previously but may have significant implications for

commercial uses. These results provide a solid foundation for our continued study of nanofluids, but with many questions remaining unanswered. There was a need to more fully investigate the fundamental heat transfer properties of nanofluids.

2. Specific Heat and Viscosity

Thermal conductivity and heat transfer performance have always been the main research focus of nanofluids. The influence of nanoparticles specific heat c_p seems too small to be considered due to the low particle concentration [24, 45]. However, in most cases, it has been supposed to be strongly dependent on the volume concentration of nanoparticles [17, 70-74]. In this study, specific heat capacity of nanofluids c_p was determined thorough the equation:

$$c_p = \frac{heat\ flow\ (w/g)}{heat\ rate\ (°C/s)} \tag{12}$$

where heat flows of all fluids were measured by DSC at a temperature range of 30°C to 100°C with an increment of 2°C. Heat rate represents the speed of temperature increase as a function of time.

Results for specific heat tests are presented in Figure 4.2.1 – 4.2.3 where all three types of nanofluids showed similar trend. Specific heat increased linearly with increasing temperature from 40°C to 100°C. If we compare specific heats for nanofluids with different concentrations at same temperature, we can also conclude that the specific heat of a nanofluid decreases with increasing particle concentration. This is in good agreement with Zhou and colleagues work [75] when specific heat of Al_2O_3/water nanofluids were measured.

In the study of viscosity, an important concept used to distinguish between different fluids is whether the apparent viscosity of the fluid is shear-rate dependent. In other words, is the fluid Newtonian or non-Newtonian? These two types of fluids have completely different rheological behaviors. The viscosity is independent of shear rate in the case of a Newtonian fluid, whereas for non-Newtonian fluid, the viscosity is a function of shear rate. In the field of nanofluids, some have been observed to exhibit Newtonian behaviors [17, 18, 24, 76] while others have been determined to be non-Newtonian [21, 49, 77, 78].

The viscosity of PAO oil (base fluid) as a function of shear rate at a temperature range of 30°C to 90°C is shown in Figure 4.3.1. It can be seen that the viscosity of PAO oil is independent of the shear rate over the entire temperature range, which indicates a Newtonian behavior. While many studies use water or ethylene glycol based nanofluids, there are relatively few studies using oil-based nanofluids. One study by Zhou and colleagues [79] found that the viscosity in the nanofluids where alumina nanospheres were suspended into PAO lubricant showed very little shear rate dependence at most volume fractions and only a very weak shear rate dependence at the highest nanoparticle volume fraction of 3.0%. The results from this study were found to be in close agreement for PAO oil based nanofluids.

Viscosities at various temperatures for three sizes of nanofluids with three different sizes of nanoparticles in the same particle loading of 2.0wt% were shown in Figure 4.3.2 – 4.3.4. Newtonian fluid behavior were observed for the Cu25-4 nanofluid as viscosity remained constant with very little fluctuation as shear rate was increased. Similar behaviors were found on the Cu40 and Cu60 nanofluids. From an engineering

point of view, these nanofluids with low particle loading can be approximated as Newtonian fluids. Since PAO oil was used, and oil viscosity is dependent on temperature, nanofluids with different weight fractions showed strong temperature dependence on their viscosity. As temperature is increased, the viscosity of nanofluid decreases significantly.

3. Effect of Reynolds number on Heat Transfer Enhancement

The experiments of Cu nanofluids were conducted over a wide range of Reynolds numbers ($95 < Re < 4700$). All measurements for base and nanofluids show an increasing heat transfer coefficient as the average flow velocity Q and Reynolds number Re increases. Data for the heat transfer coefficient in the turbulent flow regime is limited but enhancements were observed. From Figure 4.4.1.5, it is clearly shown that there is close to a 10% enhancement for Cu25-4 in the turbulent as well as in the laminar flow regime. Cu40-4 nanofluid (Figure 4.4.2.5) achieved a 9.9% increase in the heat transfer coefficient at Reynolds number of 4500 while Cu60-4 (Figure 4.4.3.5) reached a 4.8% enhancement at Reynolds number of 4700. While promising, the data in turbulent flow are still insufficient to determine any specific trends for enhancement of the heat transfer coefficient as a function of particle concentration. Heat transfer enhancement in laminar and transition flow regimes will be more fully discussed in the following sections.

4. Effect of Fluid Temperature on Heat Transfer Enhancement

The initial fluid temperature was controlled by the water bath in the heat transfer measurement system. Three temperatures (40°C, 65°C, and 90°C) were used during the

measurement of the heat transfer coefficient. Due to the heat loss in the copper tube, the inlet temperature is slightly lower than the preset temperature of the water bath but will not affect the accuracy of the measurement.

From Figure 4.4.1.1 – 4.4.1.3, the heat transfer coefficient decreases as the fluid temperature increases at the same flow rate for both the base and Cu25 nanofluids. A similar decrease is found for Cu40 and Cu60 nanofluids when comparing Figures 4.4.2.1 – 4.4.2.3 or Figures 4.4.3.1 – 4.4.3.3. This is in good agreement with our conclusions from the preliminary results where the heat transfer coefficient is significantly lower at 80°C than at 60°C.

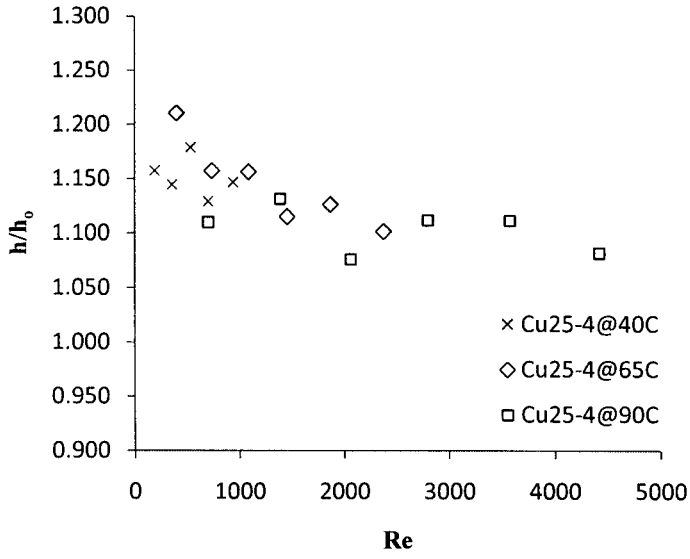

Fig. 5.4.1 Effect of fluid temperature on enhancement of heat transfer coefficient for Cu25-4 nanofluids.

The enhancement of heat transfer coefficient is reflected in the ratio of the heat transfer coefficient of the nanofluid h_0 to the base fluid h. Figure 5.4.1 shows that, at 40°C, Cu25-4 has a typical increase in heat transfer coefficient of 15.1% over the base fluid. However, at 65°C, the heat transfer coefficient enhancements average 14.4%. At

90°C, the average enhancement is only 10.3%. Similar to what was concluded in preliminary results, the enhancement of heat transfer coefficient decreases with increasing fluid temperature. In transportation applications, this could be an important issue because of the high working temperature of the motor oil in a car engine. Furthermore, there's a clear downward trend of enhancement ratio with respect to Reynolds number as the fluid reaches the transition flow regime at fluid temperature at 65°C. However, the trend is close to a horizontal line throughout the laminar and turbulent flow regime at fluid temperature of 90°C.

There are several mechanisms that lead to smaller improvements in heat transfer coefficient between the nanofluids and the base fluids at higher temperatures. A possible explanation is the depletion of particles in the near-wall fluid phase [80], which leads to the development of a lower thermal conductivity layer at the wall. Another possible explanation is the alignment of nanoparticles in the laminar flow regime.

At the lower temperature of 65°C, the viscosity of the nanofluid is higher which means there is less Brownian motion and collisions of the nanoparticles. The lateral movement of nanoparticles (perpendicular to the direction of the flow) is less intense compared to higher temperature of 90°C where the Brownian motion is more intense. Based on the results shown in Figure 5.4.1, Brownian motion seems to have a negative effect on the enhancement of heat transfer coefficient, indicating that the main contribution to the enhancement of the heat transfer coefficient is the contact between the nanoparticles and the base fluid rather than the collision between the nanoparticles. As the Reynolds number reaches the transition flow regime, the enhancement for Cu25-4 nanofluid at 65°C decreases to around 10% which is close to the enhancement at 90°C.

This could be due to the fact that the main reason for the enhancement of heat transfer coefficient in turbulent flow is the convective heat transfer of the fluid. At higher Reynolds number, the effect of the nanoparticles becomes smaller. That also explains the steady trend of enhancement ratio at a fluid temperature of 90°C in transition and turbulent flow regime as Brownian motion would be more prevalent at the higher temperatures and lower viscosities.

5. Effect of Particle Size of Nanofluids on Heat Transfer Enhancement

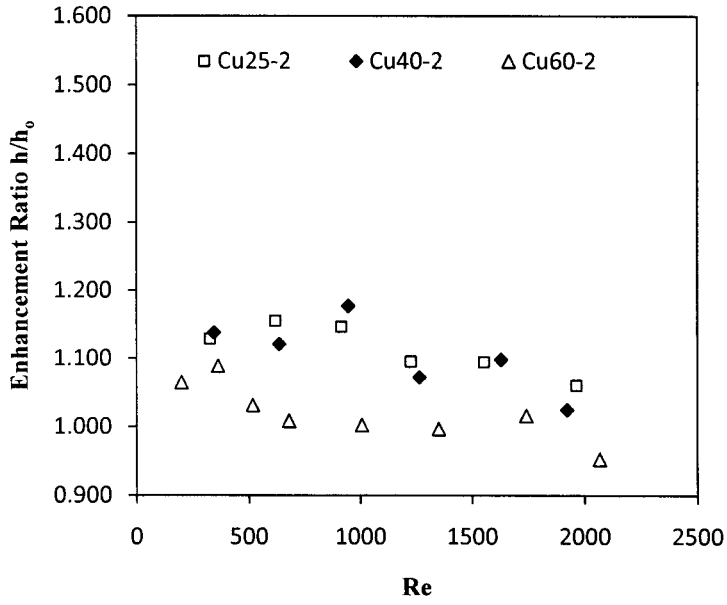

Fig 5.5.1 Enhancement ratio of heat transfer coefficient versus Reynolds number of 3 sizes of Cu nanofluids with particle loading of 1.0wt% with an inlet fluid temperature of 65°C.

The study of effect of nanoparticle size in heat transfer enhancement is limited since most studies focus on using a single size of nanoparticle at different concentrations. This effect is studied by plotting the enhancement ratio of the heat transfer coefficient under same conditions versus Reynolds number. Results for 1.0wt% nanofluids at an inlet

fluid temperature of 65°C are shown in Fig 5.5.1. The enhancement of the heat transfer coefficient for Cu25-2 averages about 11.4%. For Cu40-2 nanofluids, the enhancement is 10.5%. Only a 2.1% enhancement is found for Cu60-2 nanofluids at 65°C.

To find a possible explanation for this decrease in enhancement as the particle size increases, we start by calculating the decrease in the total number of particles in the fluid for each of the different sizes. For each weight fraction, a consistent mass of Cu nanoparticles is added to the base fluid. Since the density of copper stays the same, the total volume, V, added is the same for three nanoparticles. For sphere nanoparticles, the total number of particles of each size can be calculated as:

$$\#\ of\ particles = \frac{V}{\frac{4}{3}\pi r^3} \tag{13}$$

Using the average diameter of the sphere Cu nanoparticles of 25, 50 and 70nm, the ratio of total number of particles in each fluid is approximately 22.0 : 2.74 : 1 based on the calculation of through Eq. (13).

Another possible explanation of this phenomenon is the decrease of total surface area of nanoparticles. Again, we assumed the same amount of Cu nanoparticles added which means that the total volume, V added is the same for three nanoparticles. Therefore, the total surface area of each type of nanoparticles can be calculated through the following equation:

$$A_{total} = \frac{V}{\frac{4}{3}\pi r^3} \cdot 4\pi r^2 = \frac{3V}{r} \tag{14}$$

Based on this equation, the ratio of total particle surface area for these three different sizes of nanoparticle is approximately 4 : 2 : 1.43. Given the small decrease in the magnitude of the enhancement ratio, the change in total surface area ratio is more

believable explanation as compared to the high change in the ratio of the number of particles. The decrease of total surface area of nanoparticles could weaken the interaction between the nanoparticles and base fluid molecules therefore reduce heat transfer performance of the nanofluid.

As the weight fraction is increased to 2.0% at 65°C, the trend of decreasing heat transfer enhancement is clearer and, more importantly higher enhancement was observed as shown in Figure 5.5.2, especially for Cu25-4 nanofluid. A 21% of enhancement of heat transfer coefficient was achieved for Cu25-4 nanofluids at lowest Reynolds number of 398. An enhancement of only 16% was found for Cu40-4 and less than 10% for Cu60-4 at the same Re range.

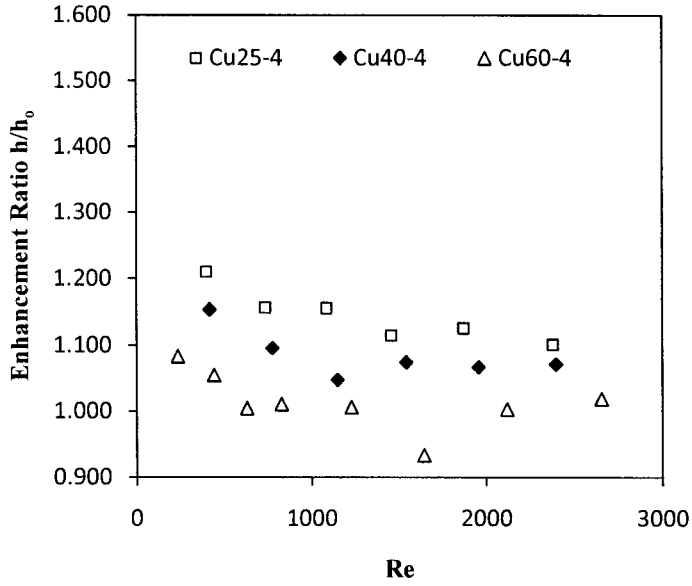

Fig 5.5.2 Enhancement ratio of heat transfer coefficient versus Reynolds number of 3 sizes of Cu nanofluids with particle loading of 2.0wt% with an inlet fluid temperature of 65°C.

Similar trend can be found for fluid temperature at 90°C. Comparing Figure 4.4.1.4, 4.4.2.4, and 4.4.3.4, it can be seen that Cu25-3 showed an average enhancement

of 12.7%, 6.3% for Cu40-4 and only 3.3% for Cu60-3. When the particle loading was increased to 2.0wt%, there was 10.4% enhancement for Cu25-4, 9.2% enhancement for Cu40-4 and only 5.2% enhancement for Cu60-4 (Figure 4.4.1.5, 4.4.2.5 and 4.4.3.5).

All the data shows that nanoparticle size does have a significant impact on the enhancement of the heat transfer coefficient. The smallest particle size of 25nm showed the best heat transfer performance. This could be due to the increased surface area of nanoparticles that intensified the random movement and collision between nanoparticles and base fluid molecules. Interestingly, the enhancement of heat transfer coefficient seems to decrease as Reynolds number is increased over the laminar flow regime. The maximum enhancement is always at the lowest Reynolds number and a clear downward trend can be seen from Figure 5.5.1, which has never been reported by others to the best knowledge of the author.

6. Effect of Nanoparticle Loading of Nanofluids on Heat Transfer Enhancement

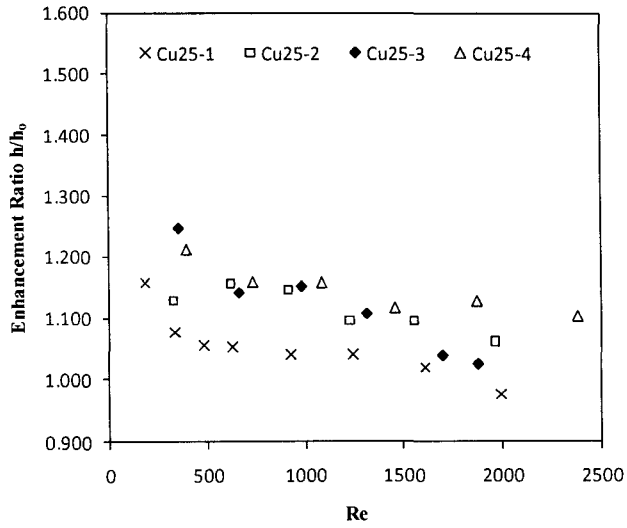

Fig 5.6.1 Enhancement ratio of heat transfer coefficient versus Reynolds number of Cu25 nanofluids with different particle loadings at inlet fluid temperature of 65°C.

A summary of results for the effect of nanoparticle loadings at 65°C are plotted in Figure 5.6.1. Enhancement of heat transfer coefficient is observed for all 4 concentrations of Cu25 nanofluids except Cu25-1 at a Reynolds number of 2000. A maximum enhancement of 25% is found for Cu25-3 at lowest Reynolds number around 400. Cu25-1 shows the least enhancement through the entire Reynolds number range although it reaches a maximum enhancement of 16% at a Reynolds number of 185. This is most likely due to the very small particle loading (0.25wt%) of Cu nanoparticles. The other 3 types of nanofluids show a very similar enhancement performance below a Reynolds number of 1500. It should be noted that only Cu25-4 is able to maintain a 10% enhancement above a Reynolds number of 1500. Each of the other particle loadings show a marked decrease in enhancement above this value.

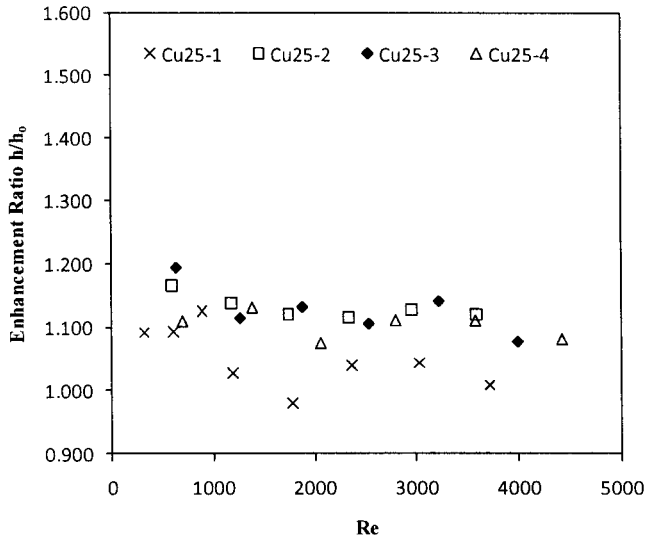

Fig 5.6.2 Enhancement ratio of heat transfer coefficient versus Reynolds number of Cu25 nanofluids with different particle loadings at inlet fluid temperature of 90°C.

As fluid temperature was increased to 90°C, test fluids were able to cover the entire transition flow regime and part of turbulent flow regime (Re>4000) due to the significant decrease in fluid viscosity. Cu25-1 showed least heat transfer enhancement again with average increase around only 5% while similar average enhancement of 11% were observed for other three nanofluids. This is in marked contrast to the results at 65°C and again suggests that viscosity may play a significant role in these systems. A possible explanation to this phenomenon is that as the concentration of nanoparticles increases, they may aggregate and cause the size to increase and leads to a decrease in the heat transfer performance. In other words, the effect of surface area increase by the increasing amount of nanoparticle is offset by the effect of particle agglomeration. An example of aggregation after 4 weeks for 60-80nm nanofluids is shown in Figure 5.6.3.

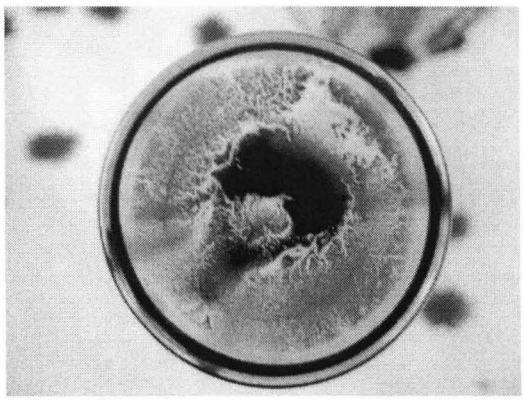

Fig 5.6.3 Example of nanoparticles aggregation after 4 weeks of settling.

7. Theoretical Modeling of Heat Transfer Coefficient

The modeling of heat transfer coefficient is starting to receive more attention from researchers because it is a better indicator of heat transfer performance than thermal conductivity. However, theoretical modeling of the heat transfer coefficient is limited due to the fact that nanofluids are multi-component systems with complex morphology. Most

correlations were established based on several traditional correlations for homogenous liquids such as Eqs. (9) – (12). Unfortunately, they are only valid for certain nanofluids in small parameter ranges.

7.1 Estimation of thermal conductivity

Most correlations for heat transfer coefficient are based on finding the Nusselt number for the system in question. In order to obtain values for the heat transfer coefficients, the thermal conductivities of both the base and nanofluids are needed. The best way to measure thermal conductivity is through the transient hot-wire method as discussed earlier. In lieu of direct measurement, the thermal conductivities of the test fluids are estimated using Eq. (4).

$$k_{eff} = \left[\frac{k_p+2k_w+2(k_p-k_w)(1+\beta)^3\phi}{k_p+2k_w-(k_p-k_w)(1+\beta)^3\phi}\right]k_w \tag{4}$$

A summary of results are shown in Table 6. Due to the low volume fraction of nanoparticles, only small enhancements in the thermal conductivities were found. The standard thermal conductivity of the PAO oil at 25°C is obtained from Amsoil.

Table 6 Thermal Conductivity of Nanofluids

	Weight fraction	Volume fraction	Thermal conductivity k (W/mK)
Base fluid	0	0	k_{bf}= 0.1395
Cu-1	0.25 wt%	0.02386 vol%	k_{nf}= 1.001 k_{bf} = 0.1396
Cu-2	1.0 wt%	0.09546 vol%	k_{nf}= 1.0038 k_{bf} = 0.1400
Cu-3	1.5 wt%	0.1432 vol%	k_{nf}= 1.0057 k_{bf} = 0.1403
Cu-4	2.0 wt%	0.1910 vol%	k_{nf}= 1.0076 k_{bf} = 0.1406

7.2 Theoretical models

There are several models that could be used to predict the heat transfer coefficient under different conditions. Based on Dittus - Boetler's model, Das et al. [60] introduced a model in 2003 which is defined as follows:

$$Nu = cRe_b^m Pr^{0.4} \tag{17}$$

where c and m are particle volume concentration dependent parameters. However, this model does not directly consider the effect of nanoparticle concentration and size which, according to the results of this study, will impact the heat transfer coefficient significantly. Oliver's correlation and Eubank and Proctor's correlation were also discussed earlier. These two models address the natural convection that will occur in a laminar flow. However, it was found that both correlations predicted heat transfer coefficients that are much lower than the experimental data in this study.

7.3 Xuan et al.'s model

Li and Xuan [81] studied the convective heat transfer and flow characteristics of Cu/water nanofluids. Spherical Cu nanoparticles with diameters less than 100nm were dispersed in deionized water with the addition of a fatty acid salt to prevent aggregation. They developed a new correlation for heat transfer coefficient of nanofluids in a horizontal tube as:

$$Nu = 0.4328(1.0 + 11.285\Phi^{0.754}Pe_d^{0.218})Re^{0.333}Pr^{0.4} \tag{18}$$

$$Nu = 0.0059(1.0 + 7.628\Phi^{0.6886}Pe_d^{0.001})Re^{0.9238}Pr^{0.4} \tag{19}$$

in which Eq. (18) is for laminar flow and Eq. (19) is for turbulent flow. Pe_d is the particle Peclet number that is defined as:

$$Pe_d = \frac{u_m d_p}{\alpha_{nf}} \tag{20}$$

where u_m is the mean velocity, d_p is the average diameter of the nanoparticle. The thermal diffusivity of the nanofluid α_{nf} is defined as:

$$\alpha_{nf} = \frac{k_{nf}}{(\rho c_p)_{nf}} \tag{21}$$

When compared with more conventional approaches used to find the heat transfer coefficient, several parameters including Peclet number Pe and volume fraction Φ are taken into consideration in the correlations above. The Peclet number represents the thermal dispersion attributed to the nanoparticles. All exponential factors and prefactors are empirical parameters. The differences between Eq. (18) and Eq. (19) are exponents of Reynolds and Peclet numbers, the particle volume fraction and the prefactors. In laminar flow, suspended nanoparticles contribute more to overall heat transfer than in turbulent flow. As the fluid reaches turbulent flow region, the exponents in the bracket in Eq. (19) decreases and Reynolds number exponent increases. This indicates that the convective flow of the test fluid contributes more than the movement of nanoparticles to overall heat transfer. These trends are qualitatively similar to what was experimentally measured during this study.

This correlation is used in this study because it was established using spherical Cu nanoparticles, which is the same material as this project. Although we used PAO formulated oil while they used water as a base fluid, and oil is not as good as a heat transfer fluid compared with water, we may still modify Xuan et al.'s correlation to predict heat transfer coefficient. This is a reasonable conclusion since the PAO based nanofluid is still a Newtonian fluid in spite of its higher viscosity and poor thermal conductivity leading to similar behavior. In laminar flow regime, the exponent and

prefactor for Reynolds number can be replaced with a and b in Eq. (18), which can now be re-written as:

$$Nu = aRe^{b}(1.0 + 11.285\Phi^{0.754}Pe_d^{0.218})Pr^{0.4} \quad (22)$$

The data obtained in this study can be fitted using Eq. (22). Results for values of a and b are listed in Table 7. It should be noted that for the same type of nanofluid, the coefficients a and b will not change with concentration because the volume fraction term Φ is included as a separate factor in the above equation. For the base fluid, the concentration of nanoparticles is 0, so the second term in the bracket of Eq. (22) is 0. The Reynolds number exponent b of all nanofluids is fairly close to that of the base fluid at the same fluid temperature. As the fluid temperature is increased, the value of b decreases. This effect is more apparent for nanofluids than the base fluid.

Table 7 Results for coefficients *a* and *b* of Eq. (22)

Fluid temperature	Fluid type	a	b
40°C	base	1.4715	0.342
	Cu25	1.4715	0.349
	Cu40	1.4715	0.349
	Cu60	1.4715	0.340
65°C	base	1.4282	0.320
	Cu25	1.4715	0.320
	Cu40	1.4932	0.315
	Cu60	1.4282	0.311
90°C	base	1.2335	0.323
	Cu25	1.3850	0.313
	Cu40	1.3417	0.313
	Cu60	1.3417	0.304

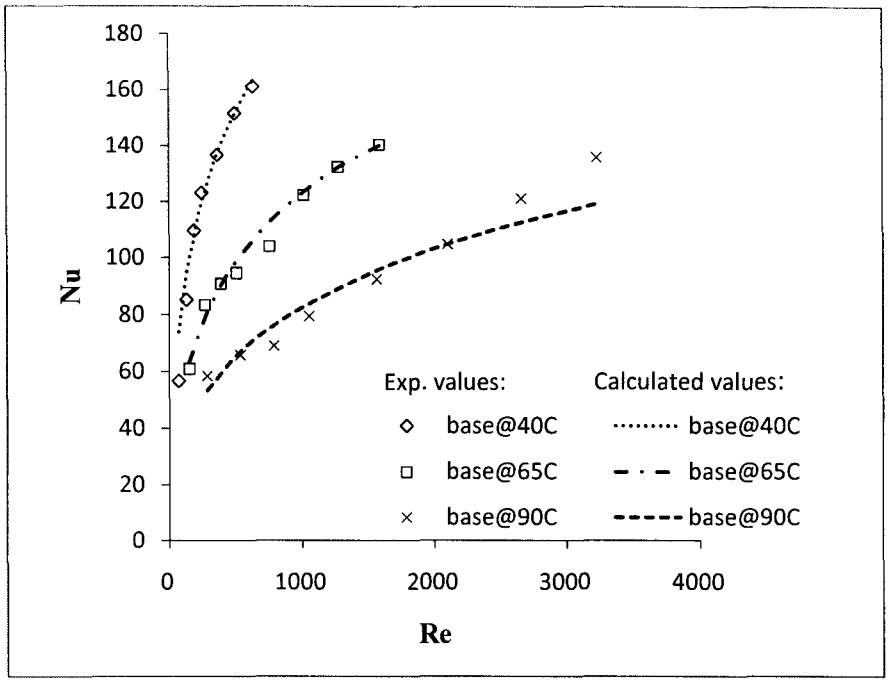

Fig 5.7.3.1 Comparison between experimental data and calculated values for base fluid at 40°C, 65°C, and 90°C.

Figure 5.7.3.1 gives the calculated and experimental results for the base fluid at each experimental temperature. Comparison shows that the calculated results from Eq. (20) are in good agreement with the experimental data at the lower temperatures and Reynolds numbers. The only divergence from the correlation seems to appear at fluid temperature for 90°C for the two *Nu* values at Reynolds number greater than 2500. This correlation underpredicted heat transfer coefficient in turbulent flow. It could be due to the relatively high shear rate that can disperse clustered nanoparticles especially in turbulent flow. However, the dispersing effect is relatively small in laminar flow system. Another possible explanation is that the nanoparticles tend to align in the direction of the flow in laminar flow regime. The random movement of the nanoparticles becomes more intense as well as the thermal dispersion in turbulent flow which will accelerate the energy exchange process in the fluid. This order to disorder transition could lead to the

under prediction of heat transfer coefficient in turbulent flow. Therefore, the original equation is only valid to predict heat transfer coefficient in laminar flow. As the fluid reaches transition flow regime, the correlation is no longer applicable.

The comparison between experimental data and calculated values for Cu25 nanofluid are plotted in Figures 5.7.3.2 – 5.7.3.5. Results for Cu25 nanofluid with 4 concentrations are presented using same coefficient values for *a* and *b*. Calculated results show good agreement with experimental data. Again, at Reynolds number greater than 2500, experimental values show more than 8% discrepancy with calculated data. More experimental data is needed to establish correlations for turbulent flow regime. Complete results are summarized in Appendix D.

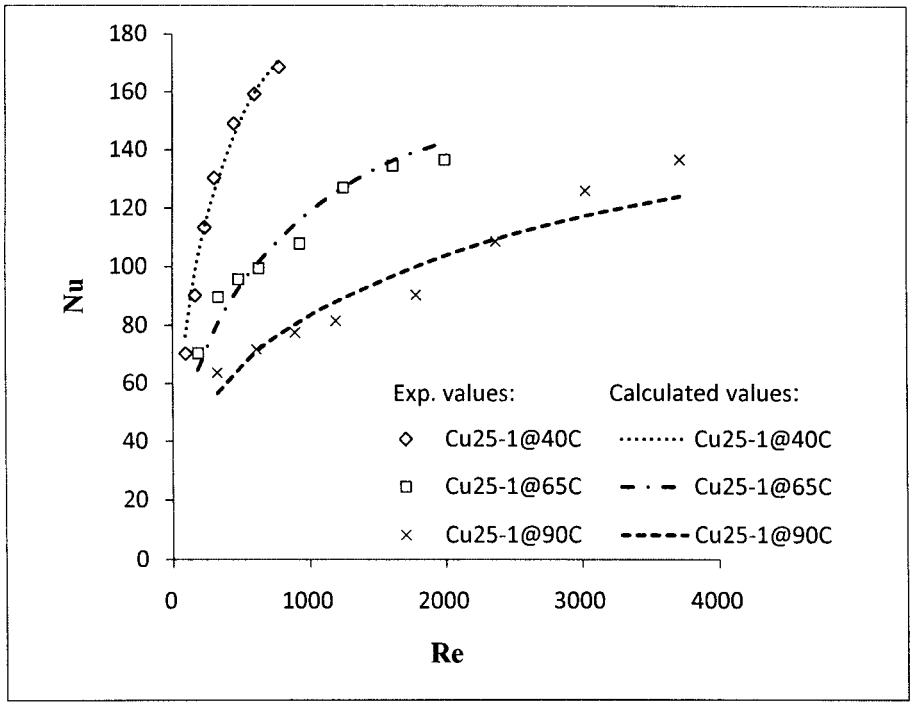

Fig 5.7.3.2 Comparison between experimental data and calculated values for Cu25-1 nanofluid at 40°C, 65°C, and 90°C.

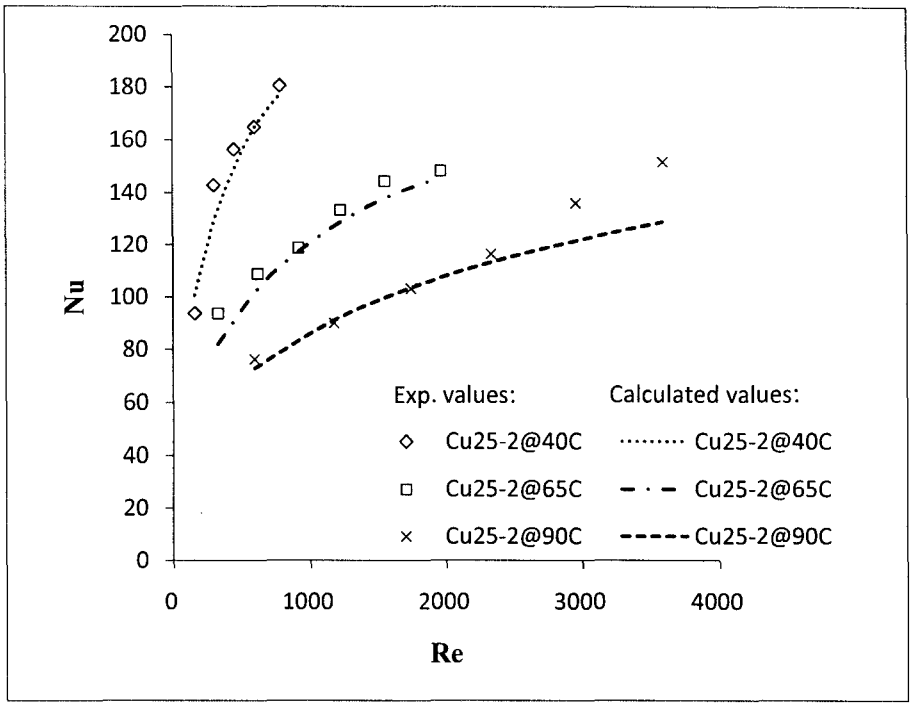

Fig 5.7.3.3 Comparison between experimental data and calculated values for Cu25-2 nanofluid at 40°C, 65°C, and 90°C.

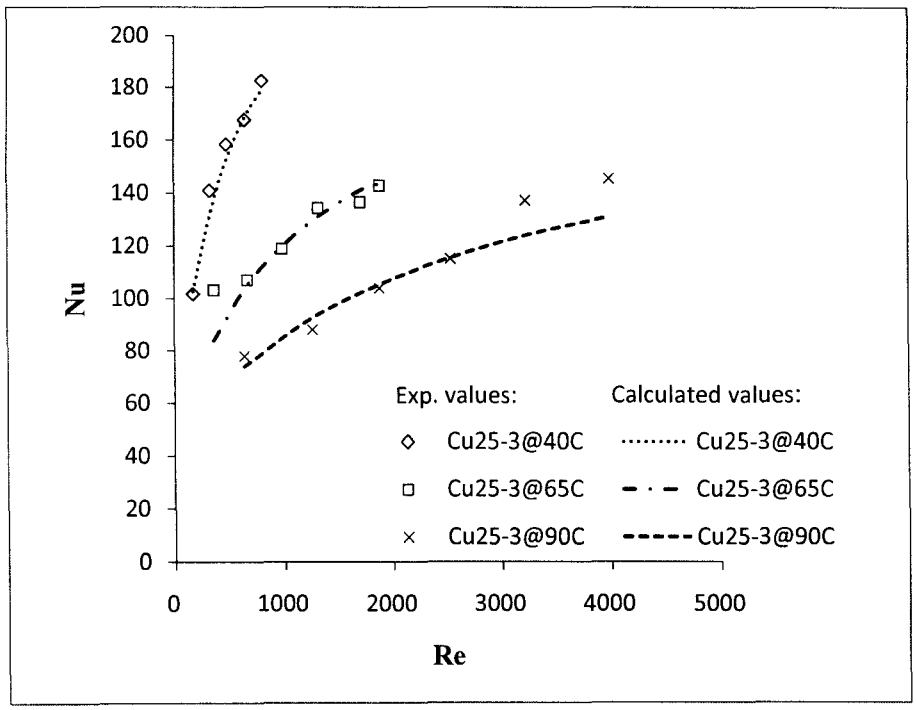

Fig 5.7.3.4 Comparison between experimental data and calculated values for Cu25-3 nanofluid at 40°C, 65°C, and 90°C.

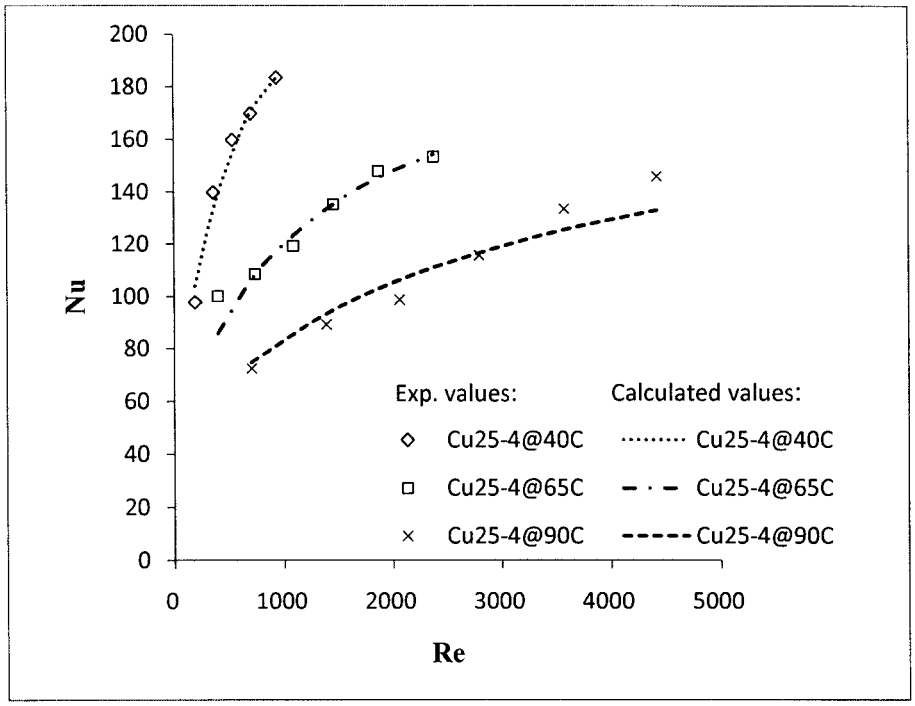

Fig 5.7.3.5 Comparison between experimental data and calculated values for Cu25-4 nanofluid at 40°C, 65°C, and 90°C.

7.4 Yang et al.'s model

In 2005, Yang and colleagues [24] developed a model to predict the heat transfer coefficient for their graphite-in-transmission fluid and graphite-in-synthetic oil nanofluids in laminar flow. Their equation is based on the Seider – Tate equation [65] and is defined as:

$$Nu = cRe^{m}Pr^{1/3}\left(\frac{D}{L}\right)^{1/3}\left(\frac{\mu_b}{\mu_w}\right)^{0.14} \tag{23}$$

where c and m are nanofluid and temperature dependent empirical parameters.

Experimental data sets were correlated using Eq. (23) and results for values of c and m are listed in Table 8. For fluid temperature at 90°C, the average temperature at the tube wall was over 95°C. Since there is no dynamic viscosity data for all test fluids at temperatures over 90°C, viscosity values at 100°C were assumed based on viscosity

decrease profile as a function of temperature.

Table 8 Results for coefficients *c* and *m* of Eq. (23)

Fluid temperature	Fluid type	c	m
40°C	base	12.741	0.347
	Cu25-1	12.834	0.351
	Cu25-2	12.834	0.357
	Cu25-3	12.834	0.357
	Cu25-4	13.020	0.355
65°C	base	12.927	0.310
	Cu25-1	13.392	0.310
	Cu25-2	13.578	0.315
	Cu25-3	13.206	0.315
	Cu25-4	13.336	0.315
90°C	base	12.462	0.291
	Cu25-1	13.020	0.287
	Cu25-2	13.392	0.298
	Cu25-3	13.206	0.296
	Cu25-4	13.113	0.291

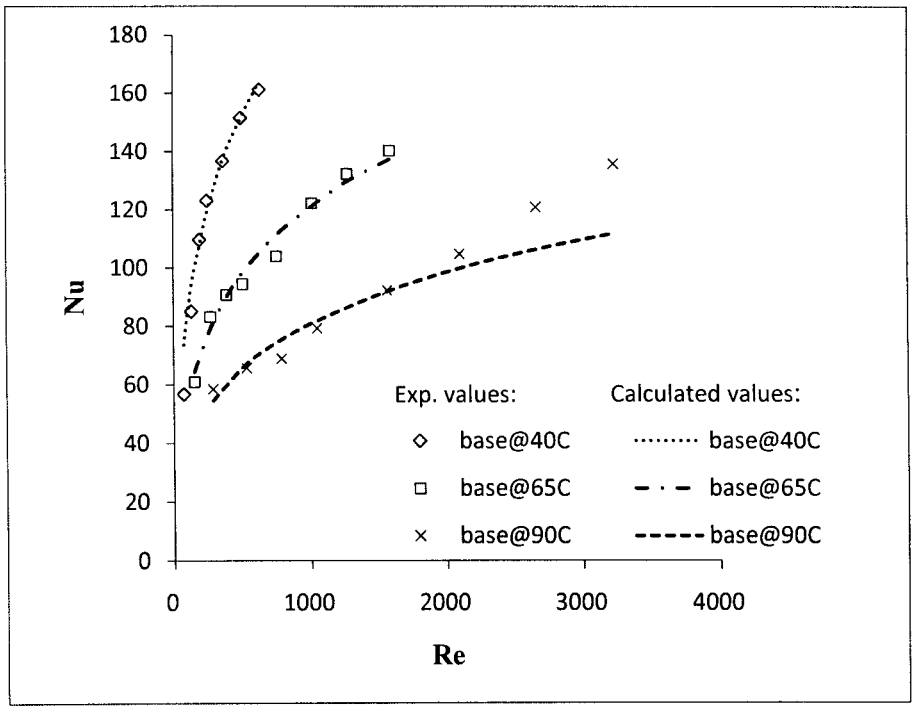

Fig 5.7.4.1 Comparison between experimental data and calculated values for base fluid at 40°C, 65°C, and 90°C.

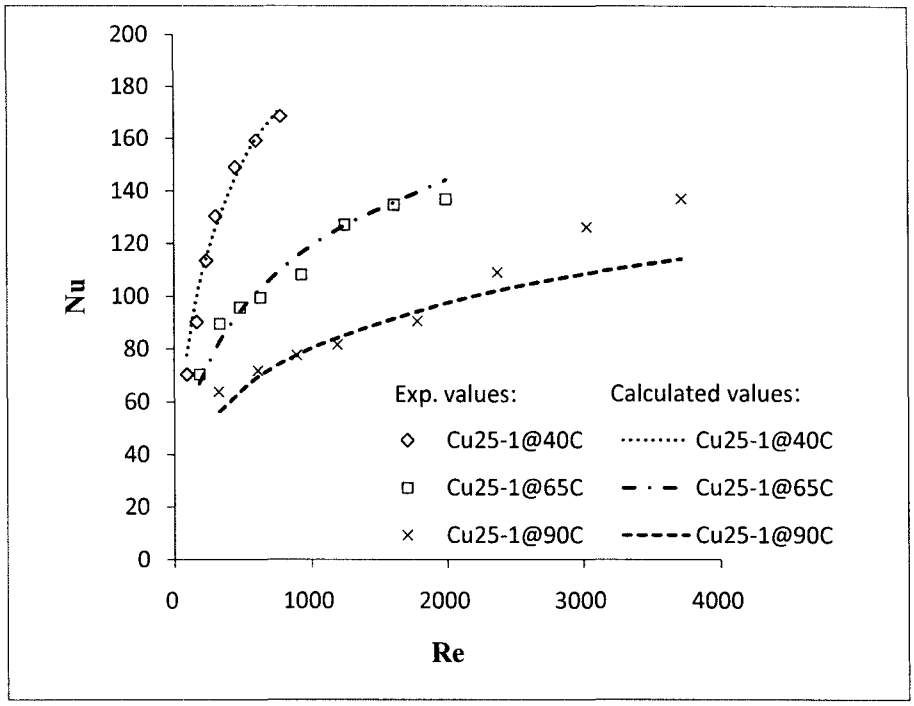

Fig 5.7.4.2 Comparison between experimental data and calculated values for Cu25-1 nanofluid at 40°C, 65°C, and 90°C.

Results for base fluid and Cu25-1 nanofluid are presented in Figures 5.7.4.1 and 5.7.4.2. By applying proper coefficients, our experimental data fit Yang et al.'s model fairly well except for lowest Reynolds number at 40°C. At a Reynolds number of 72, the experimental *Nu* value is 30% lower than calculated value for base fluid. For Cu25-1 nanofluid, the *Nu* value is off by only 10% is found at lowest Reynolds number of 94. Near wall particle depletion is a possible reason for this phenomenon. However, at fluid temperature of 90°C, this model greatly underpredicts the heat transfer coefficients in the transition and turbulent flow regime. Complete results for Cu25 nanofluids are included in Appendix E.

In summary, we examined several models that could be used to predict heat transfer coefficient of base and nanofluids in our system. Two correlations introduced by

Xuan et al. and Yang et al. seem to fit our data fairly well in laminar flow. Both models discussed above use an empirical prefactor and Reynolds number exponent to predict the heat transfer coefficient. Yang et al.'s correlation considers the radial variation of fluid properties, the effect of natural convection and the dimension of heat exchange section. But a drawback of their correlation is the lack of consideration of nanoparticle concentration and size, which are included in Xuan et al.'s model. It is concluded that both nanoparticle concentration and size will affect the enhancement of heat transfer coefficient significantly. Moreover, calculation of the natural convection effect term $(\frac{\mu_b}{\mu_w})^{0.14}$ in Yang et al.'s correlation with any precision will require knowledge of the radial temperature profile for test fluid within the heat exchange section which would be difficult to measure. A linear increase of temperature within the heat exchange section was assumed in this study to calculate dynamic viscosity which may potentially increase the range of error of the results. However, both correlations underpredict the heat transfer coefficient of base and nanofluids in turbulent flow regime. More data is needed in turbulent flow to develop any correlations.

CHAPTER VI

CONCLUSIONS AND FUTURE DIRECTIONS

1. Conclusions

This dissertation has demonstrated the development of study on the enhancement of thermal conductivity and heat transfer coefficient using nanofluids. Many research groups determined significant enhancement for thermal conductivity by dispersing different types of nanoparticles into water, ethylene glycol or oil. However, there are limited studies on the enhancement of heat transfer coefficient of nanofluids especially oil-based nanofluids.

Three different sizes (25nm, 40-60nm, 60-80nm) of spherical Cu nanoparticles were used to dispersed into PAO (Poly Alpha Olefin) formulated motor oil using a sonic dismembrator. By adding dodecanethiol as a surfactant, stable nanofluid suspensions were made. Different sizes and concentrations of nanoparticles were added to create nanofluids. Viscosities of base and nanofluids were measured using a cone-and-plate rheometer. Results showed that all base and nanofluids appeared to be Newtonian fluids as the shear stress was increased linearly with the increasing shear rate. Specific heats were measured using a Differential Scanning Calorimeter (DSC). As the particle concentration of the nanofluid was increased, the specific heat value was decreased.

By using a lab-built heat transfer test rig, the temperature rise was measured

within the heat exchange section so that heat transfer coefficient can be calculated. Results showed that heat transfer coefficients of base and nanofluids increase as the average flow velocity Q and Reynolds number Re increases. As the fluid temperature is elevated, the heat transfer coefficient decreases. As for heat transfer enhancement, all nanofluids exhibited enhancement of heat transfer coefficient over the base fluid. Nanofluids with the smallest particle size (25nm) showed the best enhancement. This could be due to the increased total surface area as the size of nanoparticle is decreased. The effect of particle loading on heat transfer enhancement is minimal in this tested range. A possible explanation is that those nanoparticles tend to agglomerate as the particle loading increases, therefore decrease the total surface area. The decrease of total surface area offset the effect of increased loading of nanoparticles.

Finally, a theoretical model to predict heat the transfer coefficient of nanofluids is modified to use in this study based on previously published correlations; the results of which are in excellent agreement with the experimental data.

2. Future Directions

Several important directions of further research can be identified.

1. Other metal nanoparticles such as Al or Au can be used to make nanofluids to determine if particle type will have an impact on the heat transfer coefficient.
2. Heat transfer performance of Cu/PAO oil nanofluids in turbulent flow can be investigated in future to confirm the downtrend of enhancement ratio we observed in laminar flow.
3. Transient hot-wire method can be used to determine thermal conductivity values

for base and nanofluids.

4. To investigate the effect of alignment of nanoparticles in nanofluids, a magnetic field can be installed in the heat exchange section to ensure the nanoparticles move only in the direction of the flow.

REFERENCES

1. Gribbin, J., *Richard Feynman: A Life in Science.* Dutton, 1997: p. 170.

2. Taniguchi, N., *On the Basic Concept of "Nano-Technology".* Proc. Intl. Conf. Eng. Tokyo, Part II, Japan Society of Precision Engineering, 1974.

3. Chopra, A., V. Kundra, and P. Weiser, *National Nanotechnology Initiative Strategic Plan.* 2011.

4. Yu, W., et al., *Review and Assessment of Nanofluid Technology for Transportation and Other Applications.* 2007.

5. Xuan, Y. and Q. Li, *Heat transfer enhancement of nanofluids.* International Journal of Heat and Fluid Flow, 2000. **21**(1): p. 58-64.

6. Martinek, K., et al., *Micellar Enzymology.* European Journal of Biochemistry, 1986. **155**(3): p. 453-468.

7. Martinek, K., et al., *Micellar Enzymology - Its Relation to Membranology.* Biochimica Et Biophysica Acta, 1989. **981**(2): p. 161-172.

8. Martinek, K., et al., *Micellar Enzymology - Potentialities in Applied Areas (Biotechnology).* Collection of Czechoslovak Chemical Communications, 1987. **52**(10): p. 2589-2602.

9. Romano, J.M., J.C. Parker, and Q.B. Ford, *Application Opportunities for Nanoparticles Made from Condensation of Physical Vapor.* Advances in Powder Metallurgy and Particulate Materials, 1997. **2**: p. 12-13.

10. Assael, M.J., et al., *Thermal conductivity of suspensions of carbon nanotubes in water.* International Journal of Thermophysics, 2004. **25**(4): p. 971-985.

11. Wen, D.S. and Y.L. Ding, *Experimental investigation into convective heat transfer of nanofluids at the entrance region under laminar flow conditions.* International Journal of Heat and Mass Transfer, 2004. **47**: p. 5181-5188.

12. Assael, M.J., et al., *Thermal conductivity enhancement in aqueous suspensions of carbon multi-walled and double-walled nanotubes in the presence of two different*

dispersants. International Journal of Thermophysics, 2005. **26**(3): p. 647-664.

13. Chon, C.H., et al., *Empirical correlation finding the role of temperature and particle size for nanofluid (Al2O3) thermal conductivity enhancement.* Applied Physics Letters, 2005. **87**(15).
14. Hong, T.K., H.S. Yang, and C.J. Choi, *Study of the enhanced thermal conductivity of Fe nanofluids.* Journal of Applied Physics, 2005. **97**(6).
15. Liu, M.S., et al., *Enhancement of thermal conductivity with carbon nanotube for nanofluids.* International Communications in Heat and Mass Transfer, 2005. **32**(9): p. 1202-1210.
16. Marquis, F.D.S. and L.P.F. Chibante, *Improving the heat transfer of nanofluids and nanolubricants with carbon nanotubes.* Jom, 2005. **57**(12): p. 32-43.
17. Pak, B.C. and Y.I. Cho, *Hydrodynamic and heat transfer study of dispersed fluids with submicron metallic oxide particles.* Experimental Heat Transfer, 1998. **11**(2): p. 151-170.
18. Putra, N., W. Roetzel, and S.K. Das, *Natural convection of nano-fluids.* Heat and Mass Transfer, 2003. **39**(8-9): p. 775-784.
19. Xuan, Y.M. and Q. Li, *Investigation on convective heat transfer and flow features of nanofluids.* Journal of Heat Transfer-Transactions of the Asme, 2003. **125**(1): p. 151-155.
20. Zhou, D.W., *Heat transfer enhancement of copper nanofluid with acoustic cavitation.* International Journal of Heat and Mass Transfer, 2004. **47**(14-16): p. 3109-3117.
21. He, Y.R., et al., *Heat transfer and flow behaviour of aqueous suspensions of TiO2 nanoparticles (nanofluids) flowing upward through a vertical pipe.* International Journal of Heat and Mass Transfer, 2007. **50**(11-12): p. 2272-2281.
22. Bucak, S., *Importance of defining when applying.* Chemical Engineering & Process Technology, 2011. **2**(1).
23. Jang, S.P. and S.U.S. Choi, *Effects of various parameters on nanofluid thermal conductivity.* Journal of Heat Transfer-Transactions of the Asme, 2007. **129**(5): p. 617-623.
24. Yang, Y., et al., *Heat transfer properties of nanoparticle-in-fluid dispersions (nanofluids) in larninar flow.* International Journal of Heat and Mass Transfer, 2005. **48**(6): p. 1107-1116.
25. Eastman, J.A., et al., *Enhanced thermal conductivity through the development of*

nanofluids. Materials Research Society Symposium Proceeding, 1997. **457**.

26. Xie, H., et al., *Thermal Conductivity of Suspensions Containing Nanosized SiC Particles.* International Journal of Thermophysics and Heat Transfer, 2002. **23**: p. 571-580.
27. Shaikh, S., K. Lafdi, and R. Ponnappan, *Thermal conductivity improvement in carbon nanoparticle doped PAO oil: An experimental study.* Journal of Applied Physics, 2007. **101**(6): p. 1-8.
28. Keblinski, P., et al., *Mechanisms of heat flow in suspensions of nano-sized particles (nanofluids).* International Journal of Heat and Mass Transfer, 2002. **45**(4): p. 855-863.
29. Nagaska, Y. and A. Ngashima, *Absolute measurement of the thermal conductivity of electrically conducting liquids by the transient hot-wire method.* J. Phys. E:Sci. Instrum., 1981. **14**: p. 1435-1440.
30. Davis, W.R., *Hot-Wire Method for the Measurement of the Thermal Conductivity of Refractory Materials.* Compendium of Thermophysical Property Measurement Methods, Vol. 1 Survey of Measurement Techniques, 1984: p. 161.
31. Maxwell, J.C., *A Treatise on Electricity and Magnetism* Clarendon Press, Oxford, UK, 1881. **1**: p. 435.
32. Hamilton, R.L. and O.K. Crosser, *Thermal Conductivity of Heterogeneous Two-Component System.* IEC Fundam., 1962. **1**: p. 182-191.
33. Murshed, S.M.S., K.C. Leong, and C. Yang, *Enhanced thermal conductivity of TiO2 - water based nanofluids.* International Journal of Thermal Sciences, 2005. **44**(4): p. 367-373.
34. Yu, W. and S.U.S. Choi, *The role of interfacial layers in the enhanced thermal conductivity of nanofluids: A renovated Maxwell model.* Journal of Nanoparticle Research, 2003. **5**(1-2): p. 167-171.
35. Wang, X.Q. and A.S. Mujumdar, *Heat transfer characteristics of nanofluids: a review.* International Journal of Thermal Sciences, 2007. **46**(1): p. 1-19.
36. Sathyanarayanan, P.L. and R. Ramprabhu, *Study on the effect of different combinations of engine coolant additives on the heat dissipation rate of radiators.* Proceedings of the Institution of Mechanical Engineers Part D-Journal of Automobile Engineering, 2005. **219**(D10): p. 1173-1179.
37. Corsico, G., et al., *Poly(internal olefins) - Synthetic Lubricants and high-performance functional fluids.* Marcel Dekker, 1999: p. 53-62.

38. Lawrence, M., *All about oil.* California Scientific. December 11 2008. Web. April 20. 2010.

39. Torbjornsen, T., *Is synthetic oil better?* Aol Autos. June 01 2008. Web. December 12 2010.

40. Lee, S., et al., *Measuring Thermal Conductivity of Fluids Containing Oxide Nanoparticles.* Journal of Heat Transfer-Transactions of the Asme, 1999. **121**: p. 280-289.

41. Wang, X., X. Xu, and S.U.S. Choi, *Thermal Conductivity of Nanoparticle-Fluid Mixture.* Journal of Thermophysics and Heat Transfer, 1999. **13**: p. 474-480.

42. Xie, H., et al., *Thermal Conductivity Enhancement of Suspensions Containing Nanosized Alumina Particles.* Journal of Applied Physics, 2002. **91**: p. 4568-4572.

43. Masuda, H., et al., *Alteration of Thermal Conductivity and Viscosity of Liquid by Dispersing Ultra-Fine Particles.* Netsu Bussei, 1993. **7**: p. 227-233.

44. Das, S.K., et al., *Temperature dependence of thermal conductivity enhancement for nanofluids.* Journal of Heat Transfer-Transactions of the Asme, 2003. **125**(4): p. 567-574.

45. Wen, D.S. and Y.L. Ding, *Formulation of nanofluids for natural convective heat transfer applications.* International Journal of Heat and Fluid Flow, 2005. **26**(6): p. 855-864.

46. Li, C.H. and G.P. Peterson, *Experimental investigation of temperature and volume fraction variations on the effective thermal conductivity of nanoparticle suspensions (nanofluids).* Journal of Applied Physics, 2006. **99**(8).

47. Hong, K.S., T.K. Hong, and H.S. Yang, *Thermal conductivity of Fe nanofluids depending on the cluster size of nanoparticles.* Applied Physics Letters, 2006. **88**(3).

48. Xie, H.Q., et al., *Dependence of the thermal conductivity of nanoparticle-fluid mixture on the base fluid.* Journal of Materials Science Letters, 2002. **21**(19): p. 1469-1471.

49. Ding, Y.L., et al., *Heat transfer of aqueous suspensions of carbon nanotubes (CNT nanofluids).* International Journal of Heat and Mass Transfer, 2006. **49**(1-2): p. 240-250.

50. Eastman, J.A., et al., *Anomalously increased effective thermal conductivities of ethylene glycol-based nanofluids containing copper nanoparticles.* Applied Physics Letters, 2001. **78**(6): p. 718-720.

51. Yang, Y., et al., *Thermal and rheological properties of carbon nanotube-in-oil dispersions.* Journal of Applied Physics, 2006. **99**(11).

52. Choi, S.U.S. and J.A. Eastman, *Enhancing thermal conductivity of fluids with nanoparticles.* Developments and Applications of Non-newtonian Flows, 1995. **FED 231**: p. 99-105.

53. Li, Q. and Y.M. Xuan, *Experimental investigation of transport properties of nanofluids.* Heat Transfer Science & Technology. Higher Education Press, 2000: p. 757-762.

54. Chun, B.H., H.U. Kang, and S.H. Kim, *Effect of alumina nanoparticles in the fluid on heat transfer in double pipe heat exchanger system.* Korean Journal of Chemical Engineering, 2008. **25**: p. 966-971.

55. Choi, C., H.S. Yoo, and J.M. Oh, *Preparation and heat transfer properties of nanoparticle-in-transformer oil dispersions as advanced energy-efficient coolants.* Current Applied Physics, 2008. **8**(6): p. 710-712.

56. Heris, S.Z., S.G. Etemad, and A.N. Esfahany, *Experimental investigation of oxide nanofluids laminar flow convective heat transfer.* International Communications in Heat and Mass Transfer, 2006. **33**(4): p. 529-535.

57. Dittus, F.W. and L.M.K. Boelter, *Pioneers in Heat-Transfer - Heat-Transfer in Automobile Radiators of the Tubular Type (Reprinted from University of California Publications in Engineering, Vol 2, Pg 443-461, 1930.* International Communications in Heat and Mass Transfer, 1985. **12**(1): p. 3-22.

58. Gnielinski, V., *New Equations for Heat and Mass-Transfer in Turbulent Pipe and Channel Flow.* International Chemical Engineering, 1976. **16**(2): p. 359-368.

59. Das, S.K., N. Putra, and W. Roetzel, *Pool boiling characteristics of nano-fluids.* International Journal of Heat and Mass Transfer, 2003. **46**(5): p. 851-862.

60. Das, S.K., N. Putra, and W. Roetzel, *Pool boiling of nano-fluids on horizontal narrow tubes.* International Journal of Multiphase Flow, 2003. **29**(8): p. 1237-1247.

61. Bang, I.C. and S.H. Chang, *Boiling heat transfer performance and phenomena of Al2O3-water nano-fluids from a plain surface in a pool.* International Journal of Heat and Mass Transfer, 2005. **48**(12): p. 2407-2419.

62. Wen, D.S. and Y.L. Ding, *Experimental investigation into the pool boiling heat transfer of aqueous based gamma-alumina nanofluids.* Journal of Nanoparticle Research, 2005. 7(2): p. 265-274.

63. Timofeeva, E.V., et al., *Thermal conductivity and particle agglomeration in alumina nanofluids: Experiment and theory.* Physical Review E, 2007. **76**(6).

64. Dittus, P.W. and L.M.K. Boelter, University of California (Berkley) Pub. Eng., 1930. **2**(13): p. 443-461.

65. Seider, E.N. and G.E. Tate, *Heat transfer and pressure drop of liquids in tubes.* Industrial & Engineering Chemistry Research, 1936. **28**(12): p. 1429-1435.

66. Oliver, D.R., *Effect of Natural Convection on Viscous-Flow Heat Transfer in Horizontal Tubes.* Chem. Eng. Sci., 1962. **17**: p. 335-350.

67. Eubank, C.C. and W.S. Proctor, *Effect of Natural Convection on Heat Transfer with Laminar Flow in Tubes.* Master of Science Thesis in Chemical Engineering, Massachusetts Institute of Technology, Cambridge, MA, 1951.

68. Watson, E.S., *Differential Microcalorimeter.* 1966.

69. Wunderlich, B., *Thermal Analysis.* New York: Academic Press, 1990: p. 137-140.

70. Maiga, S.E.B., et al., *Heat transfer behaviours of nanofluids in a uniformly heated tube.* Superlattices and Microstructures, 2004. **35**(3-6): p. 543-557.

71. Venerus, D.C., et al., *Study of thermal transport in nanoparticle suspensions using forced Rayleigh scattering.* Journal of Applied Physics, 2006. **100**(9).

72. Nnanna, A.G.A., *Experimental model of temperature-driven nanofluid.* Journal of Heat Transfer-Transactions of the Asme, 2007. **129**(6): p. 697-704.

73. Buongiorno, J., *Convective transport in nanofluids.* Journal of Heat Transfer-Transactions of the Asme, 2006. **128**(3): p. 240-250.

74. Lee, J. and I. Mudawar, *Assessment of the effectiveness of nanofluids for single-phase and two-phase heat transfer in micro-channels.* International Journal of Heat and Mass Transfer, 2007. **50**(3-4): p. 452-463.

75. Zhou, S.Q. and R. Ni, *Measurement of the specific heat capacity of water-based Al2O3 nanofluid.* Applied Physics Letters, 2008. **92**(9).

76. Prasher, R., et al., *Measurements of nanofluid viscosity and its implications for thermal applications.* Applied Physics Letters, 2006. **89**(13).

77. Tseng, W.J. and K.C. Lin, *Rheology and colloidal structure of aqueous TiO2 nanoparticle suspensions.* Materials Science and Engineering a-Structural Materials Properties Microstructure and Processing, 2003. **355**(1-2): p. 186-192.

78. Studart, A.R., et al., *Rheology of concentrated suspensions containing weakly attractive alumina nanoparticles.* Journal of the American Ceramic Society, 2006. **89**(8): p. 2418-2425.

79. Zhou, S.Q., R. Ni, and D. Funfschilling, *Effects of shear rate and temperature on viscosity of alumina polyalphaolefins nanofluids.* Journal of Applied Physics, 2010. **107**(5).

80. Kok, P.J.A.H., et al., *Near-wall particle depletion in a flowing colloidal suspension.* Journal of Rheology, 2002. **46**(2): p. 481-493.

81. Li, Q. and Y.M. Xuan, *Convective heat transfer and flow characteristics of Cu-water nanofluid.* Science in China Series E-Technological Sciences, 2002. **45**(4): p. 408-416.

82. Choi, S.U.S., et al., *Anomalous thermal conductivity enhancement in nanotube suspensions.* Applied Physics Letters, 2001. **79**(14): p. 2252-2254.

83. Patel, H.E., et al., *Thermal conductivities of naked and monolayer protected metal nanoparticle based nanofluids: Manifestation of anomalous enhancement and chemical effects.* Applied Physics Letters, 2003. **83**(14): p. 2931-2933.

84. Xie, H.Q., et al., *Nanofluids containing multiwalled carbon nanotubes and their enhanced thermal conductivities.* Journal of Applied Physics, 2003. **94**(8): p. 4967-4971.

85. Wen, D. and Y. Ding, *Effective Thermal Conductivity of Aqueous Suspensions of Carbon Nanotubes (Carbon Nanotube Nanofluids).* Journal of Thermophysics and Heat Transfer, 2004. **18**: p. 481-485.

86. Hwang, Y., et al., *Thermal Conductivity and Lubrication Characteristics of Nanofluids.* Current Applied Physics, 2006. **6S1**: p. e67-e71.

87. Lee, D., J.W. Kim, and B.G. Kim, *A new parameter to control heat transport in nanofluids: Surface charge state of the particle in suspension.* Journal of Physical Chemistry B, 2006. **110**(9): p. 4323-4328.

88. Liu, M.S., et al., *Enhancement of thermal conductivity with Cu for nanofluids using chemical reduction method.* International Journal of Heat and Mass Transfer, 2006. **49**(17-18): p. 3028-3033.

89. Faulkner, D.J., et al., *Enhanced Heat Transfer through the Use of Nanofluids in Forced Convection.* Proceedings of IMECE 2004.

90. Wen, D.S. and W. Ding, *Natural convective heat transfer of suspensions of titanium dioxide nanoparticles (Nanofluids).* Ieee Transactions on

Nanotechnology, 2006. **5**(3): p. 220-227.

91. Heris, S.Z., M.N. Esfahany, and S.G. Etemad, *Experimental investigation of convective heat transfer of Al2O3/water nanofluid in circular tube.* International Journal of Heat and Fluid Flow, 2007. **28**(2): p. 203-210.
92. Nguyen, C.T., et al., *Heat transfer enhancement using Al2O3-water nanofluid for an electronic liquid cooling system.* Applied Thermal Engineering, 2007. **27**(8-9): p. 1501-1506.

93. Williams, W., J. Buongiorno, and L.W. Hu, *Experimental investigation of turbulent convective heat transfer and pressure loss of alumina/water and zirconia/water nanoparticle colloids (nanofluids) in horizontal tubes.* Journal of Heat Transfer-Transactions of the Asme, 2008. **130**(4).

94. Jwo, C.S., et al., *Performance of overall heat transfer in multi-channel heat exchanger by alumina nanofluid.* Journal of Alloys and Compounds, 2010. **504S**: p. S385-S388.

95. Lee, J.K., et al., *The effects of nanoparticles on absorption heat and mass transfer performance in NH3/H2O binary nanofluids.* International Journal of Refrigeration, 2010. **33**: p. 269-275.

APPENDIX A

ENHANCEMENT OF THERMAL CONDUCTIVITY

Author/Year	Nanofluid	Particle size (nm)	Concentration (vol%)	Enhancement ratio
Masuda et al./1993[43]	Al_2O_3/water			
	(31.85°C)	13	1.30 – 4.30	1.109 – 1.324
	(46.85°C)	13	1.30 – 4.30	1.100 – 1.296
	(66.85°C)	13	1.30 – 4.30	1.092 – 1.262
	SiO_2/water			
	(31.85°C)	12	1.10 – 2.30	1.010 – 1.011
	(46.85°C)	12	1.10 – 2.30	1.009 – 1.010
	(66.85°C)	12	1.10 – 2.30	1.005 – 1.007
	TiO_2/water			
	(31.85°C)	27	3.25 – 4.30	1.080 – 1.105
	(46.85°C)	27	3.25 – 4.30	1.084 – 1.108
	(66.85°C)	27	3.15 – 4.30	1.075 – 1.099
Lee et al./1999[40]	Al_2O_3/water	38.4	1.00 – 4.30	1.03 – 1.10
	CuO/water	23.6	1.00 – 3.41	1.03 – 1.12
	Al_2O_3/ethylene glycol	38.4	1.00 – 5.00	1.03 – 1.18
	CuO/ethylene glycol	23.6	1.00 – 4.00	1.05 – 1.23
Wang et al./1999[41]	Al_2O_3/water	28	0.19 – 1.59	1.01 – 1.10
	CuO/water	23		
	Al_2O_3/ethylene glycol	28	5.00 – 8.00	1.25 – 1.41
	CuO/ethylene glycol	23	6.20 – 14.80	1.24 – 1.54
	Al_2O_3/engine oil	28	2.25 – 7.40	1.05 – 1.30
	Al_2O_3/pump oil	28	5.00 -7.10	1.13 – 1.20
Xuan et al./2000[5]	Cu/water	100	2.50 – 7.50	1.22 – 1.75
	Cu/transformer oil	100	2.50 – 7.50	1.12 – 1.43
Choi et al./2001[82]	MWCNT/ PAO oil	25x50000	0.04 – 1.02	1.02 – 2.57

Xie et al./2002[26]	SiC/water	26 sphere	0.78 – 4.18	1.03 – 1.17
		600 cylinder	1.00 – 4.00	1.06 – 1.24
	SiC/ethylene glycol	26 sphere	0.89 – 3.50	1.04 – 1.13
		600 cylinder	1.00 – 4.00	1.06 – 1.23
Xie et al./2002[48]	Al_2O_3/water	60.4	5.00	1.23
	Al_2O_3ethylene glycol	60.4	5.00	1.29
	Al_2O_3/pump oil	60.4	5.00	1.38
Das et al./2003[44]	CuO/water			
	(21°C)	28.6	1.00 – 4.00	1.07 – 1.14
	(36°C)	28.6	1.00 – 4.00	1.22 – 1.26
	(51°C)	28.6	1.00 – 4.00	1.29 – 1.36
Patel et al./2003[83]	Citrate-reduced			
	Ag/water (30°C)	60-70	0.001	1.030
	(60°C)	60-70	0.001	1.04
	Citrate-reduced			
	Au/water (30°C)	10-20	0.00013	1.03
		10-20	0.00026	1.05
	(60°C)	10-20	0.00013	1.05
		10-20	0.00026	1.08
	Thiolate-coverd			
	Au/toluene			
	(30°C)	3-4	0.005	1.03
		3-4	0.008	1.06
		3-4	0.011	1.06
	(60°C)	3-4	0.005	1.05
		3-4	0.008	1.07
		3-4	0.011	1.09
Xie et al./2003[84]	MWCNT/water	15x30000	0.40 – 1.00	1.03 – 1.07
	MWCNT/ ethylene glycol	15x30000	0.23 – 1.00	1.02 – 1.13
Wen et al./2004[85]	MWCNT/water (20°C)	20-60	0.04 – 0.84	1.04 – 1.24
	MWCNT/water (45°C)	20-60	0.04 – 0.84	1.05 – 1.31
Assael et al./2005[12]	DWCNT/water	0.75	5	1.03
		1.00	5	1.08
	MWCNT/water	0.60	130x>10000	1.34
		0.60	130x>10000	1.28
Chon et al./2005[13]	Al_2O_3/water	11	1.00	1.09
	(21°C)	47	1.00	1.03
		150	1.00	1.004
		47	4.00	1.08
	Al_2O_3/water	11	1.00	1.15
	(71°C)	47	1.00	1.10
		150	1.00	1.09

		47	4.00	1.29
Hong et al./2005[14]	Fe/ethylene glycol	10	0.20 – 0.55	1.13 – 1.18
Liu et al./2005[15]	MWCNT/ ethylene glycol	20 - 50	0.20 – 1.00	1.02 – 1.12
	MWCNT/ engine oil	20 - 50	1.00 – 2.00	1.09 – 1.30
Marquis et al./2005[16]	SWCNT/ diesel oil	10-50x 0.3-10 μm	0.25 – 1.00	1.10 – 1.46
		20-300x 1-100μm	0.25 – 1.00	1.30 – 2.17
	MWCNT/PAO oil	20-300x 1-100μm	1.00	2.83
Murshed et al./2005[33]	TiO_2(+CTAB)/ water	15	0.50 – 5.00	1.05 – 1.30
		10 x 40	0.50 – 5.00	1.08 – 1.33
Wen et al./2005[45]	Al_2O_3/water		0.31 – 0.72	1.02 – 1.06
Ding et al./2006[49]	MWCNT/ water (20°C)		0.05 – 0.49	1.00 – 1.10
	MWCNT/ water (25°C)		0.05 – 0.49	1.07 – 1.27
	MWCNT/ water (30°C)		0.05 – 0.49	1.18 – 1.79
Hwang et al./2006[86]	CuO/water		1.00	1.05
	SiO_2/water		1.00	1.03
	MWCNT/water		1.00	1.07
	CuO/ethylene glycol		1.00	1.09
	MWCNT/miner al oil		0.50	1.09
Lee et al./2006[87]	CuO/water (pH=3)	25	0.03 – 0.30	1.04 – 1.12
	CuO/water (pH=6)	25	0.03 – 0.30	1.02 – 1.07
Liu et al./2006[88]	Cu/water		0.05	1.04
		50 - 100	0.10	1.24
		75 - 100	0.10	1.24
		100 - 200	0.05	1.12
		100 - 300	0.10	1.11
		130 - 200	0.05	1.09
		130 - 300	0.20	1.10
		250	0.20	1.04
		200 x 500	0.20	1.13

Li et al./2006[46]	Al_2O_3/water (27.5°C)	36	2.00 – 10.00	1.08 – 1.11
	Al_2O_3/water (32.5°C)	36	2.00 – 10.00	1.15 – 1.22
	Al_2O_3/water (34.7°C)	36	2.00 – 10.00	1.18 – 1.29
	CuO/water (28.9°C)	29	2.00 – 6.00	1.35 – 1.36
	CuO/water (31.3°C)	29	2.00 – 6.00	1.35 – 1.50
	CuO/water (33.4°C)	29	2.00 – 6.00	1.38 – 1.51
Yang et al./2006[51]	MWCNT/PAO oil		0.04 – 0.34	1.06 – 3.00
Shaikh et al./2007[27]	CNT/PAO oil	10 -15nm	0.1 – 1.0	1.34 – 2.61
	Exfoliated graphite /PAO oil		0.1 – 1.0	1.18 – 2.31
	Carbon nanofiber /PAO oil		0.1 – 1.0	1.11 – 2.03
Choi et al./2008[55]	Al_2O_3 (sphere)/ pure oil	13	0.5 – 4.0	1.05 – 1.21
	Al_2O_3 (fiber)/pure oil	2 x 20-200	0.5	1.04
	AIN/pure oil	50	0.5	1.08

APPENDIX B

ENHANCEMENT OF HEAT TRANSFER COEFFCIENTS

Author/Year	Nanofluid	Particle size (nm)	Concentration (vol%)	Enhancement ratio
Pak and Cho /1998[17]	Al_2O_3/water	13	1.34	1.07 – 1.30
		13	2.78	1.24 - 1.35
	TiO_2/water	27	0.99	0.93 - 1.09
		27	2.04	0.98 - 1.16
Putra et al./2003[18]	Al_2O_3/water	131.2	1.00	0.85 – 1.02
	(L/D=0.5)	131.2	4.00	0.70 – 0.85
	Al_2O_3/water	131.2	1.00	0.87 – 1.04
	(L/D=1.0)	131.2	1.00	0.63 – 0.82
Xuan et al./2003[19]	Cu/water	<100	0.30	0.99 – 1.05
		<100	0.50	1.01 – 1.08
		<100	0.80	1.07 – 1.13
		<100	1.00	1.13 – 1.15
		<100	1.20	1.14 – 1.21
		<100	1.50	1.23 – 1.27
		<100	2.00	1.25 – 1.35
Faulkner et al./2004 [89]	MWCNT/water		1.10	1.01 – 4.69
	q"=0.1W/cm^2		2.20	1.93 – 2.21
			4.40	1.20 – 1.71
	MWCNT/water		1.10	0.48 – 1.99
	q"=0.5W/cm^2		2.20	1.17 – 1.63
			4.40	0.90 – 1.19
Wen et al./2004[11]	Al_2O_3/water	42	0.60	1.04 – 1.12
	(x/D=63)	42	1.00	1.09 – 1.22
		42	1.60	1.25 – 1.38
	Al_2O_3/water	42	0.60	1.10 – 1.20
	(x/D=116)	42	1.00	1.12 – 1.20
		42	1.60	1.26 – 1.35
Zhou et al./2004[20]	Cu/acetone	80-100	0.0-4.0g/l	HTC

				increases with addition of Cu nanoparticles
Wen et al./2005[45]	TiO_2/water (pH=3)	34	0.19	0.85 – 0.98
Yang et al./2005[24]	Graphite/ transmission Fluid (50°C)	1000-2000x2	0.77	0.97 – 1.02
		0-40	0.97	1.21 – 1.31
	Graphite/ transmission Fluid (70°C)	1000-2000x2	0.77	0.97 – 1.03
		0-40	0.97	1.14 – 1.29
	Graphite/mixture of two syn. oils (50°C)	1000-2000x2	0.75	0.99 – 1.05
		0-40	0.75	1.01 – 1.05
	Graphite/mixture of two syn. oils (70°C)	1000-2000x2	0.75	1.05 – 1.15
		0-40	0.75	1.05 – 1.13
Wen et al./2006[90]	TiO_2/water (pH=3)	34	0.35	0.77 – 0.95
		34	0.57	0.64 – 0.87
Ding et al./2006[49]	MWCNT/water x/D=26.2		0.048	1.63 – 1.93
	MWCNT/water x/D=63.3		0.048	1.96 – 2.27
	MWCNT/water x/D=116.		0.048	1.63 – 2.28
	MWCNT/water x/D=147		0.048	1.49 – 2.65
	MWCNT/water x/D=174		0.048	1.33 – 2.53
Heris et al./2006[56]	Al_2O_3/water	20	0.20	1.04 – 1.10
		20	1.00	1.12 – 1.19
		20	2.00	1.13 – 1.31
		20	2.50	1.12 – 1.38
		20	3.00	1.08 – 1.41
	CuO.water	50-60	0.20	1.02 – 1.11
		50-60	1.00	1.06 – 1.20
		50-60	2.00	1.03 – 1.27
		50-60	2.50	1.02 – 1.36
		50-60	3.00	1.02 – 1.38
He et al./2007[91]	TiO_2/water	20	0.24	0.99 – 1.03
		20	0.60	1.06 – 1.24
		20	1.10	1.16 – 1.22
Nguyen et al./2007[92]	Al_2O_3/water	47	1.0	1.10 – 1.15
		47	3.1	1.16 – 1.19
		47	6.8	1.37 – 1.41
Choi et al./2008[55]	Al_2O_3 (sphere)/	13	0.5	1.01 – 1.03

	pure oil			
	Al_2O_3 (fiber)/pure oil	2 x 20-200	0.5	1.14 – 1.17
	AIN/pure oil	50	0.5	1.24 – 1.29
Williams et al./2008 [93]	ZrO_2/water	46 60	0.9-3.6 0.2-0.9	Considerable enhancement observed
Jwo et al./2010[94]	Al_2O_3/water (30°C)	20 20	0.5 wt% 1.0 wt%	1.01 – 1.06 1.13 – 1.18
	Al_2O_3/water (40°C)	20 20	0.5 wt% 1.0 wt%	1.02 – 1.08 1.12 – 1.18
Lee et al./2010[95]	Al_2O_3/mix of NH_3/H_2O	35 35 35 35	0.01 0.02 0.04 0.06	1.14 1.29 1.21 1.2
	CNT/mix of NH_3/H_2O	25 x 10000 25 x 10000 25 x 10000 25 x 10000 25 x 10000	0.01 0.02 0.04 0.06 0.08	1.09 1.18 1.17 1.15 1.15

APPENDIX C

RESULTS OF HEAT TRANSFER MEASUREMENT

1. 25nm Cu nanofluids (Cu25)

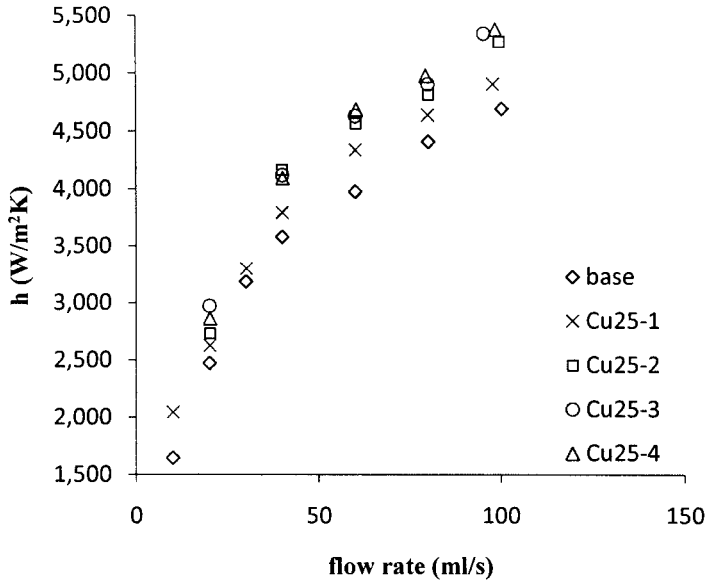

Fig C.1.1 Heat transfer coefficient (h) as a function of flow rate at 40°C.

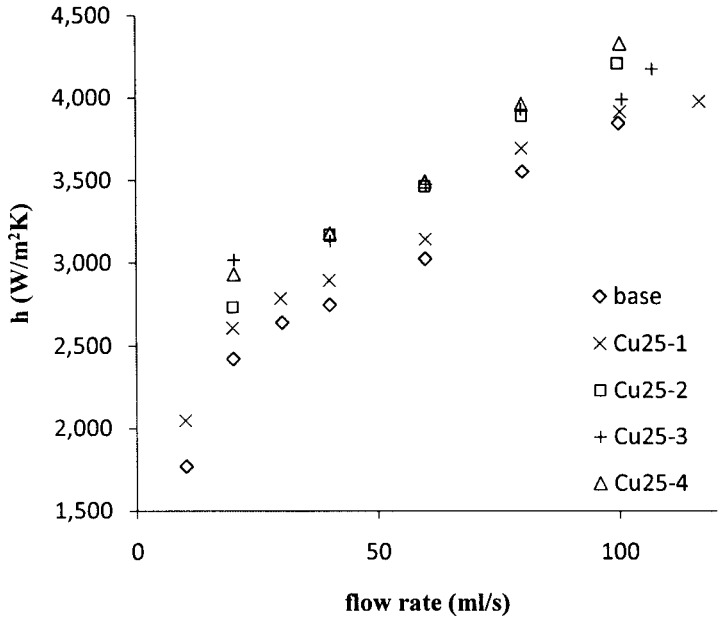

Fig C.1.2 Heat transfer coefficient (h) as a function of flow rate at 65°C.

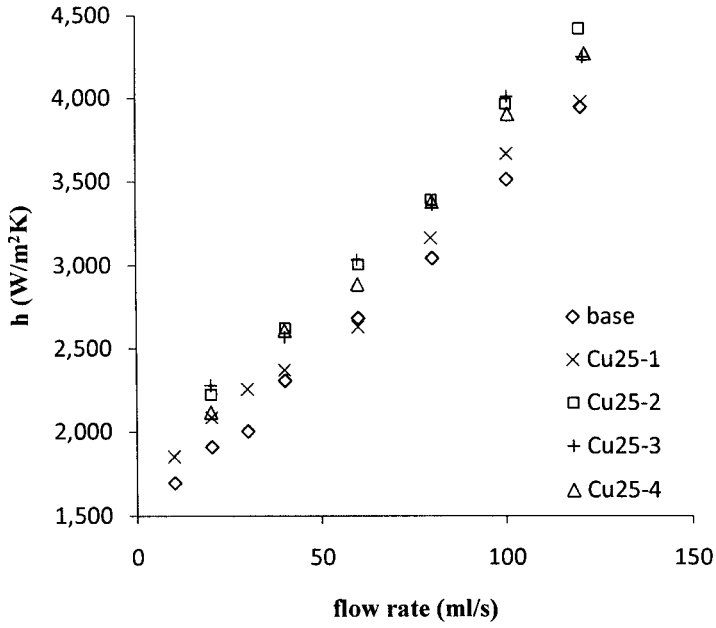

Fig C.1.3 Heat transfer coefficient (h) as a function of flow rate at 90°C.

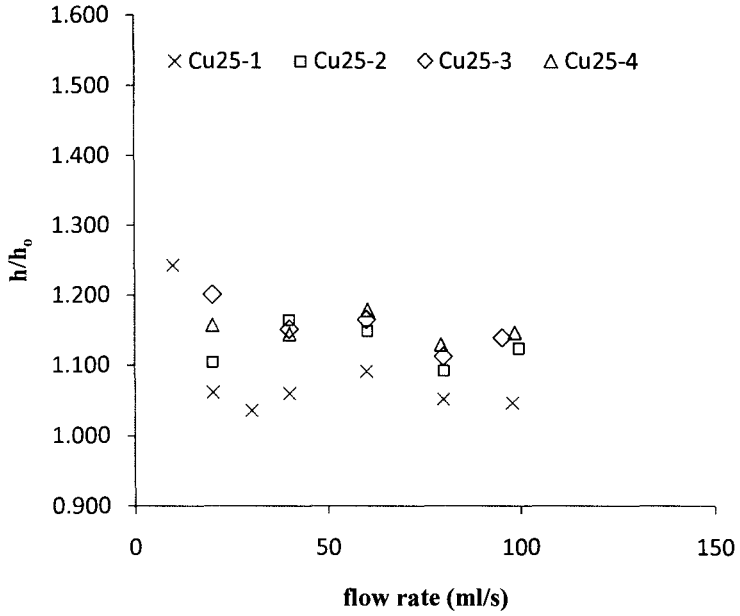

Fig C.1.4 Enhancement ratio (h/h_0) as a function of flow rate at 40°C.

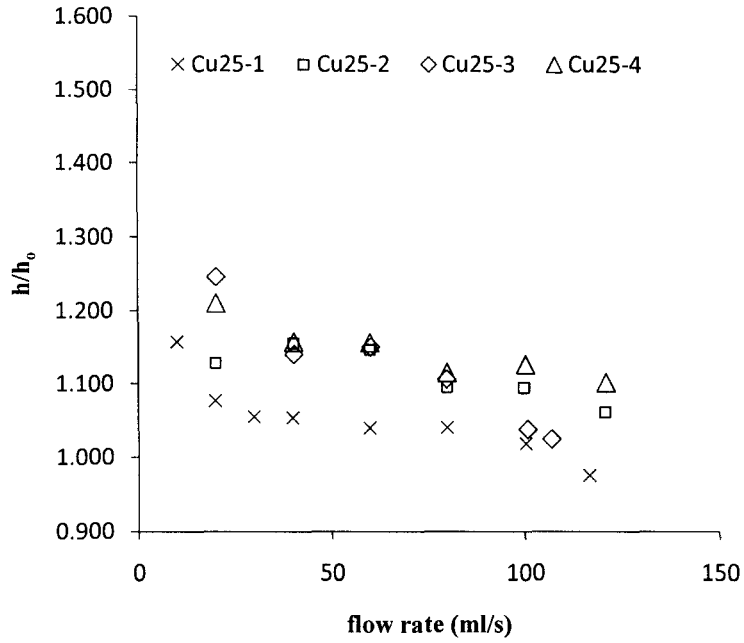

Fig C.1.5 Enhancement ratio (h/h_0) as a function of flow rate at 65°C.

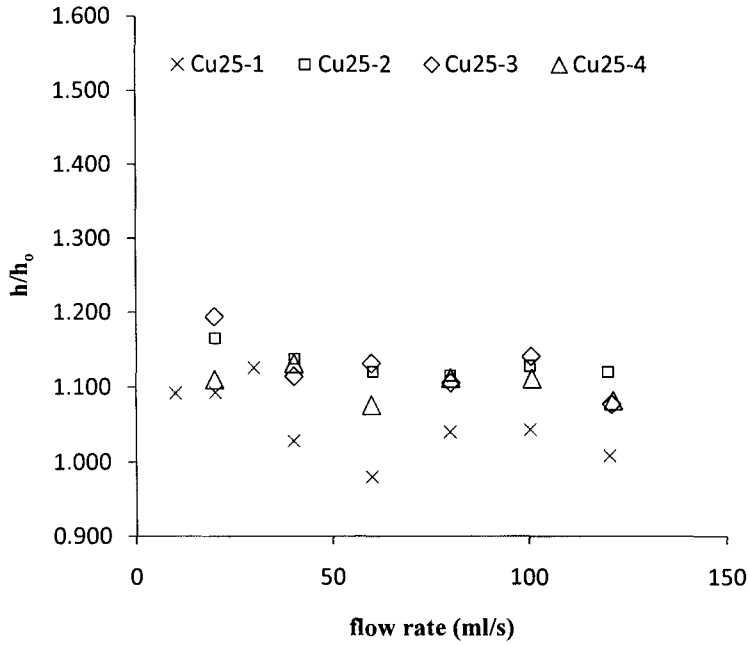

Fig C.1.6 Enhancement ratio (h/h_0) as a function of flow rate at 90°C.

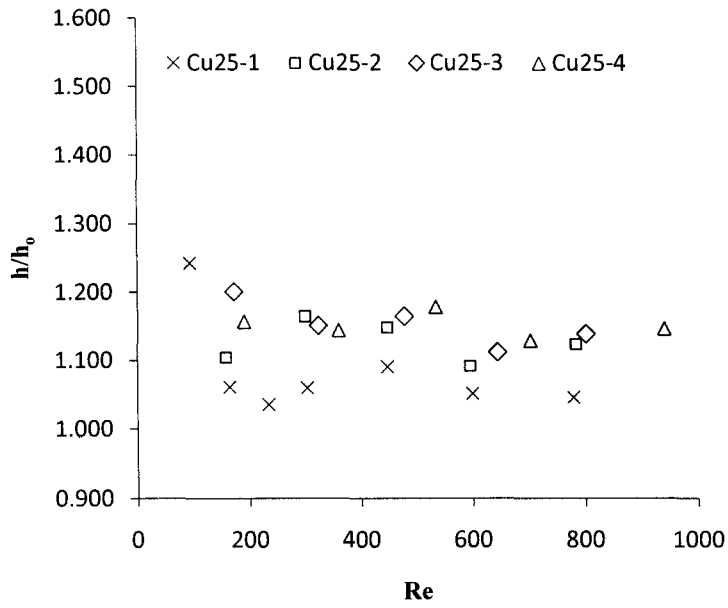

Fig C.1.7 Enhancement ratio (h/h_0) as a function of Reynolds number (Re) at 40°C.

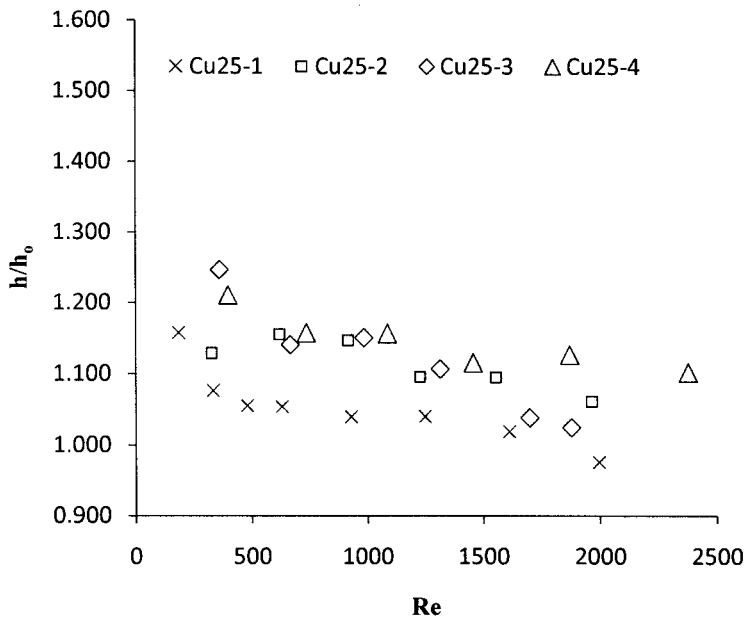

Fig C.1.8 Enhancement ratio (h/h_0) as a function of Reynolds number (Re) at 65°C.

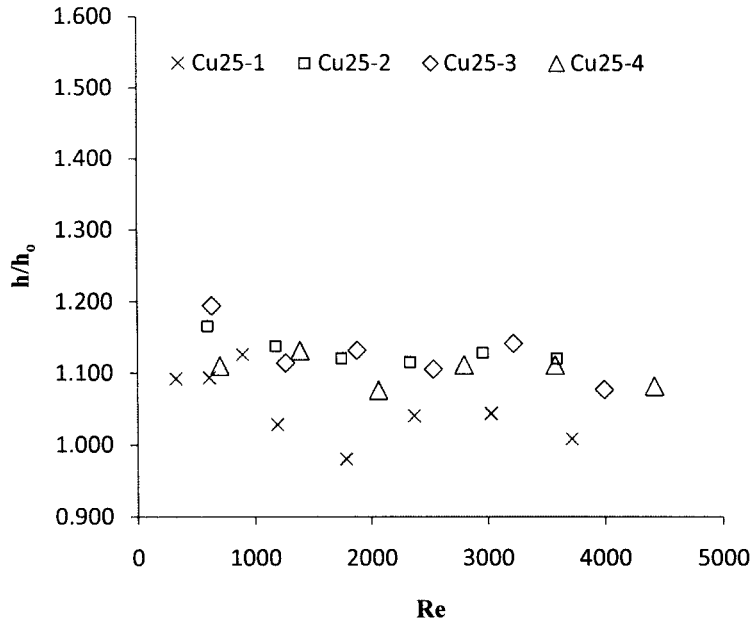

Fig C.1.9 Enhancement ratio (h/h_0) as a function of Reynolds number (Re) at 90°C.

2. 40-60nm Cu nanofluids (Cu40)

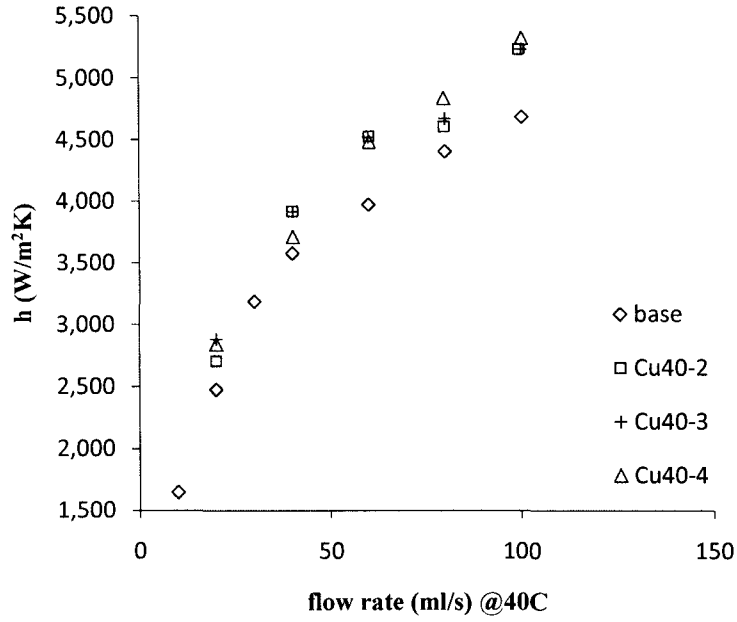

Fig C.2.1 Heat transfer coefficient (h) as a function of flow rate at 40°C.

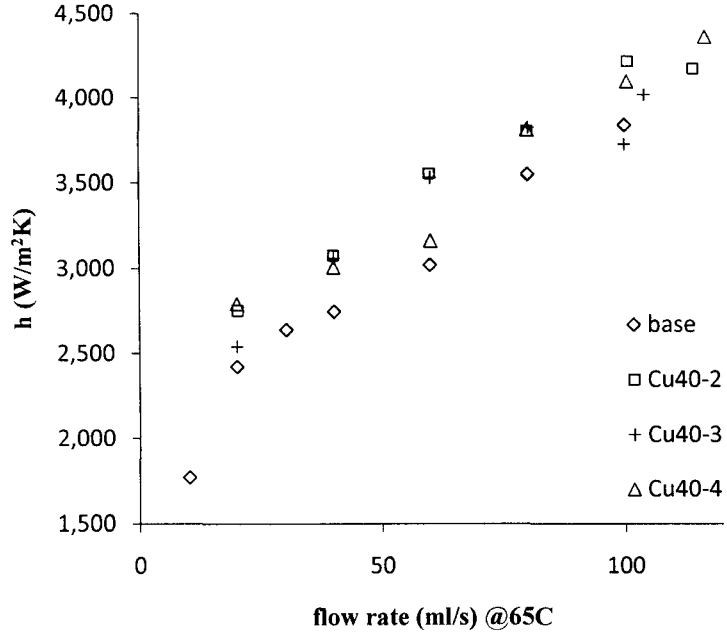

Fig C.2.2 Heat transfer coefficient (h) as a function of flow rate at 65°C.

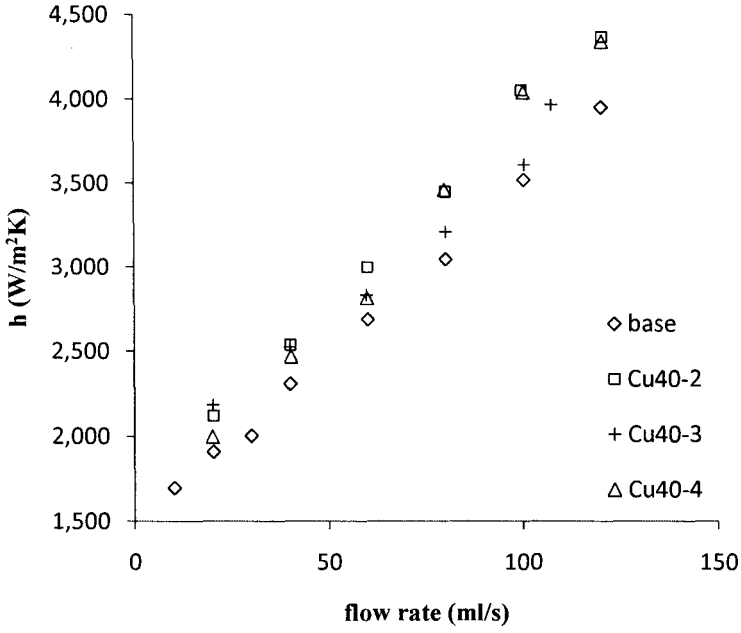

Fig C.2.3 Heat transfer coefficient (h) as a function of flow rate at 90°C.

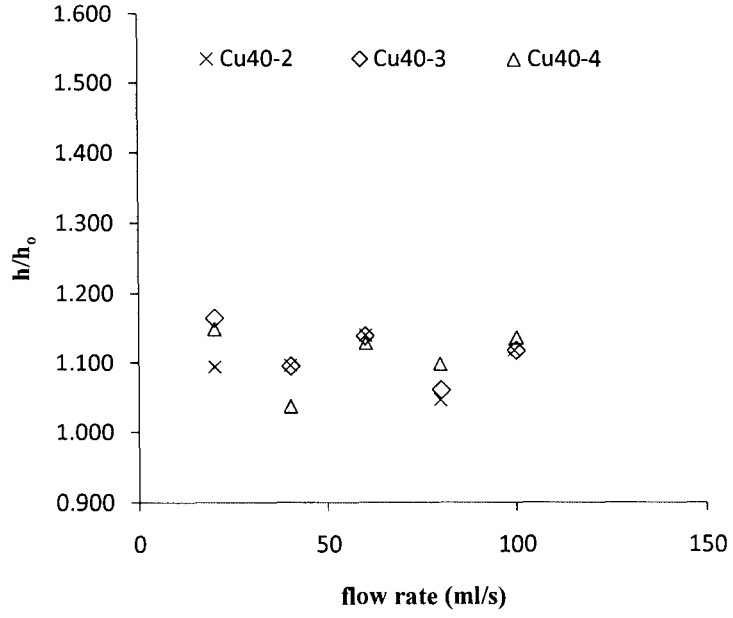

Fig C.2.4 Enhancement ratio (h/h_0) as a function of flow rate at 40°C.

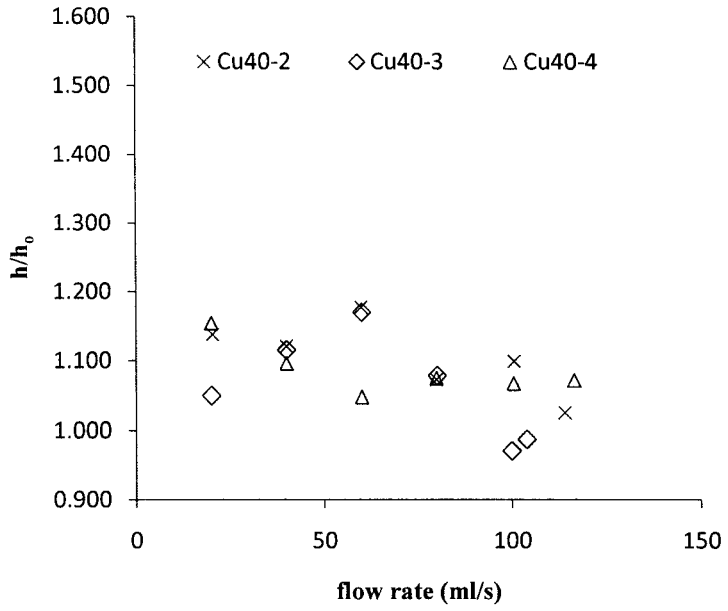

Fig C.2.5 Enhancement ratio (h/h_0) as a function of flow rate at 65°C.

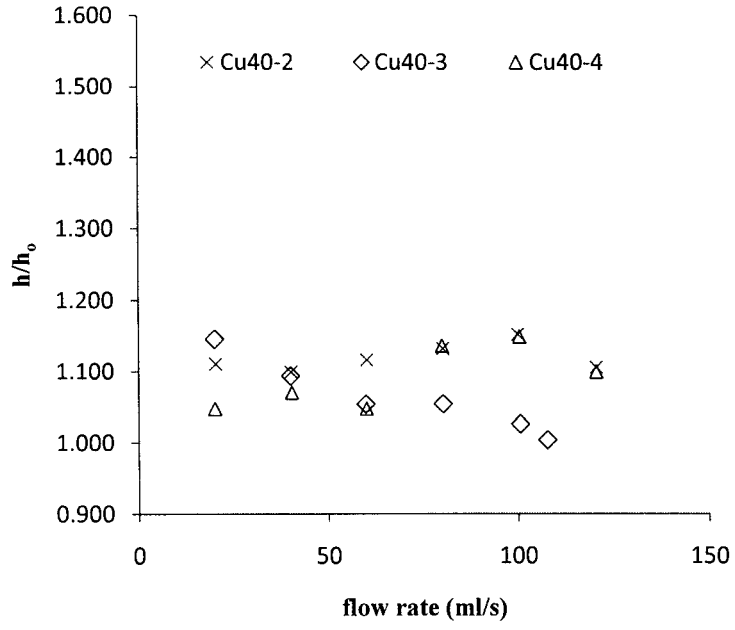

Fig C.2.6 Enhancement ratio (h/h_0) as a function of flow rate at 90°C.

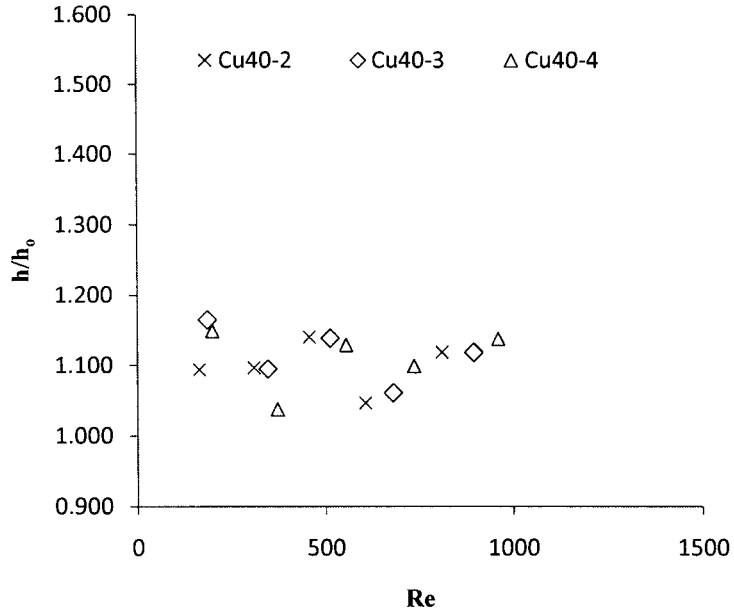

Fig C.2.7 Enhancement ratio (h/h_0) as a function of Reynolds number (Re) at 40°C.

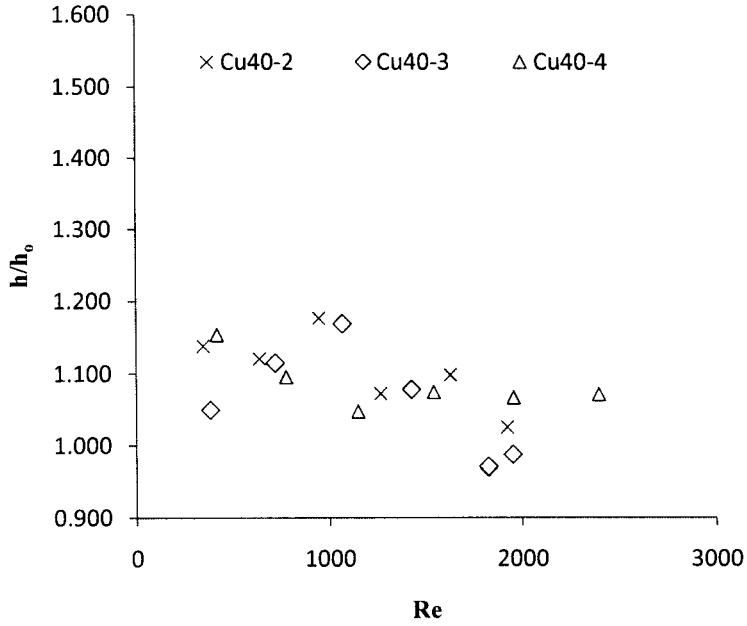

Fig C.2.8 Enhancement ratio (h/h_0) as a function of Reynolds number (Re) at 65°C.

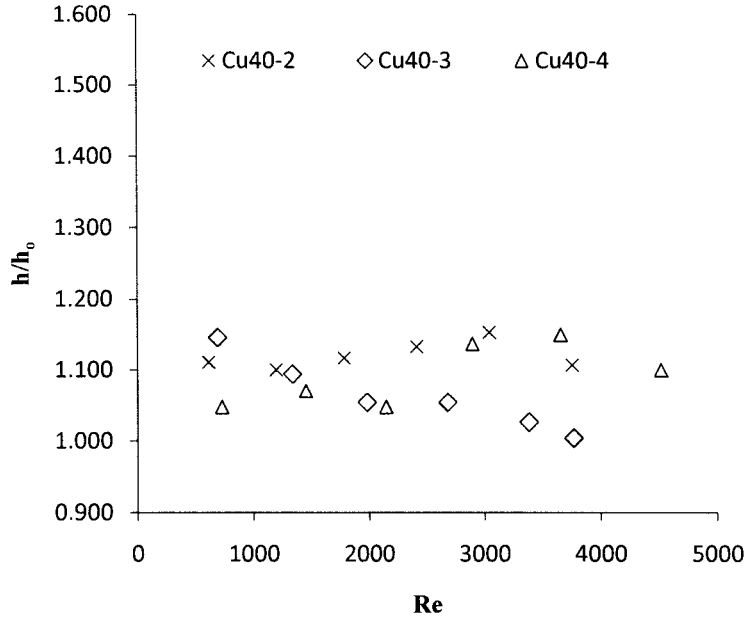

Fig C.2.9 Enhancement ratio (h/h_0) as a function of Reynolds number (Re) at 90°C.

3. 60-80nm Cu nanofluids (Cu60)

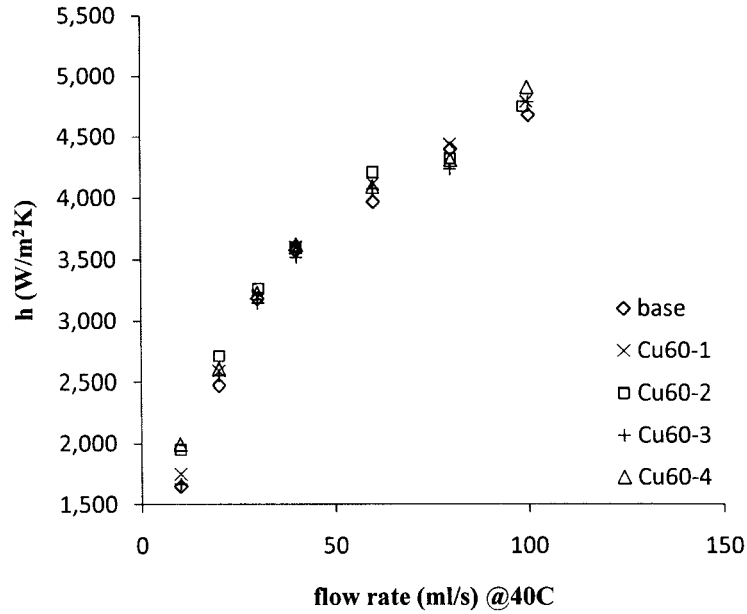

Fig C.3.1 Heat transfer coefficient (h) as a function of flow rate at 40°C.

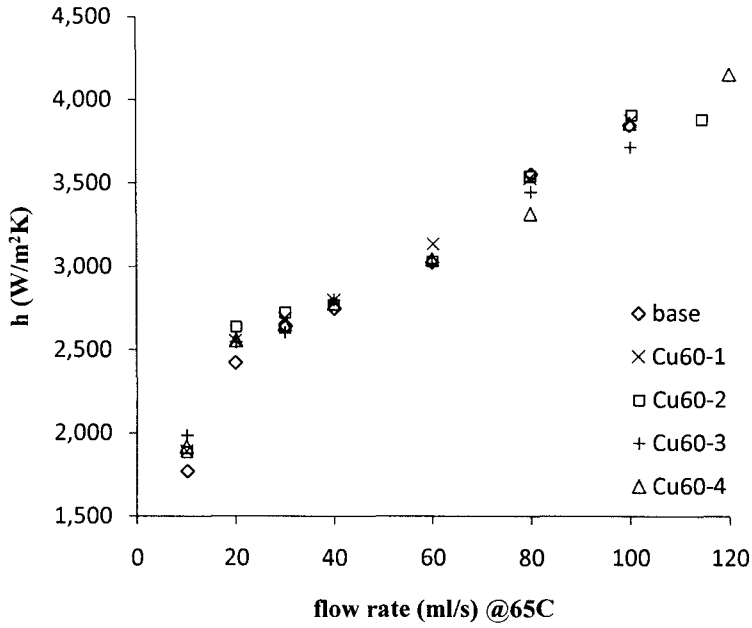

Fig C.3.2 Heat transfer coefficient (h) as a function of flow rate at 65°C.

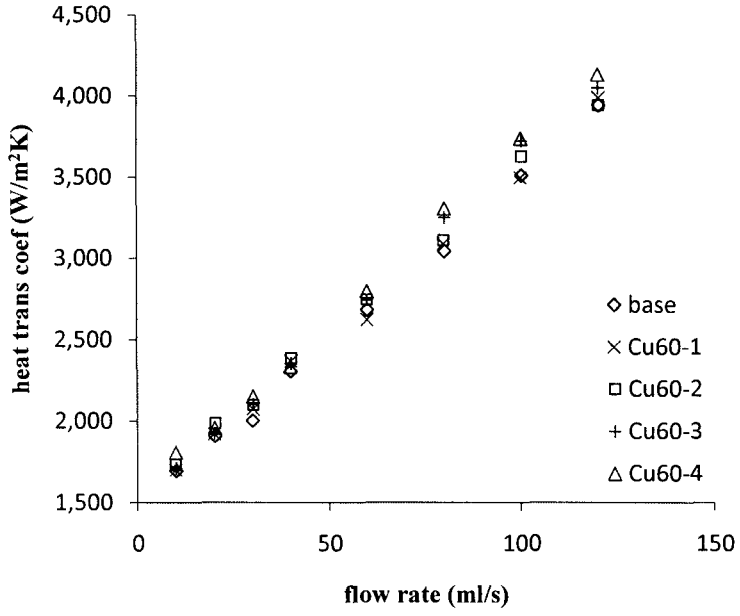

Fig C.3.3 Heat transfer coefficient (h) as a function of flow rate at 90°C.

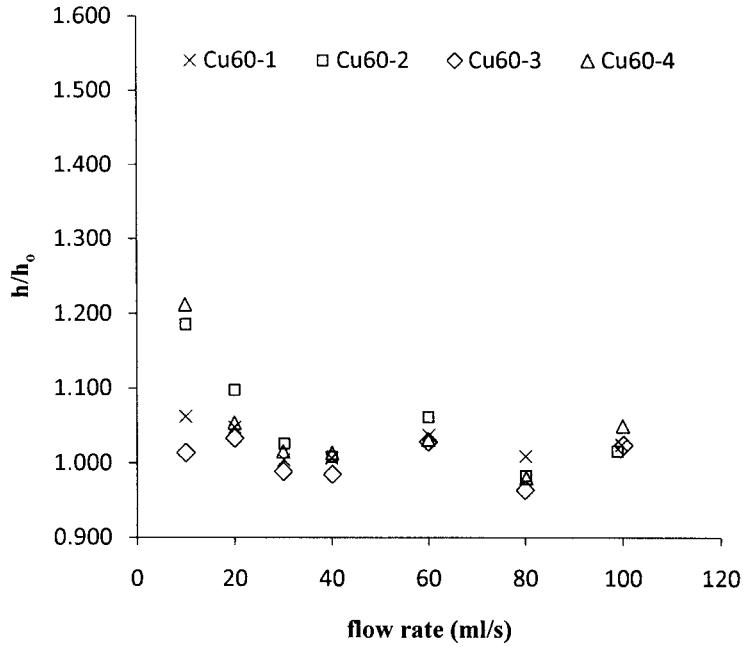

Fig C.3.4 Enhancement ratio (h/h_0) as a function of flow rate at 40°C.

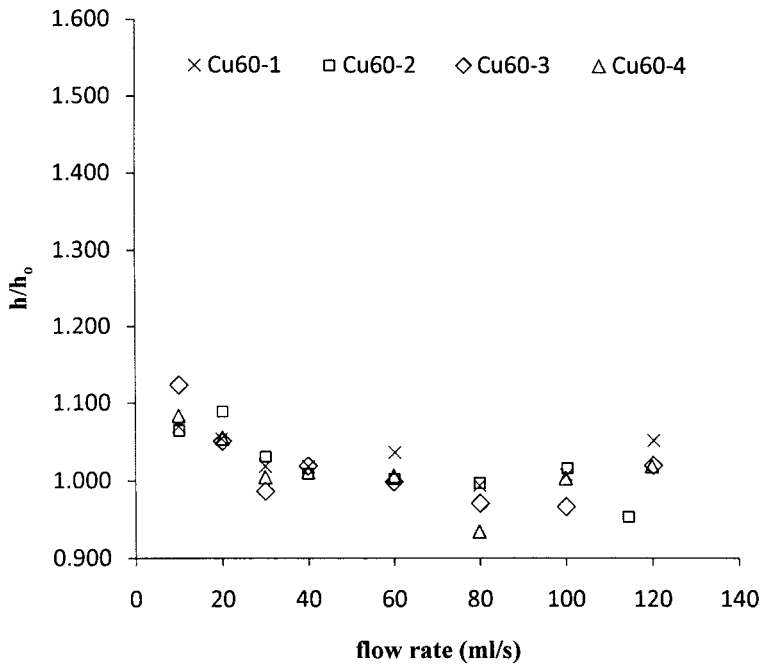

Fig C.3.5 Enhancement ratio (h/h_0) as a function of flow rate at 65°C.

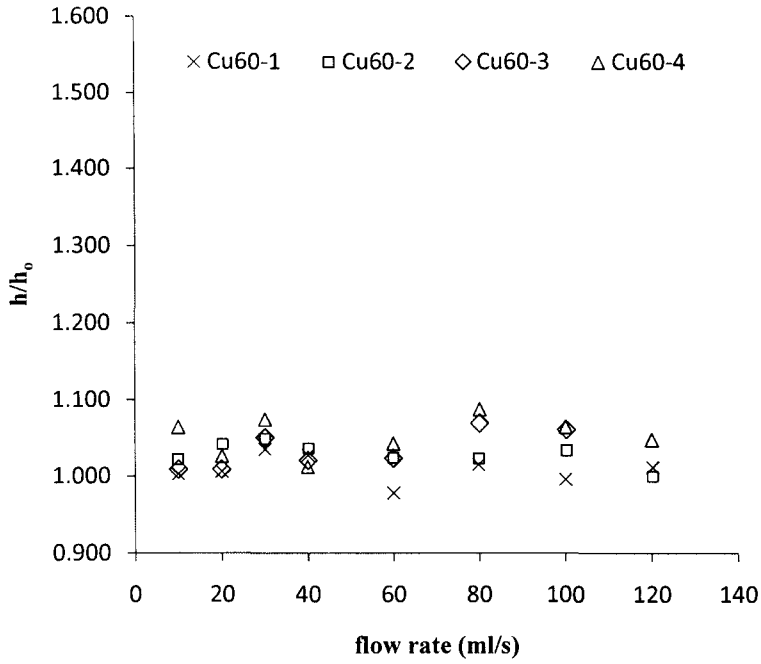

Fig C.3.6 Enhancement ratio (h/h_0) as a function of flow rate at 90°C.

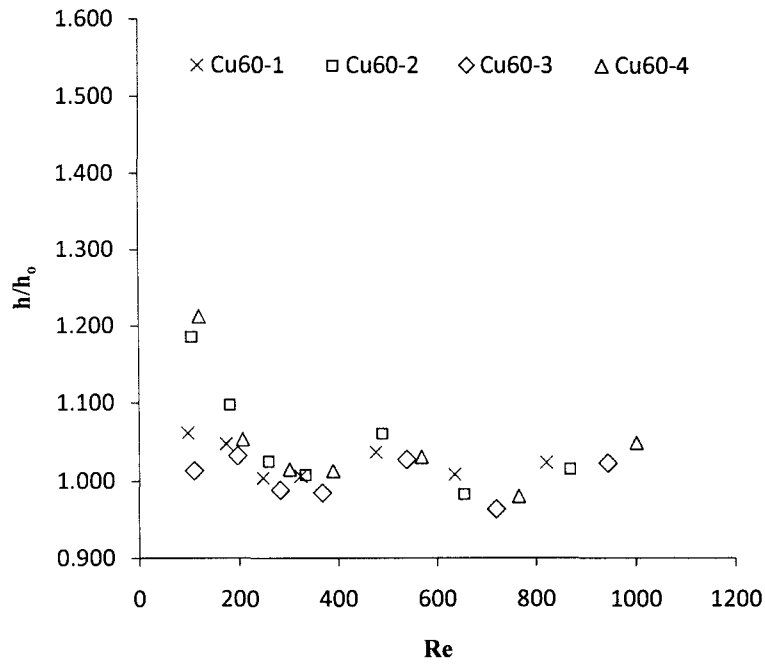

Fig C.3.7 Enhancement ratio (h/h_0) as a function of Reynolds number at 40°C.

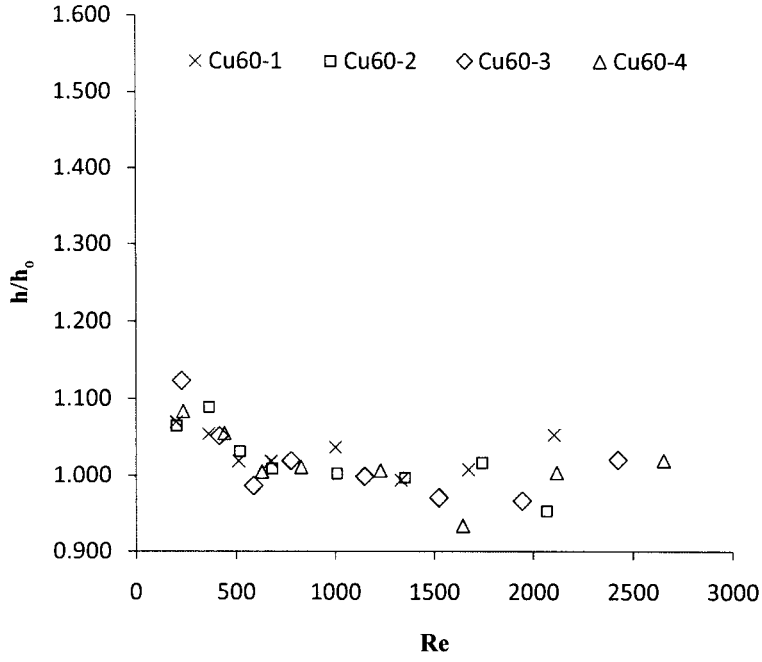

Fig C.3.8 Enhancement ratio (h/h_0) as a function of Reynolds number at 65°C.

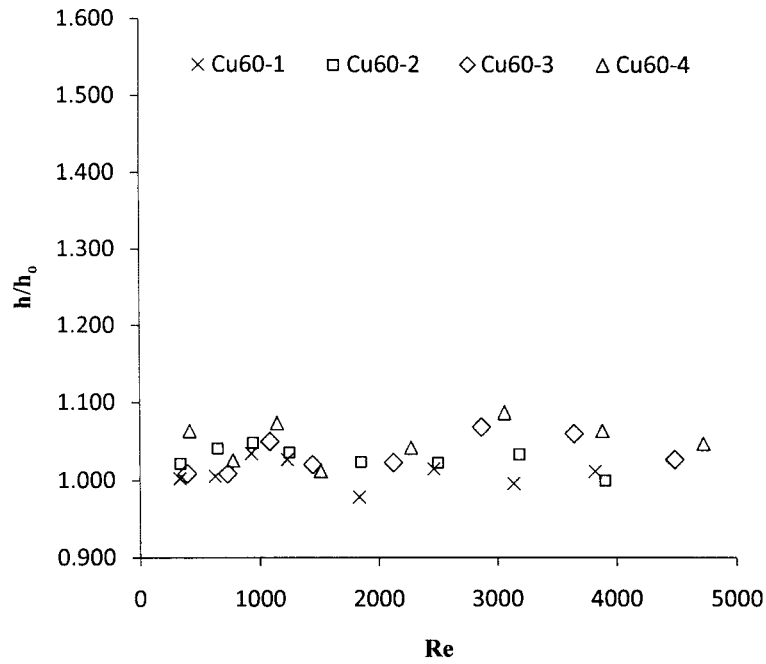

Fig C.3.9 Enhancement ratio (h/h_0) as a function of Reynolds number at 90°C.

APPENDIX D

RESULTS BASED ON MODIFIED XUAN ET AL.'S CORRELATION

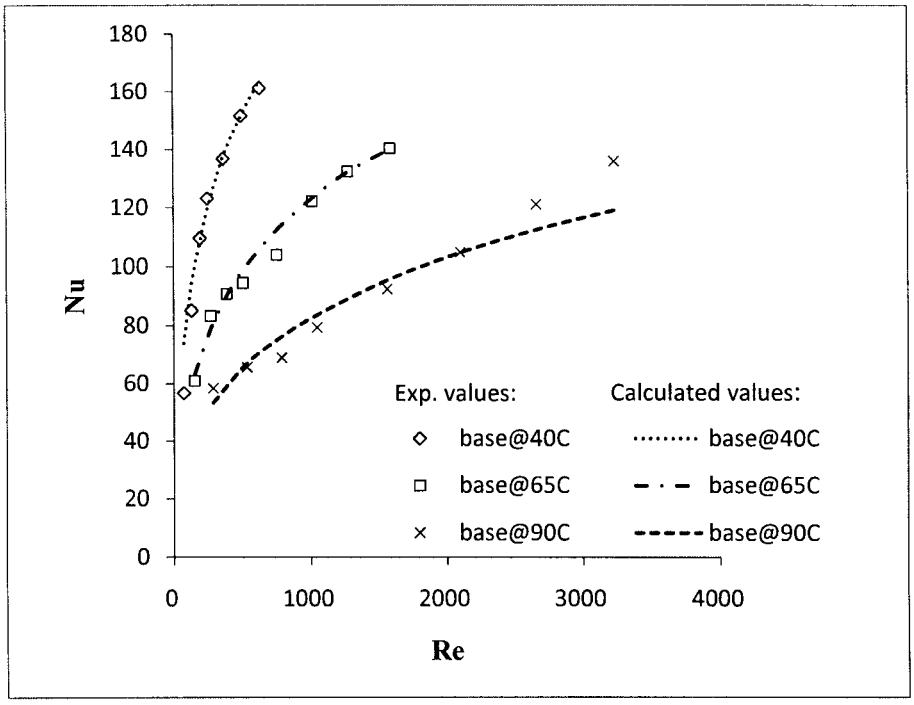

Fig D.1 Comparison between experimental data and calculated values for base fluid at 40°C, 65°C, and 90°C.

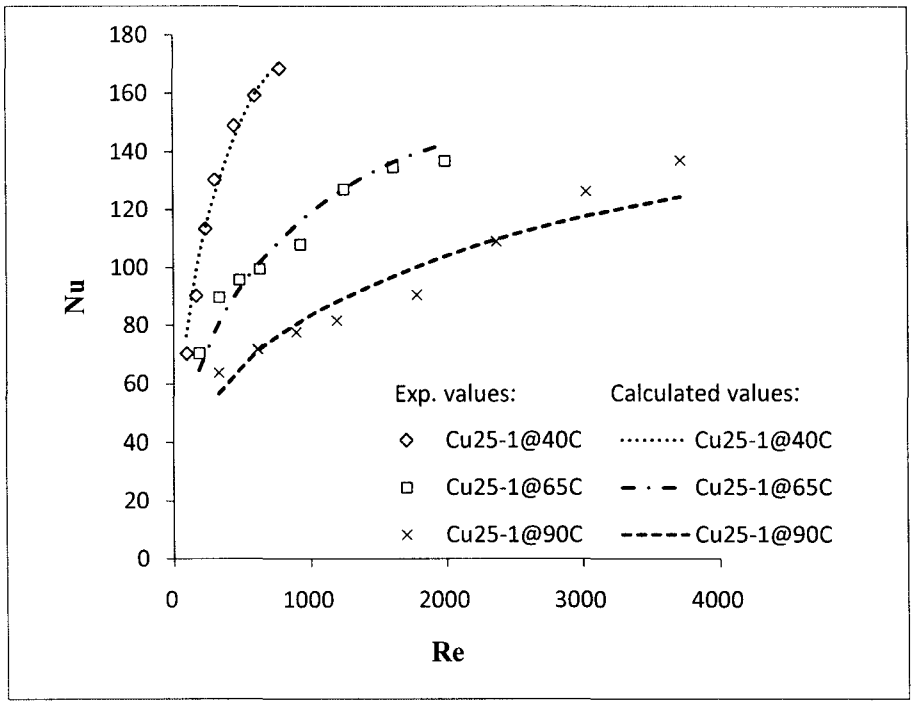

Fig D.2 Comparison between experimental data and calculated values for Cu25-1 nanofluid at 40°C, 65°C, and 90°C.

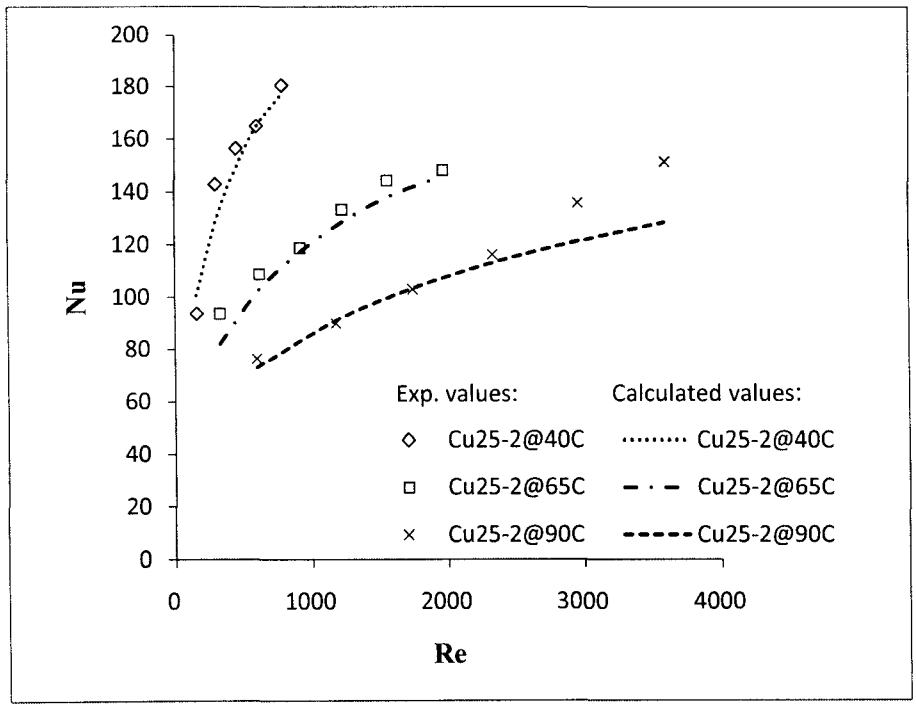

Fig D.3 Comparison between experimental data and calculated values for Cu25-2 nanofluid at 40°C, 65°C, and 90°C.

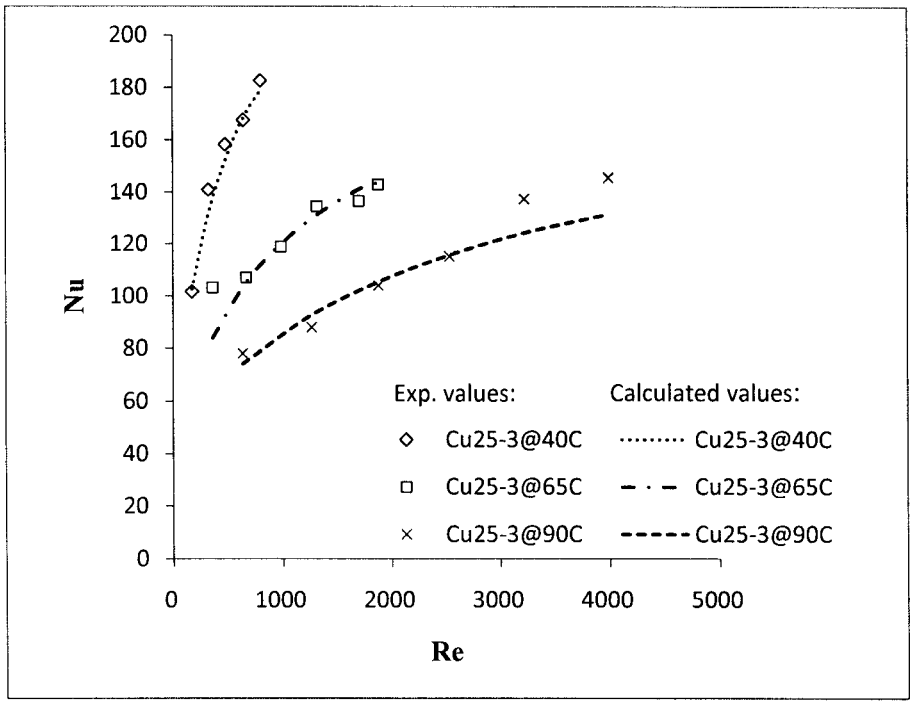

Fig D.4 Comparison between experimental data and calculated values for Cu25-3 nanofluid at 40°C, 65°C, and 90°C.

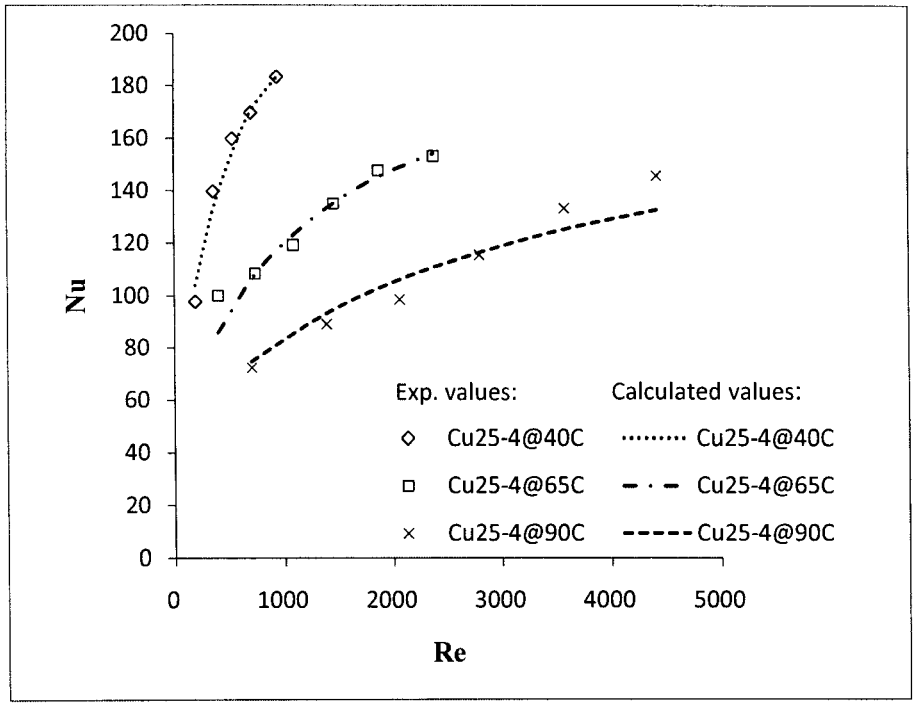

Fig D.5 Comparison between experimental data and calculated values for Cu25-4 nanofluid at 40°C, 65°C, and 90°C.

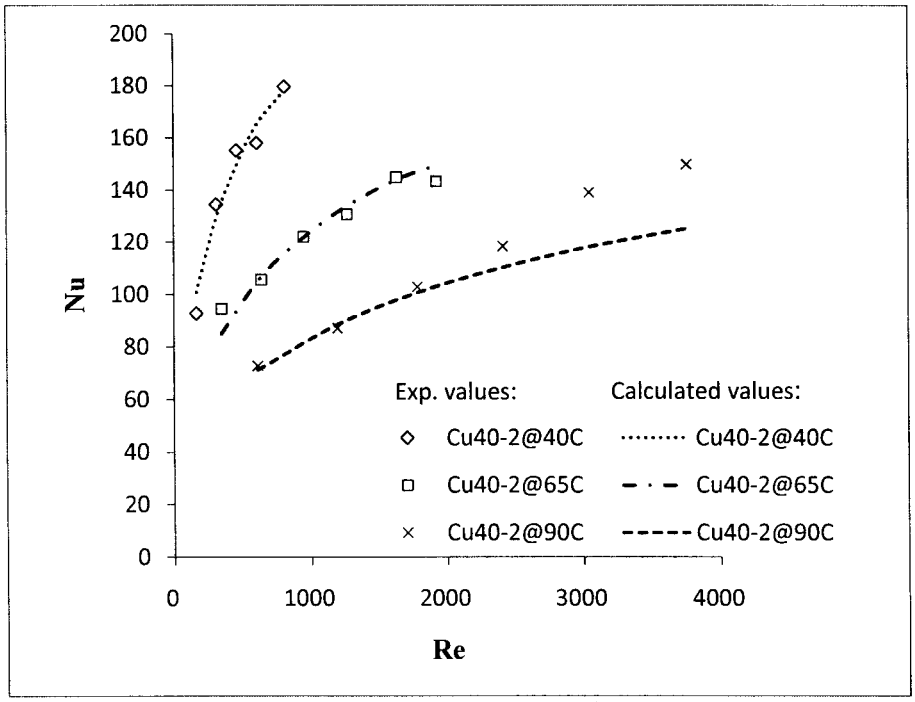

Fig D.6 Comparison between experimental data and calculated values for Cu40-2 nanofluid at 40°C, 65°C, and 90°C.

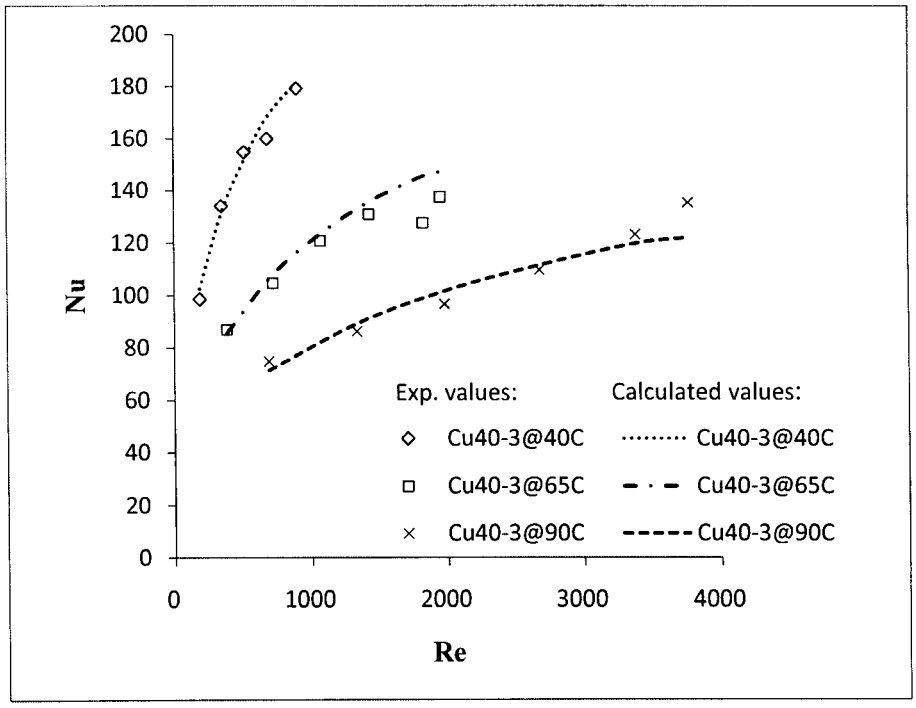

Fig D.7 Comparison between experimental data and calculated values for Cu40-3 nanofluid at 40°C, 65°C, and 90°C.

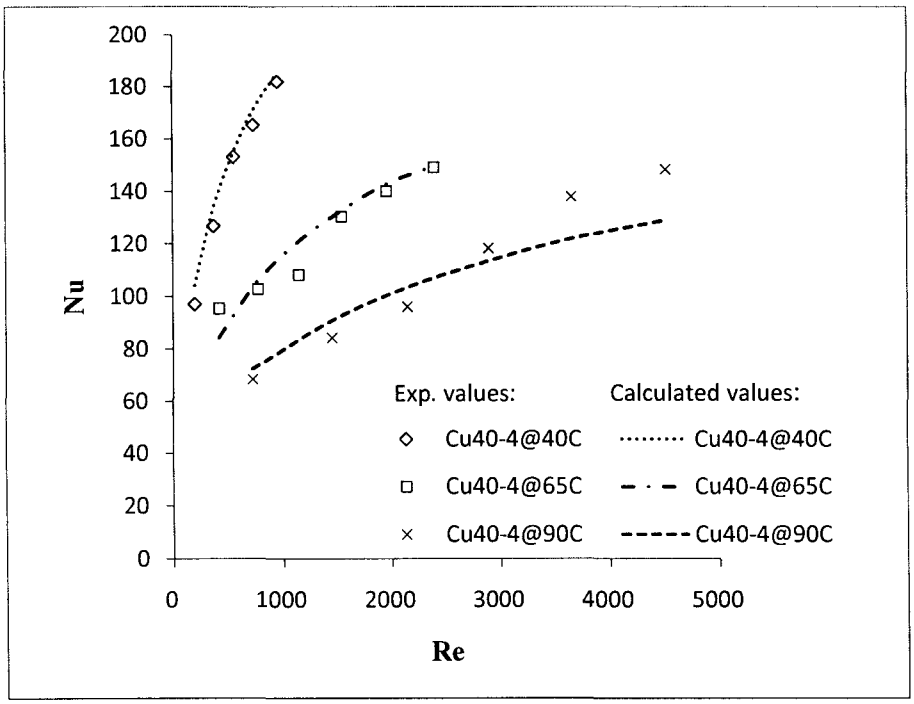

Fig D.8 Comparison between experimental data and calculated values for Cu40-4 nanofluid at 40°C, 65°C, and 90°C.

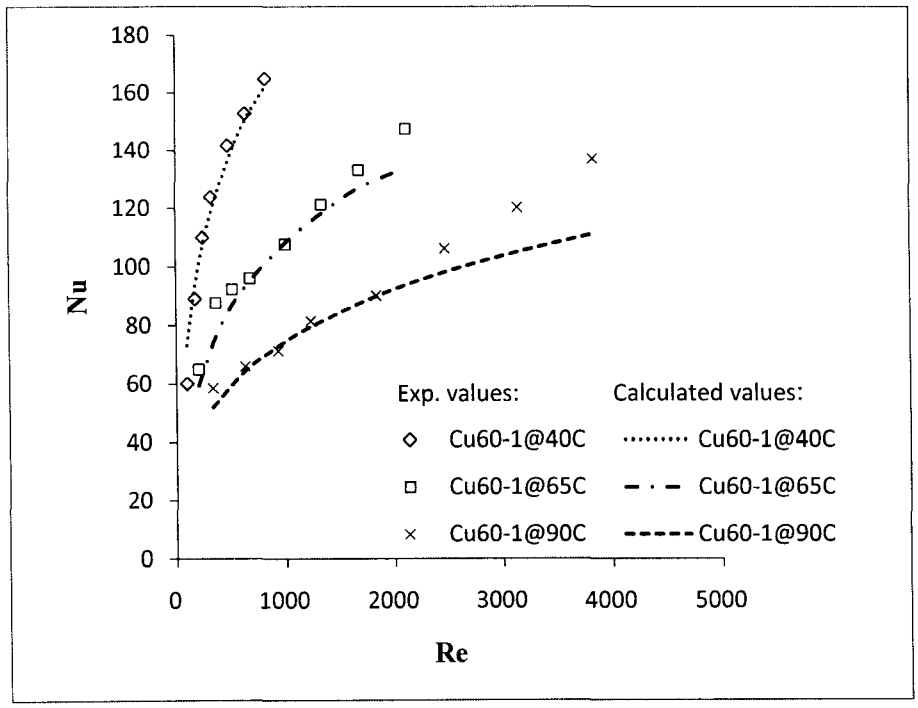

Fig D.9 Comparison between experimental data and calculated values for Cu60-1 nanofluid at 40°C, 65°C, and 90°C.

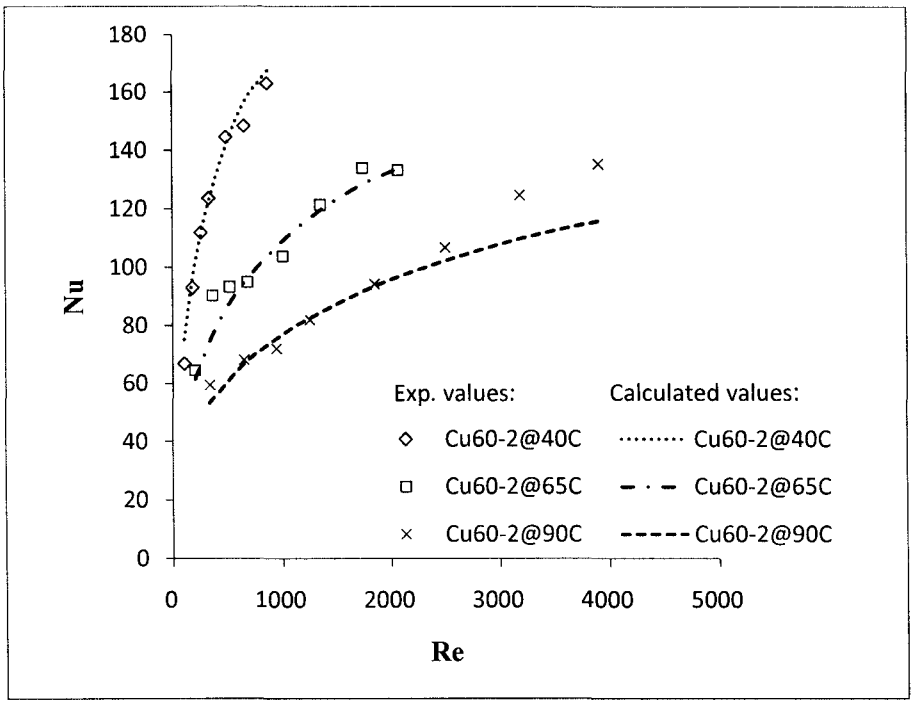

Fig D.10 Comparison between experimental data and calculated values for Cu60-2 nanofluid at 40°C, 65°C, and 90°C.

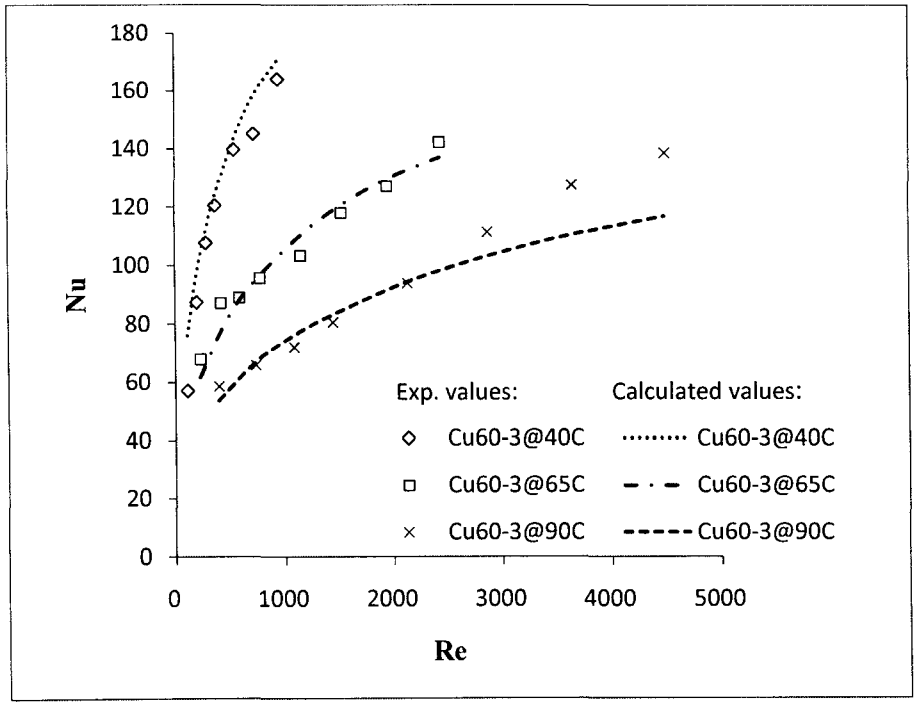

Fig D.11 Comparison between experimental data and calculated values for Cu60-3 nanofluid at 40°C, 65°C, and 90°C.

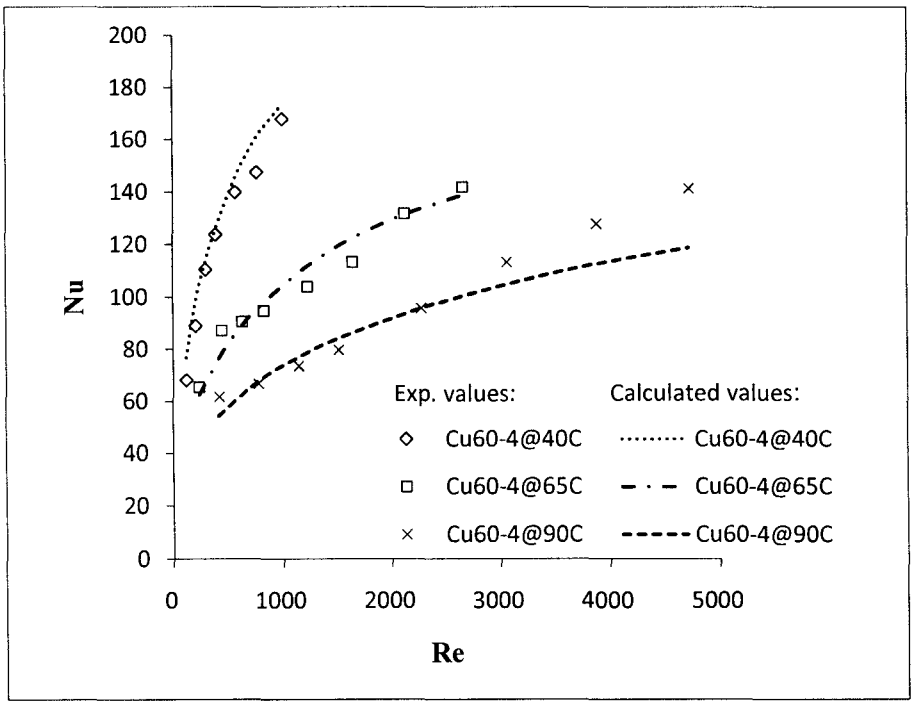

Fig D.12 Comparison between experimental data and calculated values for Cu60-4 nanofluid at 40°C, 65°C, and 90°C.

APPENDIX E

RESULTS BASED ON MODIFIED YANG ET AL.'S CORRELATION

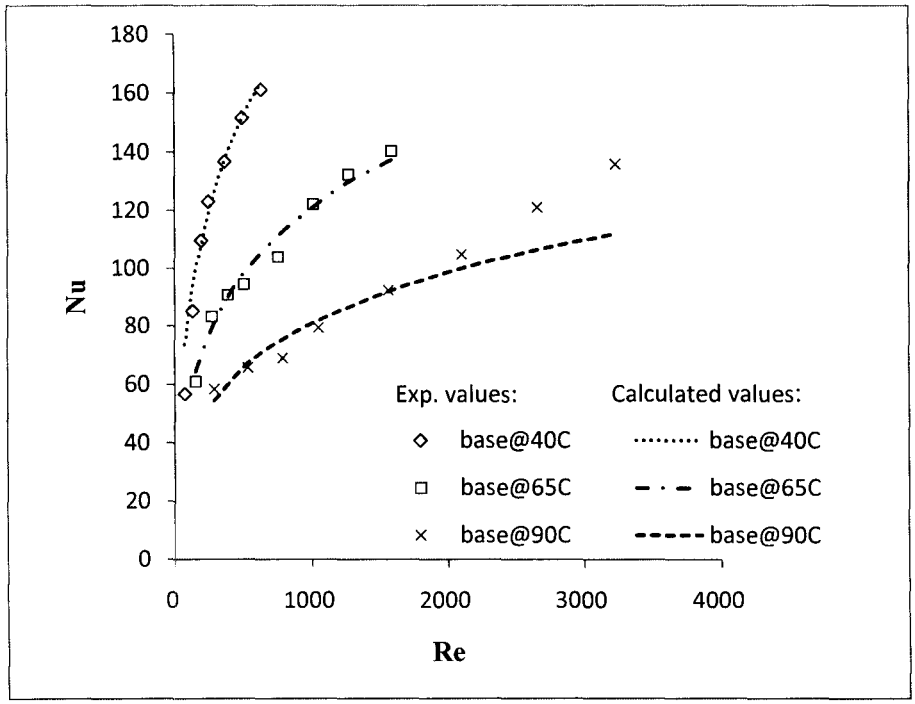

Fig E.1 Comparison between experimental data and calculated values for base fluid at 40°C, 65°C, and 90°C.

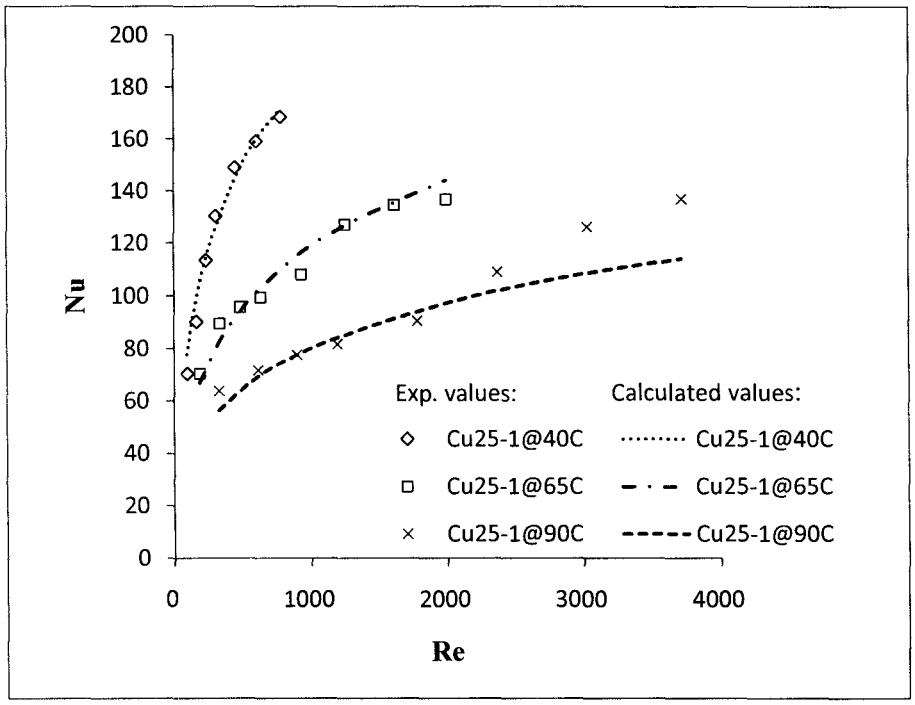

Fig E.2 Comparison between experimental data and calculated values for Cu25-1 nanofluid at 40°C, 65°C, and 90°C.

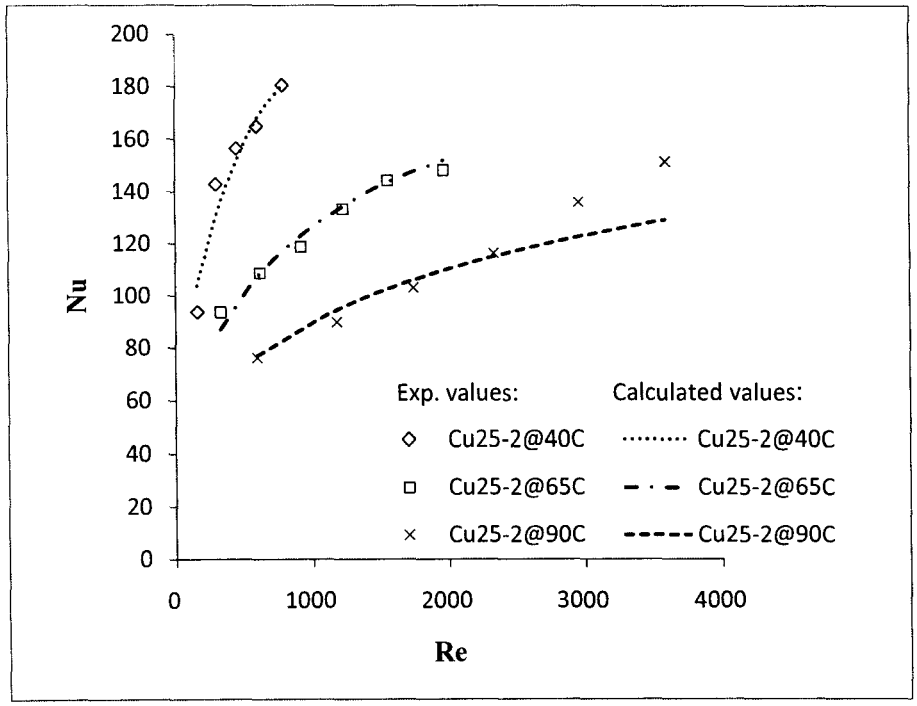

Fig E.3 Comparison between experimental data and calculated values for Cu25-2 nanofluid at 40°C, 65°C, and 90°C.

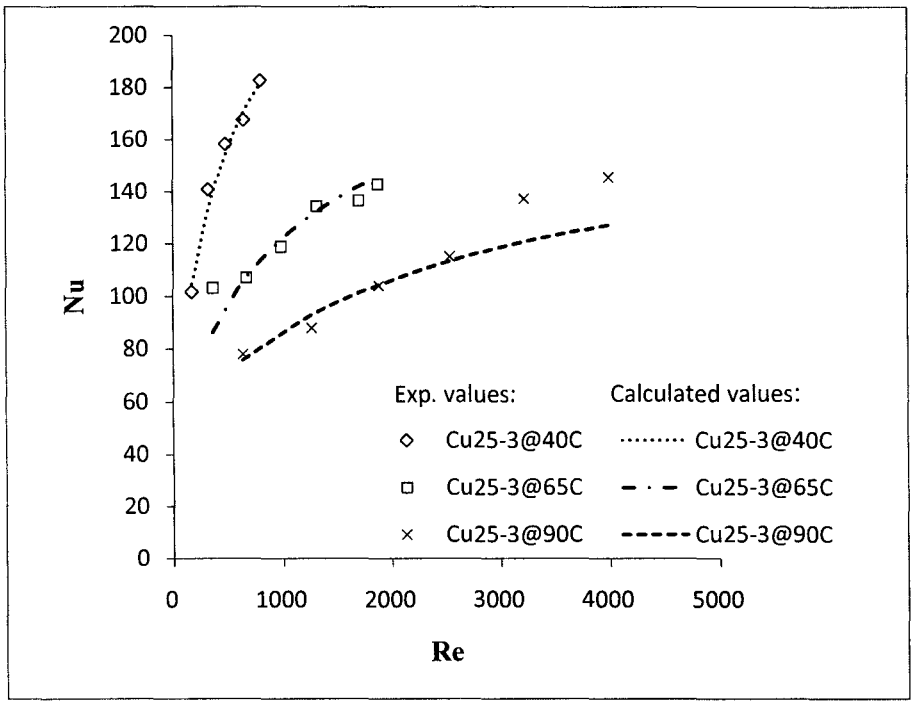

Fig E.4 Comparison between experimental data and calculated values for Cu25-3 nanofluid at 40°C, 65°C, and 90°C.

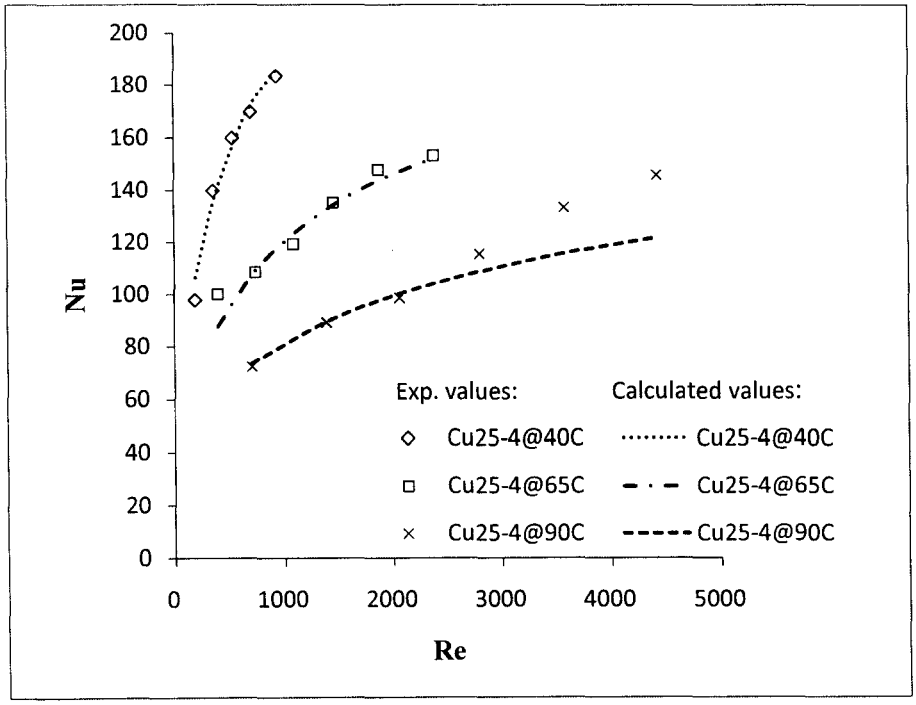

Fig E.5 Comparison between experimental data and calculated values for Cu25-4 nanofluid at 40°C, 65°C, and 90°C.

CURRICULUM VITAE

NAME: Kan Liu

ADDRESS: Department of Chemical Engineering
University of Louisville
Louisville, KY 40292

EDUCATION: B.S., Process Equipment and Control Engineering
East China University of Science and Technology
2003-2007

WORKING EXPERIENCE

Intern
Morimatsu Pressure Vessel Company, Shanghai, China
2006

Intern
Shanghai Wujing Chemical Plant, Shanghai, China
2006